Article

Density Functional Theory Estimation of Isotope Fractionation of Fe, Ni, Cu, and Zn Among Species Relevant to Geochemical and Biological Environments

Toshiyuki Fujii[1]*, Frédéric Moynier[2], Janne Blichert-Toft[3], and Francis Albarède[3]

[1] Research Reactor Institute, Kyoto University, 2-1010 Asashiro Nishi, Kumatori, Sennan, Osaka 590-0494, Japan

[2] Institut de Physique du Globe de Paris, Sorbonne Paris Cité, Université Paris Diderot, CNRS, 1 rue Jussieu, 75005, Paris, France

[3] Ecole Normale Supérieure de Lyon, Université de Lyon 1, CNRS, 46, Allee d'Italie, 69364 Lyon Cedex 7, France

*Author to whom correspondence should be addressed

tosiyuki@rri.kyoto-u.ac.jp

TEL: +81-72-451-2469, FAX: +81-72-451-2634

Abstract

This paper reports the values of reduced partition function ratios (as 1000 ln β) for Fe, Ni, Cu, and Zn bound to a number of inorganic and organic ligands. We used Density Functional Techniques to update the existing data and calculate ln β for new ligands. This work allows for the mass-dependent isotope fractionation to be predicted for various inorganic (hydrated cation, hydroxide, chloride, sulfate, sulfide, phosphate) and organic (citrate, amino acid) complexes of Fe, Ni, Cu, and Zn. Isotope fractionation among coexisting complexes of these metals was evaluated from the ln β values in a variety of geochemical and biological environments. The results provide a framework for interpretation of isotope fractionation observed in seawater and chemical sediments, in the roots and aerial parts of plants, and among the organs and body fluids of mammals.

1. INTRODUCTION

Stable isotope geochemistry uses the isotopic compositions of naturally occurring elements to shed light on the origins of natural rocks, minerals, and fluids at low and moderate temperatures (< 773 K). Non-traditional stable isotopic systems, e.g., Fe, Ni, Cu, and Zn (Albarède, 2004; Beard and Johnson, 2004; Johnson et al., 2004a,b Fujii et al., 2011a), as opposed to those of the widely used elements, H, C, N, O, and S, give important information on the environment of the modern and ancient Earth and on the origin and evolution of life.

Interpretation of the isotope composition of natural samples is elicited from experimental data obtained by modern mass spectrometry, notably multiple-collection inductively coupled plasma mass spectrometry (MC-ICP-MS). Equilibrium isotope fractionation arises during exchange of isotopes among different chemical species. It is possible to compute the electronic state of isotopologues (molecular entities that differ only by the nature of their isotopes). This means that, even for ligand exchange or electron exchange (redox), the isotope fractionation factor of equilibrium reactions can be estimated from the energy differences in the electronic states of the isotopologue reactants and products. Catalysis changes the activation energy of reactions, but does not change the electronic states of the final reactants and products. Kinetic effects can be considered as paths towards equilibrium. If the reaction rates of forward and backward reactions are not too different, the isotope effect in the process may be approximated by equilibrium fractionation. If they are very different from each other, the energy difference between the transitional isotopologues becomes the dominant factor of isotope fractionation (Bigeleisen and Wolfsberg., 1958).

This study reports the values of ln β, the logarithm of reduced partition function ratios (Bigeleisen and Mayer, 1947), computed by *ab initio* methods for a variety of chemical species of Fe, Ni, Cu, and Zn relevant to geochemistry and biochemistry. We discuss the computed values of the isotopologue partition function ratio ln β in the context of pH-dependent speciation plots, which enabled us to determine the isotope effect for coexisting species in a multi-species system. As an application to geochemistry, the isotope fractionation of Fe, Ni, Cu, and Zn under the conditions prevailing in seawater was estimated from the ln β values and related to natural data obtained in previous geochemical studies. As an application to biogeochemistry, the isotope fractionation for some compounds relevant to soil-plant systems was estimated. In view of the isotope fractionation of Fe, Cu, and Zn observed among mammal organs and body fluids (Albarede et al., 2011; Albarède, 2013; Balter et al., 2013; Moynier et al., 2013a), ln β values of Cu- and Zn-amino acid complexes were also estimated.

2. METHODS

Orbital geometries and vibrational frequencies of Fe, Ni, Cu, and Zn species were computed using the density functional theory (DFT) implemented by the Gaussian09 code (Frisch et al., 2009; Dannington et al., 2009). The DFT method employed here is a hybrid density functional consisting of Becke's three-parameter non-local hybrid exchange potential (B3) (Becke, 1993) with Lee-Yang-and Parr (LYP) (Lee et al., 1988) non-local functionals. The 6-311+G(d,p) basis set, which is an all-electron basis set, was used for H, C, N, O, P, S, Cl, Fe, Ni, Cu, and Zn. Molecules were modeled without any forced symmetry. An "ultrafine" numerical integration grid was used and the SCF (self-consistent field) convergence criterion was set to 10^{-8} or 10^{-9}. We tested whether

80 software version and database may have introduced any bias. To this effect, we
81 recalculated with Gaussian09 the Zn and Ni fractionation factors of the same species as
82 those reported by Fujii et al. (2010, 2011a,b) who used Gaussian03 and
83 B3LYP/6-311+G(d,p). The tests show that the results of the previous studies are well
84 reproduced and that changes in ln β are marginal.

85 The coordination numbers were set to 6 for Fe(II), Fe(III), Ni(II), and Zn(II), to 5
86 for Cu(II), and to 2 for Cu(I). The validity of optimized structures of model molecules
87 was checked by using spectroscopic data and thermochemical stoichiometry from the
88 literature (Fujii et al., 2006, 2010, 2011a,b, 2013). Calculations were performed for
89 single cluster model molecules. The effect of ligands beyond the first coordination
90 spheres was not considered. The bias associated with this assumption is discussed in
91 Fujii et al. (2010, 2011b).

92 For the first (3*d*) transition elements, the effect of intramolecular vibrations
93 (Bigeleisen and Mayer, 1947; Urey, 1947) is much stronger than the nuclear field shift
94 effect (Bigeleisen, 1996; Nomura et al., 1996; Fujii et al., 2010, 2011a, 2013), which
95 therefore will not be considered further. The isotope enrichment factor accordingly was
96 evaluated from the reduced partition function ratio (*s*/*s*')*f* (Bigeleisen and Mayer, 1947),
97 also noted β, such as,

$$ln\frac{s}{s'}f = \sum\left[ln\,b(u_i') - ln\,b(u_i)\right] \quad (1)$$

98 where

$$ln\,b(u_i) = -ln\,u_i + \frac{u_i}{2} + ln\left(1 - e^{-u_i}\right) \quad (2)$$

99 and

$$u_i = \frac{h\nu_i}{kT} \tag{3}$$

100

101 In the latter expression, ν stands for vibrational frequency, *s* for the symmetry number
102 of the considered compound, *h* for the Plank constant, *k* for the Boltzmann constant, and
103 *T* for the absolute temperature. The subscript *i* denotes the *i*th normal mode of
104 molecular vibration, and primed variables refer to the light isotopologue. The isotope
105 enrichment factor due to molecular vibrations can be evaluated from the frequencies ν_i
106 summed over all the different normal modes.

107 The relative enrichment of a specific compound in a multi-species system was
108 estimated by using formation constants and the ln β values of each coexisting species.
109 The standard δ notation for an element M with masses *m*' (light isotope, A') and *m*
110 (heavy isotope, A) is defined as,

$$\delta^{m}\mathrm{M} = \left(\frac{([\mathrm{A}]/[\mathrm{A}'])_{\mathrm{sample}}}{([\mathrm{A}]/[\mathrm{A}'])_{\mathrm{reference}}} - 1 \right) \times 1000 \tag{4}$$

111

112 The isotope fractionation between two different species X and Y is defined as,

$$\Delta^{m}\mathrm{M} = \delta^{m}\mathrm{M_Y} - \delta^{m}\mathrm{M_X} \tag{5}$$

113 The detailed methods used to evaluate isotope fractionation among coexisting species
114 was described by Fujii et al. (2010, 2011a, 2013) and are reproduced in *APPENDIX A*.

115 The absolute ln β values and their relative scale may vary with the calculation
116 method [e.g., DFT, HF (Hartree-Fock), MP*n* (Møller Plesset)], basis set, cluster size,
117 and solvation model (Fujii et al., 2010, 2011a,b; Rustad et al., 2010; Hill et al., 2014).
118 How different options affect the results and their overall accuracy is discussed in
119 Appendix B.

120

121 ## 3. RESULTS AND DISCUSSION

122 ### 3.1. Isotope fractionation among species in modern seawater

123 We here reproduce speciation of Cu(II) and Zn(II) inorganic species in seawater as
124 calculated by Zirino and Yamamoto (1972) for 19% chlorinity at 298 K and 1 atm total
125 pressure. The model includes activity coefficients for monovalent, divalent, and neutral
126 species. Concentrations of free HCO_3^- and CO_3^{2-} were estimated as a function of pH.
127 This model was used to estimate isotope fractionation of Fe, Ni, Cu, and Zn among
128 inorganic ligands present in seawater.

129 We expand the pH range from 7 to 9 in Zirino and Yamamoto's (1972) original
130 Cu(II) speciation model to a range of 6 to 9 (Fig. 1a). The concentrations of HCO_3^- and
131 CO_3^{2-} at pH < 7 were estimated by extrapolating the data reported using Zeebe and
132 Wolf-Gladrow (2001),

$$[HCO_3^-] = \frac{DIC}{\left(1 + \frac{[H^+]}{K_1^*} + \frac{K_2^*}{[H^+]}\right)} \quad (6)$$

133 and

$$[CO_3^{2-}] = \frac{DIC}{\left(1 + \frac{[H^+]}{K_2^*} + \frac{[H^+]^2}{K_1^* K_2^*}\right)} \quad (7)$$

134 where DIC represents the total concentration of dissolved inorganic carbon, $[CO_2]$ +
135 $[HCO_3^-]$ + $[CO_3^{2-}]$. K_1* and K_2* are the equilibrium constants, that is, K_1* =
136 $[HCO_3^-][H^+]/[CO_2]$ and K_2* = $[CO_3^{2-}][H^+]/[HCO_3^-]$. These equations were employed in
137 the extrapolation by setting DIC, K_1*, and K_2* as parameters.

138 The ln β values of various Cu species were computed by Fujii et al. (2013) for
139 fourfold and fivefold coordinations and agree with the results of Sherman (2013). For
140 example, ln β of $Cu(H_2O)_5^{2+}$ (298 K) is 4.546‰ (Fujii et al., 2013) compared with
141 4.55‰ for Sherman (2013). The $\delta^{65}Cu$ value of each species was calculated as functions
142 of pH (see *Appendix A*). As shown in Figs. 1a and 1b, at pH ~6, ^{65}Cu is enriched in
143 $CuSO_4$ and $CuHCO_3^+$, while ^{63}Cu is enriched in Cu^{2+} and $CuCl^+$. With increasing pH,
144 $Cu(OH)_2$ and $CuCO_3$ become the prevalent species. At a typical pH of seawater, 8.22
145 (Macleod et al., 1994), isotope fractionation favors ^{63}Cu in $CuCO_3$ and ^{65}Cu in $Cu(OH)_2$.
146 Figure 1c is a summary of $\delta^{65}Cu$ for the different Cu species present. At low pH,
147 positive $\delta^{65}Cu$ are found in Cu sulfates and carbonates, while $\delta^{65}Cu$ are negative in
148 hydrated Cu^{2+} and chlorides (see Figs. 1a and 1c). At high pH, $\delta^{65}Cu$ is positive in Cu
149 hydroxides and negative in carbonates.
150 The distribution of Zn(II) species in seawater at 298 K and 1 atm as functions of
151 pH was also taken from Zirino and Yamamoto (1972) (Fig. 2a). Electronic structures of
152 hydrated Zn^{2+}, chloride, carbonate, hydroxide, and sulfate were computed, and fivefold
153 coordination was found to provide a stable configuration for carbonate species. The
154 optimized structures in Cartesian coordinates are given in Table S1 of the electronic
155 supplement. The ln β values obtained are reported in Table 1. The $\delta^{66}Zn$ values for the
156 $^{66}Zn/^{64}Zn$ ratio were calculated for each relevant species as a function of pH. A
157 dominant species of free Zn^{2+} shows small isotope fractionation (Fig. 2). $ZnSO_4$ is
158 enriched in ^{66}Zn, whereas Zn chlorides are enriched in ^{64}Zn with a $\Delta^{66}Zn$ ~0.5‰ being
159 expected between Zn sulfate and chloride (Fig. 2c). With increasing pH, $Zn(OH)_2$ and
160 $ZnCO_3$ become the dominant species. Small amounts of free Zn^{2+} and $ZnCl^+$ still exist

161 at pH = 8.2. In seawater, a fractionation $\Delta^{66}Zn$ of ~1‰ is expected between Zn
162 carbonate and chloride (Fig. 2c). Zn hydroxides and sulfates do not play an important
163 role for Zn isotope fractionation for pH ≥ 8.2 (Fig. 2c).

164 A speciation model similar to that of Zirinno and Yamamoto (1972) likewise was
165 applied to Ni(II) and Fe(II) in seawater at 298 K and 1 atm. The speciation diagram of
166 Ni(II) is shown in Fig. 3a. The stability constants were taken from Byrne et al. (1988)
167 (sulfate), Foulliac and Criaud (1984) (carbonates), and Turner et al. (1981) (other
168 species). The optimized structures in Cartesian coordinates are given in Table S2 of the
169 electronic supplement. The ln β values obtained are reported in Table 2. The maximum
170 difference in ln β values among the species shown in Fig. 3b is ~0.8‰ (298 K). The
171 values of $\delta^{60}Ni$ for the isotope pair ($^{60}Ni/^{58}Ni$) are shown for each species Figs. 3b and
172 3c. At low pH, the major Ni species are hydrated Ni^{2+} and Ni chlorides, and only little
173 fractionation with $\delta^{60}Ni$ of ~0.1‰ is expected. At higher pH, ^{60}Ni is enriched in Ni
174 carbonates, which would cause +0.5‰ fractionation compared with that of chlorides.

175 The distribution of Fe(II) species in seawater at 298 K and 1 atm as a function of
176 pH is shown in Fig. 4a. The stability constant for $FeHCO_3^+$ was taken from Foulliac and
177 Criaud (1984) and the rest from Turner et al. (1981). The optimized structures of Fe(II)
178 complexes are reported in Table S3 of the electronic supplement. For example, the
179 calculation reproduces the hexahydrated structure of $Fe(H_2O)_6^{2+}$ with the Fe^{2+}-H_2O
180 distance (2.14-2.18 Å) of 2.12 Å determined by X-ray diffraction (XRD) (Magini et al.,
181 1988). The ln β values obtained (Table 3) compare well with *ab initio* studies of Fe
182 complexes (Ottonello and Zuccolini, 2009; Hill et al., 2010; Rustad et al., 2010,
183 Moynier et al., 2013b, and references therein). As shown in Figs. 4b and 4c, ^{54}Fe is
184 enriched in $FeCl^+$. Dependence of ln β on temperature is shown in Figure 5a. In the

lower pH region, ^{56}Fe is enriched in $FeSO_4$ and $FeHCO_3^+$. With increasing pH, $FeCO_3$ is becoming the prevalent species and is enriched in ^{56}Fe.

Because of the strong hydrolysis taking place in seawater, Fe(III) forms $Fe(OH)_3$ (Byrne and Kester, 1976). The values of ln β were calculated accordingly for Fe(III) species as well. The optimized structures in Cartesian coordinates are given in Table S4 of the electronic supplement. Again, the hexahydrated structure of $Fe(H_2O)_6^{3+}$ with the Fe^{3+}-H_2O distance of 2.05 Å determined by XRD (Magini et al., 1988) is well reproduced (2.06 Å). The ln β values obtained are reported in Table 4. Dependence of ln β on temperature is shown in Figure 5b. ln β of hydrated Fe^{3+} and Fe(III) chlorides calculated by *ab initio* methods has been reported previously (Fujii et al., 2006; Hill and Schauble, 2009) and the present calculations agree well with literature values. The ln β values of ferric hydroxide complexes are characteristically large. Among the hydroxides, lower order of hydrolytic species shows smaller ln β. This suggests that the dissociation of $Fe(OH)_3$ with increasing acidity enriches ^{54}Fe in both $Fe(OH)^{2+}$ and $Fe(OH)_2^+$.

Under reducing conditions, redox reactions among Fe(II) and Fe(III) species must be considered. For example, the [Fe(II)]/[Fe(III)] ratio of ~4 has been advocated for the Baltic Sea (Kononets et al., 2002). Distribution of Fe(II) and Fe(III) species in seawater at 298 K, 1 atm, and pH = 8.2 was estimated by the method of Zirinno and Yamamoto (1972) for [Fe(II)]/[Fe(III)] = 4. The resulting $\delta^{56}Fe$ values are shown in Fig. S1 of the electronic supplement. ^{56}Fe is enriched in $Fe(OH)_3$ and ^{54}Fe in free Fe^{2+}. The isotope fractionation factor $\Delta^{56}Fe$ ($Fe(OH)_3$ - Fe^{2+}) between the two species is ~4.3‰.

3.2. Euxinic seawater

208 The role of sulfides is central to a broad range of geological scenarios. The status of
209 sulfur in ancient oceans in particular is still an outstanding issue (Canfield, 1998).
210 Hydrothermal vent solutions discharging either at mid-ocean ridges (Edmond et al.,
211 1979) or along subduction zones (Mottl et al., 2004) comprise additional environments
212 dominated by sulfides. In a previous study (Fujii et al., 2011b), isotope fractionation
213 among the different Zn sulfide species present in geological fluids between 298 and 573
214 K was evaluated. Here, we extend this study to Fe, Ni, and Cu.
215 Speciation of Fe(II) in seawater-like solutions containing hydrogen sulfides has
216 been previously investigated (Rickard and Luther, 2007; Wu et al., 2012). It was
217 pointed out that Fe(II) sulfides are dominant at pH typical of seawater. The speciation
218 diagram of Fe(II) species in the seawater-like matrix at pH = 6-9 was reproduced from
219 Rickard and Luther (2007) (Fig. 6a). At pH = 8.2, the aqueous FeS is prevalent. At
220 lower pH, $FeHCO_3^+$ becomes a major Fe(II) species.
221 A characteristic feature of the speciation diagram (Fig. 6a) is the presence of the
222 higher order Fe(II) hydroxide, $Fe(OH)_3^-$. In the pH-Eh diagrams, Rickard and Luther
223 (2007) treated $FeOH^+$ and $Fe(OH)_2$ as fougerite, a hydrotalcite mineral of Fe(II) and
224 Fe(III). This may be the reason for the lack of $FeOH^+$ and $Fe(OH)_2$ in the speciation
225 diagram. The formation of $Fe(OH)_3^-$ was thermochemically confirmed by Baes and
226 Mesmer (1976), but there are no information on its stereochemical structure.
227 Hydroxylation of Fe(II) and condensation of its hydroxides form the ferrous oxide
228 (Jolivat et al., 2004). $Fe(OH)_2$ has the brucite structure, which is a layer structure with
229 hydroxyl (OH^-) groups in hexagonal close packing: each Fe(II) is octahedrally
230 coordinated to six OH^- groups and these octahedra share edges to form the layers (Zigan
231 and Rothbauer, 1967). $Fe(OH)_2(H_2O)_4$ corresponds to monomeric aqueous $Fe(OH)_2$ and

232 is treated as a *trans*-structure (Table S3 and Table 3). By reference to $Fe(OH)_2(H_2O)_4$,
233 we attempted to treat the structure of $Fe(OH)_3^-$ as $Fe(OH)_3(H_2O)_3^-$, but the species was
234 found to be unstable in our calculation as the three H_2O molecules moved away from its
235 first coordination sphere. Since the dimer $Fe_2(OH)_2(H_2O)_8^{2+}$ of $Fe(OH)^+$ is considered a
236 structural unit of the $Fe(OH)_2$ formation (Jolivat et al., 2004), its hydrolytic species
237 $Fe_2(OH)_6(H_2O)_4^{2-}$ may actually be treated as a dimer of $Fe(OH)_3^-$. The electronic states
238 of Fe_2 (Irigoras et al., 2003) was referred for the calculation of dimeric species of Fe(II).
239 The results show that Fe(II) possesses a fluttered square plane structure with four OH^-
240 ions, and H_2O molecules are bound to the OH^- moiety of $Fe_2(OH)_6^{2-}$ via hydrogen bonds.
241 We calculated ln β for $Fe_2(OH)_6^{2-}$ (Table S3 and Table 3), and found that it was close to
242 that of $Fe(OH)_2(H_2O)_4$. We therefore opted for using the value of ln β of $Fe(OH)_2$ for
243 $Fe(OH)_3^-$.

244 Iron in hydrated Fe(II) mono-hydrogensufide $FeHS(H_2O)_5^+$ would be
245 sixfold-coordinated. Rickard and Luther (2006) suggested that the structure of
246 bis-hydrogensulfide for six-coordination transition metals is similar to that of
247 *trans*-$Mn(HS)_2(H_2O)_4$. We therefore adopted the structure *trans*-$Fe(HS)_2(H_2O)_4$ in the
248 present calculations. The optimized structures of Fe(II) sulfides are shown in Table S3
249 of the electronic supplement. The ln β values obtained are shown in Table 3. Several
250 authors have reported the stability constant for $FeHS^+$ (Dyrssen, 1988; Zhang and
251 Millero, 1994; Luther et al., 1996; Al-Farawati and van den Berg, 1999; Davison et
252 al.,1999). However, the only species that were identified by Dyrssen (1988) and
253 Davison et al. (1999) was the higher order complex $Fe(HS)_2$. It may be difficult to
254 distinguish the formation of $Fe(HS)_2$ from polymerized Fe(II) sulfides denoted as

255 aqueous FeS. We therefore used the structure of *trans*-$Fe(HS)_2(H_2O)_4$ to represent
256 monomeric aqueous FeS.

257 The values of $\delta^{56}Fe$ for the $^{56}Fe/^{54}Fe$ ratio were calculated for the relevant species
258 as a function of pH (Figs. 6b and 6c). Species other than sulfides show positive $\delta^{56}Fe$ at
259 typical seawater pH. At lower pH, a $\Delta^{56}Fe$ fractionation of 0.5-1‰ may be expected
260 between these species and sulfides. At pH ≥ 8.2, $\Delta^{56}Fe$ between carbonates and sulfides
261 increases to 1.6‰.

262 The growth of FeS clusters stabilizes FeS as a solid phase. The structure of FeS
263 clusters has been computed by Rickard and Luther (2007). The stable structure of Fe_2S_2
264 is similar to the basic structural component of mackinawite. Polymerization of the
265 hydrated Fe_2S_2 molecules would make the FeS solid phase precipitate. A possible
266 structure of the hydrated Fe_2S_2 is $Fe_2S_2(H_2O)_4$ (Rickard and Luther, 2007), in which the
267 coordination number of Fe(II) is four. We successfully reproduced the structure by *ab*
268 *initio* calculations and the optimized structure of $Fe_2S_2(H_2O)_2$ is shown in Table S3. The
269 corresponding ln β values are shown in Table 3. $Fe_2S_2(H_2O)_4$ forms via dimerization of
270 Fe(II) mono-hydrogensulfides, according to,

$$2FeHS(H_2O)_5^+ \rightleftarrows Fe_2S_2(H_2O)_4 + 2H^+ + 6H_2O \quad (8)$$

271 The ln β values obtained for $Fe_2S_2(H_2O)_2$ are larger than those of Fe(II)
272 hydrogensulfides, yet still smaller than those of other aqueous Fe(II) species. This
273 suggests that the $^{56}Fe/^{54}Fe$ ratio of Fe^{2+} and Fe(II) chlorides, carbonates, and hydroxides
274 show heavier $\delta^{56}Fe$ values than that of solid FeS.

275 As for the Fe(II) case, the structures of Ni(II) hydrogensulfides were computed
276 (Table S2 of the electronic supplement). The ln β values obtained are shown in Table 2.

277 The ln β values of Ni(II) hydrogensulfides are smaller than those of the other prevalent
278 aqueous Ni(II) species. $^{60}Ni/^{58}Ni$ ratios in ferromanganese crusts suggest that
279 hydrothermal fluids entering the ocean have $\delta^{60}Ni$ ~1.5‰ (Gall et al., 2013). As shown
280 in Table 2, ln β is 1.4-1.5‰ (298 K) smaller for $Ni(HS)_2$ than for $NiCO_3$ and $NiSO_4$.
281 The ligand exchange reactions of Ni sulfide-Ni carbonate and Ni sulfide-Ni sulfate
282 possibly create $\delta^{60}Ni$ of the same magnitude as that suggested by Gall et al. (2013) for
283 hydrothermal fluids.

284 In a previous study in which Fujii et al. (2013) computed ln β at 298 K for Cu
285 species, ln β was found to be 1-2‰ smaller for Cu(II) sulfides than for Cu(II)
286 carbonates, hydroxides, and hydrated Cu^{2+}. Again, this suggests that Cu^{2+} and Cu(II)
287 chlorides, carbonates, and hydroxides are isotopically heavier than sulfides. Since
288 sulfide-bearing systems are reducing, isotope fractionation of Cu caused by the presence
289 of Cu(I) must also be considered. Taking the standard redox potentials of the HS^-/SO_4^{2-}
290 and Cu^{2+}/Cu^+ couples (Pourbaix, 1974) into account, most of inorganic Cu(II) species
291 are reduced to Cu(I) under the redox conditions in which sulfides prevail. The
292 speciation of Cu(I) under hydrothermal conditions at 573 K has been evaluated by
293 Mountain and Seward (1999) and the prevailing species were found to be CuCl, $CuCl_2^-$,
294 CuHS, and $Cu(HS)_2^-$. The higher order Cu(I) chloride complex $CuCl_3^{2-}$ is also identified,
295 but its small stability constant (Mei et al., 2013 and references therein) makes it a minor
296 species. The ln β values of these species were evaluated by *ab initio* methods by Seo et
297 al. (2007) and Sherman (2013) and the results obtained in the present study (Tables S5
298 and 5, and Fig. 7) agree with their values. At high pH and high sulfur concentration, a
299 Cu(I) dimer $Cu_2S(HS)_2^-$ exists (Mountain and Seward, 1999). As shown in Table 5,
300 increasing complexation of chlorides and sulfides results in decreasing ln β. We

evaluated the $\delta^{65}Cu$ values of Cu(I) species from the speciation model of Mountain and Seward (1999) and show the results in Fig. S2 of the electronic supplement as a function of the mole fractions of Cu(I) species. The range of isotopic variation of the Cu(I) species at 573 K is about ±0.1‰. The ln β values of Cu(II) chlorides and sulfides (Fujii et al., 2013) at 573 K are 0.2-0.5‰ higher than those of corresponding Cu(I) species (Table 5). Under hydrothermal conditions, the $\delta^{65}Cu$ value of Cu(I) should be 0.2-0.5‰ lower than that of Cu(II) with a ±0.1‰ range of variation among Cu(I) species. Cu(I) chloride may be isotopically light compared with Cu(I) sulfide (Fig. S2), and lighter if $CuCl_3^{2-}$ exists due to its small ln β (Fig. 7 and Table 5).

Dekov et al. (2013) reported $\delta^{65}Cu$ values of Cu^0 (native copper) from sedimentary layers of 0.41-0.95‰ and suggested that native Cu precipitation in the basaltic basement is a result of low temperature (293 to 358 K) hydrothermal processes under anoxic and H_2S poor conditions. These authors proposed a reduction process of Cu(I) chloride $CuCl_2^-$ to Cu^0 to explain the heavy isotope enrichment of the Cu^0. Since the ln β value of intramolecular vibrations for the uncomplexed Cu^0 atom is zero, $\Delta^{65}Cu$ between Cu^0 and $CuCl_2^-$ reduces to the negative of ln β for $CuCl_2^-$. In other words, the reduced Cu^0 should be isotopically lighter than $CuCl_2^-$. This does not match the positive $\delta^{65}Cu$ value for Cu^0 observed for native copper in the oceanic crust by Dekov et al. (2013). We here suggest that $CuCl_2^-$ was dissociated to CuCl and/or Cu^+ according to

$$CuCl_2^- + H_2O \rightleftarrows CuCl(H_2O) + Cl^- \quad (9)$$

$$CuCl_2^- + 2H_2O \rightleftarrows Cu(H_2O)_2^+ + 2Cl^- \quad (10)$$

and that the dissociated species were then irreversibly reduced to Cu^0,

$$4CuCl(H_2O) \rightarrow 4Cu^0\downarrow + 4HCl + O_2 + 2H_2O \quad (11)$$

$$4Cu(H_2O)_2^+ \rightarrow 4Cu^0\downarrow + 4H^+ + O_2 + 6H_2O \quad (12)$$

In these reactions, $\delta^{65}Cu$ for Cu^0 reflects positive $\Delta^{65}Cu$ values between $CuCl(H_2O)$ and $CuCl_2^-$ and/or between $Cu(H_2O)_2^+$ and $CuCl_2^-$. From the ln β values shown in Table 5, isotope fractionation of +0.4-0.5‰ ^{65}Cu in Cu^0 at 298-323 K may be expected.

Aggregation of Cu^0 atoms results in the formation of Cu metallic phase. Though it is difficult to simulate metals by using cluster model, intramolecular vibration of a diatomic Cu_2^0 computed gives ln β ~0.8‰ at 298-323 K. (Table S7). This suggests that the aggregation of Cu^0 atoms also give a positive isotope fractionation. Hence, the isotope fractionation larger than +0.4-0.5‰ ^{65}Cu in Cu^0 (native copper) may be possible from the above reaction scheme.

3.3. Isotope fractionation of Fe, Ni, Cu and Zn due to inorganic ligands

This section summarizes the common features of isotope fractionation for Fe, Ni, Cu, and Zn estimated by *ab initio* methods. Polyatomic inorganic ligands such as SO_4^{2-} and the phosphate ion are important for soil chemistry. Phosphate complexes of Zn and the ln β values of $^{66}Zn/^{64}Zn$ were computed by Fujii and Albarède (2012). Structures of phosphate complexes of Fe (Tables S3 and S4), Ni (Table 2S), and Cu (Table S6) were computed using the same approach as for Zn phosphates. The ln β values obtained are shown in Tables 2, 3, 4, and 5. The ln β values for a minor species, $CuHPO_4^+$, which is used only in this section, are separately shown in Table S8. Geochemical application of the results for ln β of phosphates to soil-plant systems will be discussed in Section 3.4.

341 The ln β values of the divalent states of Fe, Ni, Cu, and Zn bound to hydrated
342 cations, hydroxide, chloride, sulfate, sulfide, carbonate, and simple phosphate
343 complexes are compared in Fig. 8 (note that metal cations are denoted as M^{2+}). The
344 magnitude of ln β values varies in the order Fe < Ni > Cu > Zn. This sequence is
345 identical to that of complex stability derived from crystal field theory (Bersuker, 1996).
346 Additional stabilization energy resulting from Cu site deformation (Jahn-Teller effect,
347 Bersuker, 2006) may still be an issue.

348 The oxygen donor ligands, OH^-, SO_4^{2-}, CO_3^{2-}, HCO_3^-, HPO_4^{2-}, and $H_2PO_4^-$, tend to
349 give larger ln β values than those of hydrated cations. The values of ln β for variably
350 deprotonated ligands decrease in the order $CO_3^{2-} > HCO_3^-$ and $HPO_4^{2-} > H_2PO_4^-$, which
351 reflects that ligand protonation decreases the energy of the bond with M^{2+}. Chloride and
352 sulfide complexes show smaller ln β values than those of hydrated cations. Higher order
353 complexation of the cations with Cl^- or HS^- also results in a decrease of ln β. A similar
354 decreasing trend was found for the hydrolysis of Fe and Ni. In contrast, Cu hydroxides
355 and carbonates show a trend different from that of the other metals. This may again
356 reflect structural deformations specific to these species. In the first Cu^{2+} coordination
357 sphere, CO_3^{2-} occasionally combines with H_2O to produce HCO_3^- and OH^- (Fujii et al.,
358 2013; Sherman, 2013). Hydrolysis also makes the hydration bond of an axial H_2O
359 molecule at the first coordination sphere weaker (Fujii et al., 2013; Sherman, 2013).

360 The ln β values of Fe(II), Fe(III), Ni(II), Cu(II), and Zn(II) complexes are shown in
361 Fig. 9 as a function of the bond length with ligands. The atomic distances between M
362 and O of the oxygen donor ligands, M and Cl, and M and S of HS are used as bond
363 lengths. A minor Fe(III) sulfide species, $FeHS^{2+}$, was also computed, for which the

364 results are shown in Tables S4 and S9. The lines shown were calculated by the least
365 square method and did not take sulfides into consideration. The ln β values increase
366 with decreasing bond lengths. Since CO_3^{2-} and HCO_3^- are treated as bidentate ligands, a
367 shorter distance of M-O was shown in Fig. 9. Some of the misfit may be due to the
368 assumption of the bidentate character. The poor correlation of ln β vs bond length for
369 Cu(II) may be attributable to the distortion of complexes by the Jahn-Teller effect
370 (Bersuker, 2006). The ln β values for sulfide complexes also deviate from the
371 correlation lines and show smaller values. This can reflect the different bonding
372 energies between O and S donor ligands as explained by the hard and soft acids and
373 bases (HSAB) principle (Pearson, 1968a,b).

374 Electronegativity as originally defined by Pauling (1960) is a measure of the power
375 of an atom in a molecule to attract electrons. The term was later extended to groups
376 (Huheey, 1965). We here show that the ln β values correlate with the group
377 electronegativity of ligands (Fig. 10). The source of the values adopted for group
378 electronegativities (Allred, 1961; Huheey, 1965, 1966; Bratsch, 1985; Mullay, 1985;
379 Boyd and Boyd, 1992) are listed in Table 7. The ln β values increase with increasing
380 group electronegativity. The correlation between the ln β values of Cu(II) is stronger
381 with electronegativity (Fig. 10d) than with bond length Fig. 9d, The misfit of the ln β
382 values for sulfide complexes is also smaller for electronegativity than for bond length.

383 Overall, isotopologues with stronger chemical bonds, and therefore higher
384 intramolecular vibrational frequencies, have larger ln β (Bigeleisen and Mayer, 1947;
385 Urey, 1947). Both Figs. 9 and 10 demonstrate that the rule works even for transition
386 metal centered polyatomic molecules. Group electronegativities therefore may help

387 predict the direction and strength of isotope fractionation by ligand exchange reactions.
388 Such a property may be particularly useful for isotope fractionation induced by complex
389 metalloproteins.
390
391 **3.4. The soil-plant system**
392 $\delta^{56}Fe$ in ferrous ion (Fe^{2+}) is 1.3‰ heavier than that in ferrihydrite ($Fe_5HO_8 \cdot 4H_2O$)
393 (Beard et al., 1999). The magnitude of this fractionation is expected from the difference
394 in ln β values between Fe(II) and Fe(III) species (see Tables 3 and 4). Beard et al.
395 (1999) assigned isotope fractionation to biogenic effects via Fe-reducing bacteria and
396 suggested electron exchange reactions between Fe and organic matter. Evaluating the ln
397 β values of organometallic compounds of Fe, Cu, Ni, and Zn therefore is important.
398 The tricarboxylic citric acid is a major organic acid. The citric acid cycle known as
399 the Krebs cycle is used by aerobic organisms to generate energy through the oxidation
400 of acetate into CO_2 (Cowan, 1997). In addition, the citric acid cycle provides precursors
401 of certain amino acids. Haem biosynthesis begins in the mitochondria, with the
402 condensation of succinyl coenzyme A (CoA) produced during the citric acid cycle with
403 glycin (Crichton, 2001).
404 Citric acid also plays an important role in the transport of trace metals in the
405 soil-plant system. Citrate is released from roots of vascular plants and act as a biological
406 chelating agent for the uptake of metals from soil. Isotope fractionation induced by
407 higher plants has been found for Fe (Guelke and von Blanckenburg, 2007; Kiczka et al.,
408 2010; Moynier et al., 2013b), Ni (Estrade et al., 2013), Cu (Weinstein et al., 2011;
409 Jouvin et al., 2012), and Zn (Weiss et al., 2005; Moynier et al., 2009). In a pioneering
410 work of the isotope fractionation of Zn in the soil-plant system, Weiss et al. (2005)

411 found that Zn was isotopically lighter in the shoots relative to the roots, with a $\delta^{66}Zn$
412 difference of -0.13 to -0.26. The origin of this isotope fractionation has been explained
413 by the isotopic exchange between Zn(II) phosphates in soil and citrates (or malates) in
414 plants (Fujii and Albarède, 2012).

415 Likewise, *ab initio* calculations of Fe isotope fractionation in higher plants by
416 Moynier et al. (2013b) suggest that the roots of strategy-II plants
417 (Fe(III)-phytosiderophore) are isotopically heavier by about 1‰ (for $\delta^{56}Fe$) than the
418 upper parts of the plants. Iron is transported as Fe(III)-citrate in the xylem or
419 Fe(II)-nicotianamine in the phloem. It was suggested that, even in the absence of redox
420 reactions of Fe^{3+}/Fe^{2+}, change in speciation alone can create up to 1.5‰ isotope
421 fractionation (Moynier et al., 2013b). Here, we therefore focus on Fe(III) phosphates
422 and Fe(III) citrates and estimate $\delta^{56}Fe$ created by exchange of Fe(III) among these
423 species.

424 The $^{56}Fe/^{54}Fe$ ratio in stems is ~1‰ lighter compared to that of roots and soil
425 (Kiczka et al., 2010; Moynier et al., 2013b). Fe(III) citrates are the major Fe species in
426 the xylem of stems in strategy I plants (Kiczka et al., 2010), whereas Fe(III) phosphates
427 and hydroxides are the prevalent species in soils. The prevalent forms were determined
428 using the work of Königsberger et al. (2000) for citrates, while the results of Ciavatta
429 and Iuliano (1995) were used for Fe(III) phosphates. The chemical species of Fe(III)
430 computed are shown in Fig. 11 and Table S4 of the electronic supplement. We assumed
431 sixfold-coordination of Fe(III) for all species. Moynier et al.'s (2013b) *ab initio* results
432 for Fe citrates, Fe(cit) and $Fe(cit)_2^{3-}$, where (cit) stands for the citrate ion $C_6H_5O_7^{3-}$,
433 tested different basis sets. In the present study of Fe(cit) and $Fe(cit)_2^{3-}$, we used the
434 6-311+G(d,p) basis set. As pointed out by Fujii and Albarède (2012), HPO_4^{2-} contacts

435 hydration water around Fe^{3+}, in which H_2O is dissociated to H^+ and OH^-. For example,
436 $FeHPO_4(H_2O)_5^+$ (model molecule (b-3) of Fig. 11) acts as $FeH_2PO_4OH(H_2O)_4^+$.
437 From the stability constants of orthophosphates (Childs, 1970), Fe(III) phosphates
438 (Ciavatta and Iuliano, 1995), citrates (Königsberger et al., 2000), hydroxides (Baes and
439 Mesmer, 1976), and dissociation constants of citric acid (Königsberger et al., 2000), the
440 speciation diagram for a diluted system (activity coefficients of chemical species are
441 treated to be unity) was prepared as functions of pH (Fig. S3 of the electronic
442 supplement). At low pH < 6, various chemical exchange reactions take place among
443 Fe(III) phosphates and citrates. In the neutral pH region, partly hydrolyzed Fe(III)
444 citrates are predominant. At high pH > 8, aqueous $Fe(OH)_3$ becomes a major Fe(III)
445 species.
446 The ln β values for the $^{56}Fe/^{54}Fe$ ratio obtained are shown in Table 4. The
447 dependence of ln β on temperature is shown in Fig. 12b. The isotope fractionation
448 factors $\delta^{56}Fe$ for Fe(III) phosphates, citrates, hydroxides, and hydrated Fe^{3+} ions are
449 shown in Fig. S3 as functions of pH. $\delta^{56}Fe$ of Fe(III) citrates is ~1‰ smaller than that of
450 Fe(III) phosphates or hydroxides. Kiczka et al. (2010) observed $\delta^{56}Fe$ ~1‰ in xylem of
451 stems, where Fe(III) citrates are major species in strategy I plants. This suggests that the
452 magnitude of Fe isotope fractionation found in soil-stem (Kiczka et al., 2010) is
453 possible only by ligand exchange of Fe(III) phosphates-citrates.
454 Fe(II) nicotianamine is the major Fe species present in the central part of the plant
455 roots (stele) in strategy I plants (Kiczka et al., 2010). The $^{56}Fe/^{54}Fe$ ratio in steles was
456 more than 2‰ smaller than that of host soil (Kiczka et al., 2010). Since isotope
457 fractionation is clearly larger than the $\delta^{56}Fe$ variability expected from Fe(III) species
458 (Fig. 12b), it may be concluded that the isotope fractionation of Fe found in steles

459 results from redox reaction between Fe^{3+} and Fe^{2+}. As for the Fe(III) case, the lnβ
460 values for Fe(II) phosphates and citrates were computed by *ab initio* methods. Relevant
461 Fe(II) species were chosen from the literature (Ciavatta et al., 1992; Königsberger et al.,
462 2000). The optimized structures of Fe(II) complexes and their ln β values are shown in
463 Tables S3 and 3, and Fig. 12a. It is clear that ln β is 3-4‰ smaller for Fe(II) phosphates,
464 citrates, and hydroxides than for Fe(III) species (Table 4). These new results confirm
465 that Fe isotope fractionation in plants of 2‰ or larger is due to Fe^{3+}/Fe^{2+} redox
466 reactions.

467 A similar computational work was conducted on Ni(II) and Cu(II). The results are
468 shown in Fig. S4 (Ni) and Fig. S5 (Cu) of the electronic supplement. Since the valence
469 of Ni is fixed at (II), the transport of Ni in the soil-plant system is independent of redox
470 reactions. The relevant species of Ni(II) phosphates and citrates were chosen from the
471 literature (Taylor and Diebler, 1976; Hedwig et al., 1980). Their optimized structures
472 are given in Table S2. The ln β values obtained are shown in Table 2 and Fig. 12c. The
473 $\delta^{60}Ni$ values of Ni(II) phosphates, citrates, hydroxides, and hydrated Ni^{2+} ions are
474 shown in Fig. 16b as a function of pH. Since Ni(II) hydroxides only exist in the high pH
475 region of pH > 9 (Fig. S4), these may not be important in the soil-plant system. At
476 neutral pH, the prevalent Ni(II) species are phosphates and citrates, and the range of
477 their $\delta^{60}Ni$ values is ~0.6‰. The magnitude of isotope fractionation overlaps with the
478 recent finding (Estrade et al., 2013) of $\Delta^{60}Ni$ = 0.2‰ between the roots and leaves of a
479 plant sample. With the decrease of pH, $\delta^{60}Ni$ of phosphates and citrates become very
480 similar (Fig. S4). At pH < 6, hydrated Ni^{2+} exists in the system and may have lower
481 $^{60}Ni/^{58}Ni$ values than those of phosphates and citrates.

Potentially significant species of Cu(II) phosphates and citrates were taken from the literature (Petit-Ramel and Khalil, 1974; Ciavatta et al., 1993). The fourfold or fivefold coordinated structures were computed. The optimized structures and the ln β values obtained are shown in Table S6 and Table 6, respectively. The dependence of ln β on temperature is shown in Fig. 12d. As in the case of $FeHPO_4(H_2O)_5^+$ (model molecule (b-3) of Fig. 11), $CuH_2(PO_4)_2(H_2O)_2^{2-}$ behaves as $CuH_4(PO_4)_2(OH)_2^{2-}$. The citrate ion (cit) is a tri-negative tridentate anion, where the three carboxylic groups of the citric acid are dissociated. Most of the citrates shown in Table 6 (cit) are coordinated to Cu^{2+} as tridentate anions, and as a pseudo-bidentate anion in the $Cu(cit)_2^{4-}$ complex. This may be due to the Jahn-Teller effect (Bersuker, 2006), which involves the distortion of the Cu site. A further dissociation of the alcoholic group of (cit) was also suggested by nuclear magnetic resonance (NMR) analysis (Tananaeva et al. (1990), in the form of $C_6H_4O_7^{4-}$ denoted as $H_{-1}(cit)$. Though a complexation of Cu^{2+} with $H_{-1}(cit)$ was reported (Petit-Ramel and Khalil, 1974), $CuH_{-1}(cit)^{2-}$ was found to be unstable and the result suggests a fragmentation of (cit). This suggests that hydroxylation of Cu^{2+} takes place before deprotonation of (cit). We therefore used $Cu(OH)^+$ and $Cu(OH)_2$ as substitutes for $CuH_{-1}(cit)^{2-}$ in the speciation diagram as a function of pH (Fig. S5). The range of $\delta^{65}Cu$ for Cu(II) phosphates, citrates, hydroxides, and hydrated Cu^{2+} ions is shown in Fig. S5 as a function of pH, where the ln β values of Cu(II) hydroxides and hydrated Cu^{2+} were taken from Fujii et al. (2013). At neutral pH, major Cu(II) species are phosphates and citrates, and a range of ~0.5‰ can be expected for $\delta^{65}Cu$. This range overlaps with observations on higher plants (Weinstein et al., 2011; Jouvin et al., 2012). A reduction of Cu^{2+} to Cu^+ by a reductase within roots has also been reported by Jouvin et al. (2012). Since the range of ln β values for Cu(I) species (Table 5) is ~2‰ smaller

than those of Cu(II) species at 298 K (Table 6), a fractionation of -0.84 to -0.11‰ between roots and nutrient solutions (Jouvin et al., 2012) may be expected.

At neutral pH, Zn(II) (Fujii and Albarède, 2012), Ni(II) (Fig. S4), and Cu(II) (Fig. S5) phosphates show higher δ values than those of citrates. The δ values of Zn(II) and Ni(II) phosphates decrease with decreasing pH and become similar to those of citrates at pH ~5. This is not the case for Cu(II): δ^{65}Cu of phosphates becomes smaller than that of citrates by as much as 0.5‰ at pH = 4 (Fig. S5). The H^+ ion released by the adenosine triphosphate (ATP) proton pump (Crichton, 2001) makes the pH of extracellular fluid lower than that of the cytosol. If the pH of extracellular area close to the plasma membrane is as low as pH = 4, Cu(II) phosphates would show smaller δ^{65}Cu compared to that of Cu (II) citrates. The Cu(II) ligand exchange may have contributed to the Cu isotope fractionation observed between roots and nutrient solutions (Jouvin et al., 2012).

3.5. Amino acids

Transition metals are found in hundreds of proteins in the human body. The proteins are involved in a large spectrum of critical biological functions, such as oxygen transport (Fe), electron shuttling (Cu), structural control and protein degradation (Zn). These functions are expressed via complexation of the metals with amino acids under various structural environments, redox and pH conditions of biological fluids. Isotopic variations in metals in organs and body fluids provide an enormous source of untapped information relevant to normal and pathological conditions. In this section, we focus on isotopic fractionation of Zn(II) and Cu(II) between amino acid complexes. Substantial patterns of Zn (Balter et al., 2013; Moynier et al., 2013a) and Cu (Balter et al., 2013) isotope fractionation are observed in some organs such as the liver and the kidney, as

well as in blood components. To a large extent, these patterns reflect the binding of Zn and Cu with different amino acids, variable redox states and electronegativity (Albarède, 2013; Balter et al., 2013; Moynier et al., 2013a).

A preliminary assessment of ln β for Zn(II)-amino acid complexes without hydrated water has been done by Moynier et al. (2013a). In the present study, we present a set of ln β values for $^{66}Zn/^{64}Zn$ in aqueous Zn(II)-amino acid complexes of cysteine (Cys), glutamine (Glu), histidine (His), methionine (Met), and threonine (Thr). Inorganic aqueous Zn(II) complexes usually show sixfold coordinations (Fujii et al., 2010, 2011b, 2012), while fourfold complexation is usual for Zn(II) in proteins (Auld, 2001, 2009). We calculated both fourfold and sixfold coordinations. Amino acids possess specific dissociable groups. For example, Cys has thiol (-SH), His has imidazole ($C_3H_4N_2$), and Glu has carboxyl (-COOH) groups. The hydroxyl group (-OH) of Thr tends to bind to the metal ion from the outer coordination sphere, but when it comes closer, it is deprotonated and binds directly to the metal ion (Grenouillet et al., 1973). These functional groups were treated to be dissociated and bind to hydrated Zn^{2+}. Met possesses a functional group of thioether (C-S-C). The S donor was treated to be coordinated to hydrated Zn^{2+}. The bonding types of amino acids to cations were reviewed by Lippard and Berg (1994).

An objective of this study is to gather information on isotope fractionation of transition metals via their bonding with amino acids in proteins. Besides the functional groups, amino groups ($-NH_2$) and carboxyl groups ($-COO^-$) in the amino acids are possible to contact with metal cations (Lippard and Berg, 1994). In our calculations, redundant contacts of these groups with Zn^{2+} were restricted by protonation to be $-NH_3^+$

553 and -COOH. The protonation sites of amino acids are referred to Dinadyalane at al.
554 (2006). All Zn^{2+}-amino acid complexes are treated as 2+ charged molecules.

555 The optimized structures of Zn^{2+}-amino acid complexes are shown in Fig. 13a and
556 13b. The ln β values at temperatures ranging from 273 to 373 K are shown in Table 8.
557 The ln β values at a typical body temperature of 310 K are shown in Fig. 14a. It has
558 been pointed out that heavy isotopes tend to bind to O-donor ligands, whereas light
559 isotopes are positively fractionated by S-donor ligands (Albarède et al., 2011; Albarède,
560 2013; Balter et al., 2013; Moynier et al., 2013a). This is clearly seen in Fig. 14a for the
561 complexes with identical coordination number. The isotope fractionation correlated with
562 N-donor ligands may be intermediate between O-donor and S-donor systems or even
563 stronger than with O-donor ligands. Besides the donor type, coordination number is
564 important, implying that fourfold complexation gives larger ln β values relative to
565 complexes with sixfold coordination. ln β of $Zn(His)^{2+}$ complexes is 0.2 to 0.6‰ larger
566 than that of $Zn(Cys)^{2+}$. This matches the observation that organs rich in proteins with
567 His residues show larger $\delta^{66}Zn$ than organs in which proteins rich in Cys residues
568 dominate (Balter et al., 2013; Moynier et al., 2013a).

569 We further computed large molecules of $Zn(His)_3(Cys)^{2+}$ and $Zn(His)_3(H_2O)^{2+}$, in
570 which the coordination number of Zn(II) is four. The values at 310 K of ln β are 3.43‰,
571 and 3.83‰, respectively ($\Delta^{66}Zn$ = 0.40‰). These complexes are core structures of
572 matrix metalloproteinases (MMPs), which are capable of degrading the extracellular
573 matrix proteins (Van Wart, 1990). The displacement of the propeptide cysteine by water
574 is induced by either proteolytic cleavage and/or conformational changes of the
575 propeptide (Auld, 2009). Such a transformation switches the role of Zn from a

576 non-catalytic to a catalytic function. The potential of $\Delta^{66}Zn$ as a probe for understanding
577 the mechanism of "cystein switch" is therefore very strong.

578 The optimized structures of Cu^{2+}-amino acid complexes are shown in Fig. 13c. The
579 ln β values at temperatures ranging from 273 to 373 K are shown in Table 9. The ln β
580 values at the body temperature of 310 K typical for mammals are shown in Fig. 14b.
581 Again, the ln β of Cu^{2+} complexes with O and N-donor amino acids is ~1‰ higher than
582 those with S-donor amino acids.

583 Glutathione (L-γ-glutamyl-L-cysteinylglycine) is the most abundant intracellular
584 non-protein thiol and an essential reducing agent of the cell. Glutathione in its reduced
585 (GSH) and oxidized (GSSG) forms is responsible for important biological functions
586 such as active transport of amino acids, enzyme activity, formation of complexes with
587 microelements, e.g., Zn(II), and the redox status of the Cu^{2+}/Cu^{+} couple (Shtyrlin et al.,
588 2005). The structure of the Zn^{2+}-GSH complex $Zn(GS)^{-}$ is tetrahedral, whereas that of
589 the Cu^{2+}-GSH complex $Cu(GS)H^{0}$ is a distorted planner (Chow et al., 1975). The
590 optimized structures are shown in Fig. 13a and 13c. The ln β values at temperatures
591 ranging from 273 to 373 K are listed in Tables 8 and 9. The ln β values at 310 K are
592 shown in Fig. 14. Zn(II) and Cu(II) are bound to O-, N-, and S- donors in GSH, and
593 hence it may be reasonable to anticipate that the ln β values of $Zn(GS)^{-}$ and $Cu(GS)H^{0}$
594 lie among those of amino acid complexes. The ln β value of $Zn(GS)^{-}$ is 0.2‰ larger
595 than that of $Zn(H_2O)_6^{2+}$. An equivalent Zn isotope fractionation is therefore expected
596 upon uptake of Zn(II) by GSH. On the other hand, the ln β value of $Cu(GS)^{0}$ is close to
597 that of $Cu(H_2O)_5^{2+}$, suggesting that Cu isotopes are not fractionated by GSH uptake of
598 Cu(II). A computational study of the Cu^{2+}/Cu^{+} redox reaction in proteins indicates that

599 the fourfold coordination of Cu(II) changes to twofold coordination of Cu(I) (Pavelka
600 and Burda, 2008). This suggests that the ln β values of twofold coordination Cu(I)
601 species shown in Table 5 may be similar to ln β of the Cu(I)-GSH complex. The ln β
602 value of $Cu(GS)^0$ is 1.2‰ larger than that of $Cu(H_2O)_2^+$ estimated by Fujii et al. (2013)
603 (Fig. 14b). Isotope fractionation of this magnitude is therefore expected for the
604 Cu^{2+}/Cu^+ pair as a result of redox glutathione activity.

605 As a final note, we also report values for Cu-lactate. The observation that, in most
606 cancer cells, glycolysis is remarkably enhanced and redirected from the citric acid cycle
607 towards lactic acid fermentation, even when oxygen is available, is known as the
608 Warburg effect (Pedersen, 2007). Because Cu(II)-lactate complexes are particularly
609 strong (Piispanen, 1995) preliminary estimates of the isotope effect resulting from Cu^{2+}
610 complexation by L-lactic acid were calculated. A fivefold coordination of
611 $CuC_3H_5O_3(H_2O)_3^+$ suggested from the structure of aquobis-lactate-copper (Prout et al.,
612 1968) was computed. The ln β is shown in Table 9. Lactate shows the largest ln β value
613 of all the studied amino acid complexes, which is a hint that positive $\delta^{65}Cu$ should be
614 found in the cytosol of cancer cells. This is an additional and particularly strong
615 indication that stable isotope fractionation of the first transition series elements in
616 biology should be useful biomarkers that would help understand the detailed
617 mechanisms of some biological processes.

618

619 **Conclusions**

620 The ln β values calculated for the inorganic species of Fe, Ni, Cu, and Zn are helpful for
621 understanding the isotopic variations found in surface seawater, the deep sea, and
622 hydrothermal systems. The isotope fractionation of Fe, Ni, Cu, and Zn found in higher

623 plants is understandable via isotopic exchange reactions between phosphates and
624 citrates. The ln β values calculated for Zn-amino acid complexes provide insights into a
625 range of isotopic variations observed for organs and body fluids of mammals.
626
627 ACKNOWLEDGMENTS
628 We thank three anonymous reviewers, Merlin Méheut, and Associate Editor
629 Jean-François Boily for their useful suggestions and constructive comments on the
630 manuscript. FM acknowledges the financial support of the ANR via a Chaire
631 d'Excellence IDEX Sorbonne Paris Cité IDEX13C44 and the UnivEarthS Labex
632 program at Sorbonne Paris Cité (ANR-10-LABX-0023 and ANR-11-IDEX-0005-02),
633 and FA and JBT acknowledge support from the Lyon Institute of Origins of the Labex
634 Program.
635

636 *APPENDIX A*

637 The isotope fractionation factor of an element M, δM for an isotope pair of light isotope
638 A' and heavy isotope A, was estimated as follows. As an example, we consider a system
639 containing three chemical species X, Y, and Z.

640 Distribution of chemical species X, Y, and Z as functions of pH is calculated from
641 reported stability constants. The mole fractions of χ_X, χ_Y, and χ_Z ($\Sigma\chi = 1$) calculated are
642 set as those of isotopologues including the isotope A'. An ambient molar (mol dm^{-3}) or
643 molal (mol kg^{-1}) concentration of [M] is then set. The total concentration of A' is $[M]R_{A'}$
644 for the isotopic abundance $R_{A'}$ of A' in the whole system. The naturally occurring
645 isotopic abundance is set to be $R_{A'}$.

646 The isotopic mass balance is kept at every pH.

$$[M]R_{A'} = [M]R_{A'}\chi_X + [M]R_{A'}\chi_Y + [M]R_{A'}\chi_Z \quad \text{(a-1)}$$

647 The isotope fractionation between the species X and Y is (if ln β is given in ‰ unit, use
648 10^{-3} ln β here),

$$\ln \beta_Y - \ln \beta_X = \frac{([A]/[A'])_Y}{([A]/[A'])_X} - 1 \quad \text{(a-2)}$$

649 and hence,

$$[A]_Y = (\ln \beta_Y - \ln \beta_X + 1)\frac{[A']_Y}{[A']_X}[A]_X \quad \text{(a-3)}$$

$$= (\ln \beta_Y - \ln \beta_X + 1)\frac{\chi_Y}{\chi_X}[A]_X$$

650 Similarly, for the isotope fractionation between the species X and Z

$$[A]_Z = (\ln \beta_Z - \ln \beta_X + 1)\frac{\chi_Z}{\chi_X}[A]_X \quad \text{(a-4)}$$

651 The isotopic mass balance of A is,

$$[\mathrm{M}]R_{\mathrm{A}} = [\mathrm{A}]_{\mathrm{X}} + [\mathrm{A}]_{\mathrm{Y}} + [\mathrm{A}]_{\mathrm{Z}} \tag{a-4}$$

$$= \left(\frac{1 + \chi_Y \ln\beta_Y + \chi_Z \ln\beta_Z - (\chi_Y + \chi_Z)\ln\beta_X}{\chi_X} \right) [\mathrm{A}]_{\mathrm{X}}$$

652 The concentrations of A of species X, Y, and Z can thus be calculated. The isotope
653 fractionation in the species X is

$$\delta \mathrm{M_X}\ (‰) = \left(\frac{[A]_X / [A']_X}{([M]R_A)/([M]R_{A'})} - 1 \right) \times 1000 \tag{a-5}$$

$$= \left(\frac{\chi_X}{1 + \chi_Y \ln\beta_Y + \chi_Z \ln\beta_Z - (\chi_Y + \chi_Z)\ln\beta_X} \times \frac{1}{\chi_X} - 1 \right) \times 1000$$

$$= \frac{(\chi_Y + \chi_Z)\ln\beta_X - \chi_Y \ln\beta_Y - \chi_Z \ln\beta_Z}{1 + [\chi_Y \ln\beta_Y + \chi_Z \ln\beta_Z - (\chi_Y + \chi_Z)\ln\beta_X]} \times 1000$$

654 Similarly, $\delta \mathrm{M_Y}$ and $\delta \mathrm{M_Z}$ can be calculated. Since we treat small ln β values, in practice,
655 the number of atoms in unit volume (or weight) is more useful than using molar (or
656 molal) concentration.
657

APPENDIX B

Software B3LYP with a basis set 6-311+G(d,p) is a standard DFT method for computing aqueous species of Ni(II), Cu(II), and Zn(II). Using the code with 6-311+G(d,p) basis set or higher is recommended for estimating the accurate electronic structures (de Bruin et al., 1999; Rulíšek and Havlas, 1999). Here, we discuss the accuracy of ln β values reported in this work.

Calculating how physicochemical properties vary with hydration of the species is a common strategy for examining the accuracy of theoretical calculations of aqueous species (Fujii et al., 2010, 2011a,b). In the theoretical study on the hydration enthalpy of Fe^{2+} and Fe^{3+}, Li et al. (1996) tested a small cluster model of 6 H_2O molecules as the first coordination sphere and a large cluster model of 12 additional H_2O molecules as the second coordination sphere. For Fe^{3+}, the large cluster model brought the calculated data closer to the experimental results. For Fe^{2+}, both the small and the large cluster modes reproduced the experimental results. Similarly, the hydration enthalpies of Ni^{2+} and Zn^{2+} were appropriately reproduced by using both the small and the large cluster models (Fujii et al, 2010, 2011a).

In a pioneering computational study on hydrated Mg^{2+} (Pye and Rudolph, 1998), vibrational frequencies were well reproduced when using the large cluster of $Mg(H_2O)_{18}^{2+}$, while they were underestimated by 8-10% when the small cluster $Mg(H_2O)_6^{2+}$ was used. A similar phenomenon was confirmed for Ni^{2+} and Zn^{2+}, though the hydration enthalpies were well predicted (Fujii et al, 2010, 2011a,b). The calculation results are shown in Table B1. The totally symmetric stretching mode ν_1 of hexaaqua complexes is the fundamental intramolecular vibration mode, and the ν_1 frequency is also shown in this table. The calculated ν_1 frequencies of $Ni(H_2O)_6^{2+}$ and $Zn(H_2O)_6^{2+}$

682 are smaller than the literature values determined by Raman spectrometry. Setting 12
683 H_2O molecules at the second coordination sphere brought the calculation results closer
684 to the literature values. Adding the second hydration sphere increased ln β (298 K) by
685 +0.6‰ for Ni and +0.3‰ for Zn.

686 Continuum solvation models are known to be useful to simulate the
687 physicochemical properties of aqueous complexes (Ginovska et al., 2008). The
688 conductor-like polarizable continuum model (CPCM) of solvation was tested for
689 hydrated ions of Fe, Ni, Cu, and Zn (Table B1). For divalent and trivalent cations, the
690 use of CPCM still increases ν_1 frequency, but the effect is smaller than that of a second
691 coordination sphere. The CPCM assumption changed ln β (298 K) by less than 0.3‰.

692 The accuracy of computed ln β values for hydrated Fe^{2+} and Fe^{3+} has been
693 extensively discussed in the literature (Rustad et al., 2010; Saunier et al., 2011, and
694 references therein). It was pointed out that ln β may have been overestimated by some
695 computational studies. Rustad et al. (2010) argues that the absolute values of ln β for
696 hydrated Fe^{2+} and Fe^{3+} are well reproduced by using large $Fe(H_2O)_{18}^{2+}$ clusters with a
697 conductor-like screening model (COSMO) of solvation. Our results for ln β with a small
698 cluster is ~0.4‰ (298 K), which is larger than Rustad et al.'s (2010) results for both
699 Fe^{2+} and Fe^{3+}.

700 Isotope fractionation of $^{56}Fe/^{54}Fe$ between hydrated Fe^{3+} and Fe^{2+}, with $\Delta^{56}Fe$ =
701 $\delta^{56}Fe(Fe^{3+}) - \delta^{56}Fe(Fe^{2+})$, has been experimentally determined at 295 K (Johnson et al.,
702 2002; Welch et al., 2003). It is a standard result that $\Delta^{56}Fe$ can be approximated by the
703 difference of ln β ($^{56}Fe/^{54}Fe$) between hydrated Fe^{3+} and Fe^{2+}. At present, two
704 theoretical estimates of ln β (Ottonello and Zuccolini, 2009; Rustad et al., 2010) show

values consistent with the experimental results (Johnson et al., 2002; Welch et al., 2003) (Table B2). We computed $Fe(H_2O)_6^{2+}$ and $Fe(H_2O)_6^{3+}$ using B3LYP/6-311G with various diffuse and polarization functions. A CPCM calculation including water solvation was also tested. The results are shown in Fig. S6 of the electronic supplement. It is clear that the higher basis set as 6-311+G(d,p) (see Table B2) is required for computing the ln β values of aqueous species of iron. The use of CPCM decreased both ln β and $\Delta^{56}Fe$. The small cluster model has been shown to produce results systematically ~0.4‰ heavier than large clusters (Rustad et al., 2010) (see above). Nevertheless, the calculated $\Delta^{56}Fe$ value reproduces the experimental result of Welch et al. (2003). When the small cluster model is suspected to fail, it has been suggested to scale frequencies empirically for the effect of the second solvation sphere (Pye and Rudolph, 1998). Since we showed that the accuracy of the small cluster model to reproduce relative isotope fractionation is adequate (e.g., $\Delta^{56}Fe$, see Fig. S6 and Table B2), scaling factors were not used.

Treatment of the second coordination sphere in computational studies turns out to be more difficult when the H_2O molecules at the first coordination sphere are substituted by ligands. The large cluster model needs experimental evidence of molecular arrangement in the second coordination sphere, but experiments are fraught with technical difficulties. For the ligand-exchanged complexes, the solvation models of pure water may not be adequate. For example, chloro-complexes exist in chloride solutions, for which the solvent is not identical with pure water. Difficulties of the solvation models are discussed in Ginovska et al. (2008).

We conclude that the absolute values of ln β estimated with the large cluster model are more accurate than estimates based on the small cluster model. Introducing the

729 solvation model may improve accuracy of ln β, but its effect as shown in Table B1 is
730 probably not significant, and the scale of relative isotope fractionation still stands.
731 Although the absolute value of ln β estimated with the small cluster model may be
732 improved by addition of a second and more distant coordination spheres, the Δ values
733 estimated from Table B2 are reliable and the isotope fractionation scale presented in this
734 work can be used for predicting isotope fractionation among species in solution.
735

736 **REFERENCES**

737 Albarède F. (2004) The stable isotope geochemistry of copper and zinc. *Rev. Mineral.*
738 *Geochem*. **55**, 409-427.

739 Albarède F., Telouk P., Lamboux A., Jaouen K. and Balter V. (2011a) Isotopic evidence
740 of unaccounted for Fe and Cu erythropoietic pathways. *Metallomics* **3**, 926-933.

741 Albarède F. (2013) Isotope of desease. *Mineral. Mag*. **77**, 568-568.

742 Al-Farawati R. and van den Berg C. M. G. (1999) Metal-sulfide complexation in
743 seawater. *Mar. Chem*. **63**, 331–352.

744 Allred A. L. (1961) Electronegativity values from thermochemical data. *J. Inorg. Nucl.*
745 *Chem*. **17**, 215-221.

746 Applegarth L. M. S. G. A., Corbeil C. R., Mercer D. J. W, Pye C. C., Tremaine P. R.
747 (2014) Raman and ab initio investigation of aqueous Cu(I) chloride complexes from
748 25 to 80C°. *J Phys. Chem. B* **118**, 204-214.

749 Auld D. S. (2001) Zinc coordination sphere in biochemical zinx sites. *BioMetals* **14**,
750 271-313.

751 Auld D. S. (2009) The ions and outs of biolozical zinc sites. *BioMetals* **22**, 141-148.

752 Beard B. L., Johnson C. M (2004) Fe isotope variation in the modern and ancient earth
753 and other planetary bodies. *Rev. Mineral. Geochem*. **55**,

754 Baes, Jr., C. F. and Mesmer R. E. (1976) *The hydrolysis of cations*. John Wiley & Sons,
755 New York.

756 Balter V., Lamboux A., Zazzo A., Telouk P, Leverrier Y., Marvel J., Moloney A. P.,
757 Monahan F. J., Schmidte O., Albarède A. (2013) Contrasting Cu, Fe, and Zn isotopic
758 patterns in organs and body fluids of mice and sheep, with emphasis on cellular
759 fractionation, *Metallomics*, **5**, 1470-1482.

760 Bersuker I. B. (1996) *Electronic Structure and Properties of Transition Metal*
761 *Compounds*. John Wiley & Sons, New York.
762 Bersuker I. B. (2006) *The Jahn-Teller effect*; Cambridge Univ. Press, New York.
763 Bickley R. I., Edwards H. G. M., Knowles A., Gustar R. E., Mihara D. and Rose S. J.
764 (1993) Vibrational spectroscopic study of nickel(II) malonate,
765 $Ni(COO•CH_2•COO)•2H_2O$ and its aqueous solution. *J. Mol. Struct*. **296**, 21-28.
766 Bigeleisen J. and Mayer M. G. (1947) Calculation of equilibrium constants for isotopic
767 exchange reactions. *J. Chem. Phys*. **15**, 261-267.
768 Bigeleisen J., Wolfsberg M (1958) Theoretical and experimental aspects of isotope
769 effects in chemical kinetics. *Adv. Chem. Phys*. **1**, 15-76.
770 Bigeleisen J. (1996) Nuclear size and shape effects in chemical reactions. isotope
771 chemistry of the heavy elements. *J. Am. Chem. Soc*. **118**, 3676-3680.
772 Bratsch S. G. (1985) A group electronegativity method with Pauling units. *J. Chem.*
773 *Edu*. **62**, 101-103.
774 Byrne R. H. and Kester D. R. (1976) Solubility of hydrous ferric oxide and iron
775 speciation in seawater. *Marine Chem*. **4**, 255-274.
776 Canfield D. E. (1998) A new model for Proterozoic ocean chemistry. *Nature* **396**,
777 450-453.
778 Castro P. M., Jagodzinski P. W. (1991) FTIR and Raman spectra and structure of
779 Cu(NO3)+ in aqueous solution and acetone. *Spectrochim. Acta* **47A**, 1707-1720.
780 Chow S. T., McAuliffe C. A., Sayle B. J. (1975) Metal complexes of amino acids and
781 derivatives - IX. *J. Inorg. Nucl. Chem*. **37**, 451-454.
782 Ciavatta L., Iuliano M., Porto R (1992) Complex formation equilibria in aqueous
783 iron(II) orthophosphate solutions. *Annal. Chim*. **82**, 121-135.

784 Ciavatta L., Iuliano M., Porto R (1993) Complex formation equilibria in copper(II)
785 orthophosphate solutions. *Annal. Chim*. **83**, 19-38.
786 Ciavatta L., Iuliano M. (1995) On the formation of mononuclear
787 iron(III)-orthophosphate complexes. *Annal. Chim*. **85**, 235-255.
788 Cowan J.A. (1997) *Inorganic Biochemistry*, Wiley-VCH, New York.
789 Crichton R. (2001) *Inorganic Biochemistry of Iron Metabolism*, John Wiley & Sons,
790 Chichester.
791 Davis A. R. and Chong C. (1972) A laser Raman study of aqueous copper nitrate
792 solutions. *Inorg. Chem*. **11**, 1891-1895.
793 Davison W., Phillips N., Tabner B. J. (1999) Soluble ion sulfide species in natural
794 waters: Reappraisal of their stoichiometry and stability constants. *Aquat. Sci*. **61**,
795 23-43.
796 de Bruin T. J. M., Marcelis A. T. M., Zuilhof H. and Sudhölter E. J. R. (1999)
797 Geometry and electronic structure of bis-(glycinato)-CuII•2H_2O complexes as studied
798 by density functional B3LYP computations. *Phys. Chem. Chem. Phys.* **1**, 4157-4163.
799 Dekov V. M., Rouxel O., Asael D., Hålenius U., Munnik F. (2013) Native Cu from the
800 oceanic crust: Isotopic insights into native metal origin. *Chem. Geol*. **359**, 136-149.
801 Dennington R., Keith T. and Millam J. (2009) *GaussView, Version 5.0.8*. Semichem
802 Inc., Shawnee Mission KS.
803 Dinadayalane T. C., Sastry G. N., Leszczynski J (2006) Comprehensive theoretical
804 study towards the accurate proton affinity values of naturally occurring
805 amino acids. *Int. J. Quantum Chem*. **106**, 2920-2933.
806 Dyrssen D (1988) Sulfide complexation in surface seawater. *Mar. Chem*. **24**, 143-153.

807 Edmond J. M., Measures C., Mangum B., Grant B., Sclater F. R., Collier R., Hudson A.,
808 Gordon L. I. and Corliss J. B. (1979) On the formation of metal-rich deposits at ridge
809 crests. *Earth Planet. Sci. Lett*. **46**, 19-30.
810 Edwards H. G. M. and Knowles A. (1992) Vibrational spectroscopic study of nickel (II)
811 formate, $Ni(HCO_2)_2$, and its aqueous solution. *J. Mol. Struct*. **268**, 13-22.
812 Estrade N., Cloquet C., Deng T., Echevarria G., Sterchеman T., Morel J. L. (2013)
813 Nickel isotope fractionation in the soil to hyper-accumulating plant system. *Mineral.*
814 *Mag.* **77**, 1052-1052.
815 Frisch M. J., Trucks G. W., Schlegel H. B., Scuseria G. E., Robb M. A., Cheeseman J.
816 R., Scalmani G., Barone V., Mennucci B., Petersson G. A., Nakatsuji H., Caricato M.,
817 Li X., Hratchian H. P., Izmaylov A. F., Bloino J., Zheng G., Sonnenberg J. L., Hada
818 M., Ehara M., Toyota K., Fukuda R., Hasegawa J., Ishida M., Nakajima T., Honda Y.,
819 Kitao O., Nakai H., Vreven T., Montgomery Jr. J. A., Peralta J. E., Ogliaro F.,
820 Bearpark M., Heyd J. J., Brothers E., Kudin K. N., Staroverov V. N., Kobayashi R.,
821 Normand J., Raghavachari K., Rendell A., Burant J. C., Iyengar S. S., Tomasi J.,
822 Cossi M., Rega N., Millam N. J., Klene M., Knox J. E., Cross J. B., Bakken V.,
823 Adamo C., Jaramillo J., Gomperts R., Stratmann R. E., Yazyev O., Austin A. J.,
824 Cammi R., Pomelli C., Ochterski J. W., Martin R. L., Morokuma K., Zakrzewski V.
825 G., Voth G. A., Salvador P., Dannenberg J. J., Dapprich S., Daniels A. D., Farkas Ö.,
826 Foresman J. B., Ortiz J. V., Cioslowski J. and Fox D. J. (2009) *Gaussian 09, Revision*
827 *B.01*, Gaussian, Inc., Wallingford CT.
828 Fujii, T., Moynier, F., Telouk, P. and Albarède, F. (2006) Isotope fractionation of
829 iron(III) in chemical exchange reactions using solvent extraction with crown ether. *J.*
830 *Phys. Chem., A* **110**, 11108–11112.

831 Fujii T., Moynier F., Telouk P. and Abe, M. (2010) Experimental and theoretical
832 investigation of isotope fractionation of zinc between aqua, chloro, and macrocyclic
833 complexes. *J. Phys. Chem. A* **114**, 2543-2552.
834 Fujii T., Moynier F., Dauphas N. and Abe M. (2011a) Theoretical and experimental
835 investigation of nickel isotopic fractionation in species relevant to modern and
836 ancient oceans. *Geochim. Cosmochim. Acta* **75**, 469-482.
837 Fujii T., Moynier F. Pons M. L. and Albarède F (2011b) The origin of Zn isotope
838 fractionation in sulfides. *Geochim. Cosmochim Acta* **75**, 7632-7643.
839 Fujii T. and Albarède F. (2012) Ab initio calculation of the Zn isotope effect in
840 phosphates, citrates, and malates and applications to plants and soil. *PLoS ONE* **7**,
841 e30726.
842 Fujii T., Moynier F., Abe. M., Nemoto K., and Albarède F. (2013) Copper isotope
843 fractionation between aqueous compounds relevant to low temperature geochemistry
844 and biology. *Geochim. Cosmochim. Acta* **110**, 29-44.
845 Gall L., Williams H. M., Siebert C., Halliday A. N., Herrington R. J., Hein J. R. (2013)
846 Nickel isotopic compositions of ferromanganese crusts and the constancy of deep
847 ocean inputs and continental weathering effects over the Cenozoic. *Earth Planet. Sci.*
848 *Lett.* **375**, 148-155.
849 Ginovska B., Camaioni D. M., Dupuis M., Schwerdtfeger C. A., Gil Q. (2008)
850 Charge-dependent cavity radii for an accurate dielectric continuum model of
851 solvation with emphasis on ions: aqueous solutes with oxo, hydroxo, amino, methyl,
852 chloro, bromo, and fluoro functionalities. *J. Phys. Chem. A* **112**, 10604-10613.

853 Grenouillet P., Martin R. P., Rossi A., Ptak M. (1973) Interactions between copper(II)
854 ions and L-threonine, L-allo-threonine, and L-serine in aqueous solution. *Biochem.*
855 *Biophys Acta* **322**, 185-194.
856 Guelke, M., von Blanckenburg, F. (2007) Fractionation of stable iron isotopes in higher
857 plants. *Environ. Sci. Technol*. **41**, 1896-1901.
858 Hedwig G. R., Liddle J. R., Reeves R. D. (1980) Complex formation of nickel(II) ions
859 with citric acid in aqueous solution: a potentiometric and spectroscopic study. *Aust. J.*
860 *Chem*. **33**, 1685-1693.
861 Hester R. E., Planes R. A. (1964) Solvation of metal ions in aqueous solutions : the
862 metal-oxygen bond. *Inorg. Chem*. **3**, 768-769.
863 Hill P. S and Schauble E. A. (2008) Modeling the effects of bond environment on
864 equilibrium iron isotope fractionation in ferric aquo-chloro complexes. *Geochim.*
865 *Cosmochim. Acta* **72**, 1939-1958.
866 Hill P. S., Schauble E. A. and Young E. D. (2010) Effects of changing solution
867 chemistry on Fe^{3+}/Fe^{2+} isotope fractionation in aqueous Fe-Cl solutions. *Geochim.*
868 *Cosmochim. Acta* **74**, 6669-6689.
869 Hill P. S., Tripati A. K., Schauble E. A. (2014) Theoretical constraints on the effects of
870 pH, salinity, and temperature on clumped isotope signatures of dissolved inorganic
871 carbon species and precipitating carbonate minerals. *Geochim. Cosmochim. Acta* **125**,
872 610-652
873 Huheey J. E. (1965) The electronegativity of groups. *J. Phys. Chem*. **69**, 3284-3291.
874 Huheey J. E. (1966) The electronegativity of multiply bonded groups. *J. Phys. Chem*. **70**,
875 2086-2092.

876 Irigoras A., Michelini M. D., Sicilia E., Russo N., Mercero J. M., Ugalde J.M., The
877 electronic states of Fe_2^+. *Chem. Phys. Lett.*, **376**, 310-317.
878 Irish D. E., McCarroll B. and Young T. F. (1963) Raman study of zinc chloride
879 solutions. *J. Chem. Phys*. **39**, 3436–3444.
880 Johnson C. M., Skulan, J. L., Beard B. L. Sun H., Nealson K. H. Braterman P. S. (2002)
881 Isotopic fractionation between Fe(III) and Fe(II) in aqueous solutions. *Earth Planet*
882 *Sci. Lett*. **195**, 141-153.
883 Johnson C. M., Beard B. L., Albarède F. (2004) Overview and general concepts. *Rev.*
884 *Mineral. Geochem*. **55**, 1-24.
885 Johnson C. M., Beard B. L., Roden E. E., Newman D. K., Nealson K. H. (2004)
886 Isotopic constrains on biogeochemical cycling of Fe. *Rev. Mineral. Geochem*. **55**,
887 359-408.
888 Jolivet J. -P., Chanéac C., Tronc E (2004) Iron oxide chemistry. From molecular cluster
889 to extended solid networks. *Chem. Commun*. **5**, 481-487.
890 Jouvin, D., Weiss, D., Mason, T., Bravin, M., Louvat, P., Zhao, F., Ferec, F., Hinsinger,
891 P., Benedetti, M. (2012) Stable isotopes of Cu and Zn in higher plants: evidence for
892 Cu reduction at the root surface and two conceptual models for isotopic fractionation
893 processes. *Environ. Sci. Technol*. **46**, 2652-2660.
894 Kanno H. (1987) Correlation of the Raman ν_1 bands of aquated divalent metal ions with
895 the cation-hydrated water distance. *J. Raman Spectrosc*. **18**, 301-304.
896 Kanno H. (1988) Hydrations of metal ions in aqueous electrolyte solutions: a Raman
897 study. *J. Phys. Chem*. **92**, 4232-4236.

898 Kanno H, Hiraishi J. (1982) A Raman study of aqueous solutions of ferric nitrate,
899 Ferrous chloride and ferric chloride in the glassy state. *J. Raman Spectrosc*. **12**,
900 224-227.
901 Kiczka, M., Wiederhold, J.G., Kraemer, S.M., Bourdon, B., Kretzschmar, R. (2010)
902 Iron isotope fractionation during Fe uptake and translocation in alpine plants. *Environ.*
903 *Sci. Technol*. **44**, 6144-6150.
904 Königsberger L. C., Königsberger E.,May P. M., Hefter G. T. (2000) Complexation of
905 iron(III) and iron(II) by citrate. Implications for iron speciation in blood plasma. *J.*
906 *Inorg. Biochem*. **78**, 175-184.
907 Kononets M. Yu., Pakhomova S. V., Rozanov A. G. and Proskurnin M. A. (2002)
908 Determination of Soluble Iron Species in Seawater Using Ferrozine. *J. Anal. Chem*.,
909 **57**, 586-589.
910 Li, J., Fisher, C. L., Chen, J. L., Bashford, D. and Noodleman, L. (1996) Calculation of
911 redox potentials and pKa values of hydrated transition metal cations by a combined
912 density functional and continuum dielectric theory. *Inorg. Chem*. **35**, 4694-4702.
913 Lippard S. J. and Berg J. M. (1994) *Principles of Bioinorganic Chemistry*, University
914 Science Books, Mill Valley.
915 Luther, III, G. W., Rickard D. T., Theberg S, Olroyd A (1996) Determination of metal
916 (bi)sulfide stability constants of Mn^{2+}, Fe^{2+}, Co^{2+}, Ni^{2+}, Cu^{2+}, and Zn^{2+} by
917 voltammetric methods. *Environ. Sci. Technol*. **30**, 671-679.
918 Macleod, G., Mcneown, C., Hall, A. J., Russel, M. J. (1994) Hydrothermal and oceanic
919 pH conditions of possible relevance to the origin of life. *Origin Life Evol. Biosphere*
920 **24**, 19-41.

921 Maeda M., Ito T., Hori M. and Johansson G. (1995) The structure of zinc chloride
922 complexes in aqueous solution. *Z. Naturforsch*. **51a**, 63-70.
923 Magini M., ed. (1988) *X-Ray Diffraction of Ions in Aqueous Solutions: Hydration and*
924 *Complexation Formation*. CRC Press, Boca Raton.
925 Mei, Y., Sherman D. M., Liu W., Brugger J (2013) Ab initio molecular dynamics
926 simulation and free energy exploration of copper(I) complexation by chloride and
927 bisulfide in hydrothermal fluids, *Geochim. Cosmochim. Acta* **102**, 45-64.
928 Mink J., Németh Cs., Hajba L., Sandström M. and Goggin P. L. (2003) Infrared and
929 Raman spectroscopic and theoretical studies of hexaaqua metal ions in aqueous
930 solution. *J. Mol. Struct*. **661-662**, 141-151.
931 Mottl M. J., Wheat C. G., Fryer P., Gharib J. and Martin J. B. (2004) Chemistry of
932 springs across the Mariana forearc shows progressive devolatilization of the
933 subducting plate. *Geochim. Cosmochim. Acta* **68**, 4915-4933.
934 Moynier F, Pichat S., Pons M. L., Fike D., Balter V., Albarede F. (2009) Isotopic
935 fractionation and transport mechanisms of Zn in plants. *Chem. Geol*. **267**, 125-130.
936 Moynier F., Fujii T., Shaw A. S., Le Borgne M. (2013a) Heterogeneous distribution of
937 natural zinc isotopes in mice, Metallomics, 5, 693–699.
938 Moynier, F., Fujii, T., Wang, K., Foriel, J. (2013b) Ab initio calculations of the Fe(II)
939 and Fe(III) isotopic effects in citrates, nicotianamine, and phytosiderophore, and new
940 Fe isotopic measurements in higher plants. *Compt. Rend. Geosci.*, **345**, 230-240.
941 Mullay J. (1985) Calculation of group electronegativity. *J. Am. Chem. Soc.* **107**,
942 7271-7275.
943 Nomura M., Higuchi N. and Fujii Y. (1996) Mass dependence of uranium isotope
944 effects in the U(IV)-U(VI) exchange reaction. *J. Am. Chem. Soc*. **118**, 9127-9130.

945 Ottonello G. and Zuccolini M. V. (2009) Ab-initio structure, energy and stable Fe
946 isotope equilibrium fractionation of some geochemically relevant H-O-Fe complexes.
947 *Geochim. Cosmochim. Acta* **73**, 6447-6469.
948 Pauling L. (1960) *The nature of the chemical bond*. Cornell University Press, New
949 York.
950 Pavelka M., Burda J. V. (2008) Computational study of redox active centres of blue
951 copper proteins: a computational DFT study. *Mol. Phys*. **106**, 2733-2748.
952 Pearson R. G. (1968) Hard and soft acids and bases, HSAB, part I. Fundamental
953 principles. *J. Chem. Edu*. **45**, 581-587.
954 Pearson R. G. (1968) Hard and soft acids and bases, HSAB, part II. Underlying theories.
955 *J. Chem. Edu*. **45**, 643-648.
956 Pedersen P. L. (2007) Warburg, me and Hexokinase 2: Multiple discoveries of key
957 molecular events underlying one of cancers' most common phenotypes, the
958 "Warburg Effect", i.e., elevated glycolysis in the presence of oxygen. *J. Bioenerg.*
959 *Biomembr*. **39**, 211-222.
960 Petit-Ramel M. M., Khalil I. (1974) Étude des complex mixtes bimétalliques. I.
961 Détermination des constantes de stabilité de l'acide citrique et des citrates de cuibvre.
962 *Bull. Soc. Chim. Fr.* 1255-1258.
963 Piispanen J. Lajunen H. J. (1995) Complex formation equilibria of some aliphatic
964 α-hydroxycarboxylic acids. 2. The study of copper(II) complex. *Acta Chem. Scand*.
965 **49**, 241-247.
966 Pourbaix, M. (1974) *Atlas of electrochemical equilibria in aqueous solutions.* NACE,
967 Houston.

968 Prout C. K., Armstrong R. A., Carruthers J. R., Forrest J. G., Murray-Rust P, Rossotti F.
969 J. C. (1968) Structure and stability of carboxylate complexes. Part 1. The crystal and
970 molecular structures of copper(II) glycollate, DL-lactate, 2-hydroxy-2-methyl
971 propionate, methoxyacetate, and phenoxyacetate. *J. Chem. Soc. A* **11**, 2791-2813.
972 Pye C. C. Rudolph W. W. (1998) An ab initio and Raman investigation of
973 magnesium(II) hydration. *J. Phys. Chem*. **102**, 9933-9943.
974 Rickard D. and Luther, III, G. W. (2006) Metal sulfide complexes and clusters. *Rev.*
975 *Mineral. Geochem*. **61**, 421–504.
976 Rickard D. and Luther, III, G. W. (2007) Chemistry of iron sulfides. *Chem. Rev*. **107**,
977 514-562.
978 Rudolph W. W. and Pye C. C. (1999) Zinc(II) hydration in aqueous solution. A Raman
979 spectroscopic investigation and an ab-initio molecular orbital study. *Phys. Chem.*
980 *Chem. Phys*. **1**, 4583-4593.
981 Rulíšek, L. and Havlas, Z. (1999) Ab initio calculations of monosubstituted (CH_3OH,
982 CH_3SH, NH_3) hydrated ions of Zn^{2+} and Ni^{2+}. *J. Phys. Chem. A* **103**, 1634-1639.
983 Rustad J. R., Casey W. H., Yin Q. Z., Bylaska E. J., Felmy A. R., Bogatko S. A.,
984 Jackson V. E. and Dixon D. A. (2010) Isotopic fractionation of Mg^{2+}(aq), Ca^{2+}(aq),
985 and Fe^{2+}(aq) with carbonate minerals. *Geochim. Cosmochim. Acta* **74**, 6301-6323.
986 Sherman D. M. (2013) Equilibrium isotopic fractionation of copper during
987 oxidation/reduction, aqueous complexation and ore-forming processes: Predictions
988 from hybrid density functional theory. *Geochim. Cosmochim. Acta*, **118**, 85-97.
989 Saunier G, Pokrovski G. S., Poitrasson F. (2011) First experimental determination of
990 iron isotope fractionation between hematite and aqueous solution at hydrothermal
991 conditions. *Geochim. Cosmochim. Acta* **75**, 6629-6654.

992 Sharma S. K. (1973) Raman study of ferric perchlorate and nitrate in acidic solutions. *J.*
993 *Inorg. Nucl. Chem*. **35**, 3831-3836.
994 Shtyrlin V. G., Zyavkina Y. I., Ilakin V. S., Garipov R. R., Zakharov A. V. (2005)
995 Structure, stability, and ligand exchange of copper(II) complexes with oxidized
996 glutathione. *J. Inorg. Biochem*. **99**, 1335-1346.
997 Tananaeva N. N., Trunova E. K., Kostromina N. A., Shevchenko Yu. B. (1990) ^{13}C
998 NMR study of the dissociation of tartaric and citric acids. *Teor. Éksper. Khim*., **26**,
999 706-710
1000 Taylor R. S., Diebler H. (1976) Kinetic and equilibrium studies of the binding of
1001 nickel(II) to 5'-adenosine monophosphate and related compounds. *Bioinorg. Chem*. **6**,
1002 247-264.
1003 Turner D. R., Whitfield M. and Dickson A. G. (1981) The equilibrium speciation of
1004 dissolved components in freshwater and sea water at 25°C and 1 atm pressure.
1005 *Geochim. Cosmochim. Acta* **45**, 855–881.
1006 Urey H. C. (1947) The thermodynamic properties of isotopic substances. *J. Chem. Soc.*
1007 562-581.
1008 Van Wart H. E., Birledal-Hansen H. (1990) The cysteine switch: A principle of
1009 regulation of metalloproteinase activity with potential applicability to the entire
1010 matrix metalloproteinase gene family. *Proc. Natl. Acad. Sci. USA* **87**, 5578-5582.
1011 Weinstein, C., Moynier, F., Wang, K., Paniello, R., Foriel, J., Catalano, J., Foriel, J.
1012 (2011) Cu isotopic fractionation in plants. *Chem. Geol*. **286**, 266-271.
1013 Weiss, D.J., Mason, T.F.D., Zhao, F.J., Kirk, G.J.D., Coles, B.J., Horstwood, M.S.A.
1014 (2005) Isotopic discrimination of zinc in higher plants. *New Phytol*. **165**, 703-710.

1015 Welch S. A., Beard B. L., Johnson C. M., Braterman P. S. (2003) Kinetic enad
1016 equilibrium Fe isotope fractionation between Fe(II) and Fe(III). *Geochim.*
1017 *Cosmochim Acta* **67**, 4231-4250.
1018 Wu L., Druschel G., Findlay A., Beard B. L. and Johnson C. M. (2012) Experimental
1019 determination of iron isotope fractionations among Fe_{aq}^{2+}–FeS_{aq}–Mackinawite at low
1020 temperatures: Implications for the rock record. *Geochim. Cosmochim. Acta* **89**, 46-61.
1021 Yamaguchi T., Hayashi S. and Ohtaki H. (1989) X-ray diffraction and raman studies of
1022 zinc(II) chloride hydrate melts, $ZnCl{\bullet}RH_2O$ (R = 1.8, 2.5, 3.0, 4.0, and 6.2). *J. Phys.*
1023 *Chem*. **93**, 2620-2625.
1024 Zeebe R. E. and Wolf-Gladrow D. (2001) *CO_2 in Seawater: Equilibrium, Kinetics,*
1025 *Isotopes*, Elsevier, Amsterdam.
1026 Zhang J. -Z., Millero F. J. (1994) Investigation of metal sulfide complexes in sea water
1027 using cathodic stripping square wave voltammetry. *Anal. Chim. Acta* **284**, 497-504.
1028 Zigan F, Rothbauer R (1967) Neutronenbeugungsmessungen am Brucit. *N. Jb. Mineral.*
1029 *Monatsh. Abh.* 137-143
1030 Zirino A. and Yamamoto S (1972) A pH-dependent model for the chemical speciation
1031 of copper zinc cadmium, and lead in seawater. *Limnol. Oceanogr*. **17**, 661-671.
1032
1033
1034

Table 1 Logarithm of the reduced partition function, ln β (‰), for the pair ^{66}Zn-^{64}Zn of Zn(II) complexes.

Species	Temperature (K)					
	273	298	323	373	473	573
$Zn(H_2O)_6^{2+}$	3.854	3.263	2.797	2.119	1.334	0.915
$ZnCl(H_2O)_5^{+}$	3.702	3.136	2.689	2.039	1.285	0.882
$ZnCl_2(H_2O)_4$	3.486	2.950	2.528	1.915	1.205	0.826
$ZnCl_3(H_2O)^{-}$	3.490	2.952	2.528	1.913	1.202	0.824
$ZnCl_4^{2-}$	2.722	2.293	1.957	1.474	0.921	0.629
$ZnSO_4(H_2O)_5$	4.154	3.527	3.031	2.306	1.460	1.006
$Zn(OH)_2(H_2O)_4$	4.185	3.567	3.075	2.350	1.495	1.032
$ZnHCO_3(H_2O)_3^{+}$	4.573	3.877	3.326	2.525	1.593	1.095
$ZnCO_3(H_2O)_3$	4.940	4.199	3.612	2.752	1.745	1.202

Table 2 Logarithm of the reduced partition function, ln β (‰), for the pair ^{60}Ni-^{58}Ni of Ni(II) complexes.

Species	Temperature (K)					
	273	298	323	373	473	573
$Ni(H_2O)_6^{2+}$	6.383	5.412	4.644	3.525	2.224	1.528
$NiCl(H_2O)_5^{+}$	6.228	5.280	4.531	3.439	2.169	1.490
$NiCl_2(H_2O)_4$	6.009	5.093	4.369	3.315	2.090	1.435
$NiSO_4(H_2O)_5$	6.907	5.868	5.044	3.840	2.433	1.676
$NiOH(H_2O)_5^{+}$	6.706	5.702	4.904	3.736	2.368	1.631
$Ni(OH)_2(H_2O)_4$	6.551	5.579	4.807	3.671	2.336	1.613
$NiHCO_3(H_2O)_4^{+}$	6.790	5.757	4.941	3.751	2.368	1.627
$NiCO_3(H_2O)_4$	6.841	5.814	4.999	3.806	2.411	1.661
$NiHS(H_2O)_5^{+}$	5.609	4.753	4.077	3.092	1.949	1.338
$Ni(HS)_2(H_2O)_4$	5.191	4.401	3.776	2.866	1.809	1.243
$NiH_2PO_4(H_2O)_5^{+}$	6.806	5.774	4.958	3.767	2.380	1.636
$NiHPO_4(H_2O)_5$	6.910	5.871	5.048	3.843	2.435	1.676
$NiH_2(cit)(H_2O)_3^{+}$	6.909	5.857	5.026	3.814	2.406	1.653
$NiH(cit)(H_2O)_3$	6.876	5.833	5.008	3.805	2.404	1.653
$Ni(cit)(H_2O)_3^{-}$	6.824	5.791	4.974	3.781	2.391	1.645
$Ni(cit)_2^{4-}$	5.008	4.228	3.616	2.732	1.714	1.174

Table 3 Logarithm of the reduced partition function, ln β (‰), for the pair ^{56}Fe-^{54}Fe of Fe(II) complexes.

Species	Temperature (K)					
	273	298	323	373	473	573
$Fe(H_2O)_6^{2+}$	6.013	5.095	4.370	3.314	2.088	1.433
$FeCl(H_2O)_5^{+}$	5.746	4.869	4.176	3.166	1.995	1.369
$FeCl_2(H_2O)_4$	5.476	4.636	3.974	3.011	1.895	1.300
$FeSO_4(H_2O)_5$	6.349	5.397	4.641	3.535	2.241	1.543
$FeOH(H_2O)_5^{+}$	6.444	5.488	4.726	3.607	2.291	1.579
$Fe(OH)_2(H_2O)_4$	6.318	5.394	4.656	3.565	2.275	1.573
$Fe_2(OH)_6^{2-}$	6.372	5.407	4.643	3.527	2.227	1.530
$FeHCO_3(H_2O)_4^{+}$	6.213	5.267	4.520	3.432	2.167	1.489
$FeCO_3(H_2O)_4$	6.836	5.806	4.991	3.798	2.405	1.656
$FeHS(H_2O)_5^{+}$	5.210	4.413	3.784	2.868	1.806	1.240
$Fe(HS)_2(H_2O)_4$	4.676	3.960	3.395	2.574	1.621	1.113
$Fe_2S_2(H_2O)_4$	5.718	4.839	4.146	3.139	1.974	1.353
$FeH_2PO_4(H_2O)_5^{+}$	6.282	5.326	4.572	3.471	2.191	1.505
$FeHPO_4(H_2O)_5$	6.927	5.883	5.056	3.846	2.434	1.675
$FeH_4(PO_4)_2(H_2O)_4$	6.256	5.300	4.546	3.447	2.173	1.492
$FeH_3(PO_4)_2(H_2O)_4^{-}$	6.154	5.225	4.491	3.417	2.163	1.489
$FeH(cit)(H_2O)_3$	6.175	5.236	4.495	3.413	2.156	1.482
$Fe(cit)(H_2O)_3^{-}$	6.191	5.254	4.512	3.430	2.169	1.492
$FeH(cit)_2^{3-}$	5.443	4.603	3.942	2.983	1.877	1.288
$Fe(cit)_2^{4-}$	4.583	3.867	3.306	2.496	1.565	1.072
$Fe(cit)_2OH^{5-}$	7.880	6.695	5.756	4.383	2.777	1.913

Table 4 Logarithm of the reduced partition function, ln β (‰), for the pair ^{56}Fe-^{54}Fe of Fe(III) complexes.

Species	Temperature (K)					
	273	298	323	373	473	573
$Fe(H_2O)_6^{3+}$	9.488	8.070	6.943	5.291	3.354	2.310
$FeCl(H_2O)_5^{2+}$	8.634	7.333	6.301	4.792	3.030	2.084
$FeCl_2(H_2O)_4^{+}$	8.098	6.873	5.903	4.485	2.834	1.948
$FeSO_4(H_2O)_5^{+}$	9.883	8.420	7.256	5.543	3.527	2.435
$FeOH(H_2O)_5^{2+}$	10.559	9.026	7.799	5.982	3.824	2.647
$Fe(OH)_2(H_2O)_4^{+}$	10.838	9.277	8.025	6.166	3.950	2.737
$Fe(OH)_3(H_2O)_3$	10.986	9.392	8.114	6.222	3.974	2.749
$FeHCO_3(H_2O)_4^{2+}$	9.176	7.795	6.700	5.099	3.228	2.222
$FeCO_3(H_2O)_4^{+}$	9.225	7.849	6.755	5.151	3.269	2.253
$FeH_3PO_4(H_2O)_5^{3+}$	9.941	8.454	7.273	5.541	3.512	2.418
$FeH_2PO_4(H_2O)_5^{2+}$	10.102	8.601	7.407	5.653	3.592	2.477
$FeHPO_4(H_2O)_5^{+}$	10.695	9.119	7.862	6.010	3.825	2.640
$FeH_5(PO_4)_2(H_2O)_4^{2+}$	10.147	8.634	7.432	5.668	3.598	2.480
$FeH_4(PO_4)_2(H_2O)_4^{+}$	10.258	8.733	7.520	5.739	3.647	2.516
$FeH_3(PO_4)_2(H_2O)_4$	10.465	8.915	7.682	5.866	3.730	2.574
$FeH_7(PO_4)_3(H_2O)_3^{+}$	10.188	8.665	7.457	5.684	3.608	2.487
$FeH_6(PO_4)_3(H_2O)_3$	10.608	9.021	7.761	5.915	3.751	2.584
$Fe(cit)(H_2O)_3$	10.492	8.928	7.685	5.861	3.720	2.565
$Fe(cit)OH(H_2O)_2^{-}$	10.074	8.582	7.394	5.647	3.591	2.478
$FeH(cit)_2^{2-}$	10.002	8.491	7.295	5.547	3.510	2.415
$Fe(cit)_2^{3-}$	8.573	7.262	6.228	4.724	2.980	2.047
$Fe(cit)_2OH^{4-}$	8.204	6.970	5.992	4.562	2.890	1.990

Table 5 Logarithm of the reduced partition function, ln β (‰), for the pair ^{65}Cu-^{63}Cu of Cu(I) complexes.

Species	Temperature (K)						Reference
	273	298	323	373	473	573	
$Cu(H_2O)_2^+$	3.368	2.867	2.468	1.882	1.193	0.822	Fujii et al. (2013)
$CuCl(H_2O)$	3.401	2.887	2.480	1.885	1.191	0.818	This study
	3.40	2.89	2.48	1.89	1.19	0.82	Seo et al. (2007)
$CuCl_2^-$	2.775	2.350	2.014	1.526	0.960	0.659	This study
	2.71	2.29	1.97	1.49	0.94	0.64	Seo et al. (2007)
	2.79	2.36	2.03	1.53	0.96	0.66	Sherman (2013)
$CuCl_3^{2-}$	1.012	0.851	0.725	0.545	0.339	0.231	This study
	1.02	0.85	0.73	0.55	0.34	0.23	Seo et al. (2007)
	1.26	1.06	0.91	0.68	0.43	0.29	Sherman (2013)
$CuHS(H_2O)$	3.208	2.722	2.337	1.775	1.121	0.770	This study
	2.96	2.50	2.15	1.63	1.03	0.70	Sherman (2013)
$Cu(HS)_2^-$	2.940	2.489	2.133	1.616	1.017	0.697	This study
	2.90	2.46	2.11	1.60	1.00	0.69	Seo et al. (2007)
	2.72	2.30	1.97	1.49	0.94	0.64	Sherman (2013)
$Cu_2S(HS)_2^{2-}$	2.648	2.239	1.917	1.450	0.911	0.624	This study

Table 6 Logarithm of the reduced partition function, ln β (‰), for the pair ^{65}Cu-^{63}Cu of Cu(II) complexes.

Species	Temperature (K)					
	273	298	323	373	473	573
$CuH_2PO_4(H_2O)_4^+$	5.515	4.684	4.026	3.063	1.939	1.334
$CuH_4(PO_4)_2(H_2O)_3$	5.553	4.714	4.050	3.079	1.947	1.339
$CuH_3(PO_4)_2(H_2O)_3^-$	5.290	4.492	3.861	2.937	1.860	1.280
$CuH_2(PO_4)_2(H_2O)_2^{2-}$	6.360	5.403	4.645	3.535	2.238	1.540
$CuH_2(cit)(H_2O)_2^+$	5.286	4.486	3.852	2.927	1.850	1.272
$CuH(cit)(H_2O)_2$	5.622	4.772	4.099	3.117	1.972	1.357
$Cu(cit)(H_2O)_2^-$	6.092	5.177	4.451	3.389	2.147	1.479
$Cu(cit)_2^{4-}$	4.998	4.231	3.626	2.748	1.730	1.188

Table 7 Group electronegativities.

Group	Electronegativity	Reference
H_2O	3.57	Boyd and Boyd (1992)
OH	3.97	Mullay (1985)
Cl	3.16	Allred (1961)
SO_4	4.60	Huheey (1966)
HS	2.32	Huheey (1965)
HCO_3	3.63	[a]
CO_3	4.33	Huheey (1966)
H_3PO_4	3.23	[b]
H_2PO_4	3.96	[b]
HPO_4	5.11	[b]

[a] Calculated by a method of Bratsch (1985) with electronegativities of H (2.20) (Allred, 1961) and CO_3.

[b] Calculated by a method of Bratsch (1985) with electronegativities of H (2.20) (Allred, 1961) and PO_4 (4.50) (Huheey, 1966).

Table 8 Logarithm of the reduced partition function, ln β (‰), for the pair ^{66}Zn-^{64}Zn of Zn(II)-amino acid complexes and hydrated Zn^{2+} ion.

		Temperature (K)				
		273	298	310	323	373
fourfold	$Zn(H_2O)_4^{2+}$	4.539	3.853	3.577	3.310	2.516
	$Zn(Glu)(H_2O)_2^{2+}$	4.473	3.796	3.524	3.260	2.478
	$Zn(Thr)(H_2O)_3^{2+}$	4.774	4.056	3.767	3.487	2.654
	$Zn(His)(H_2O)_2^{2+}$	4.670	3.959	3.673	3.397	2.578
	$Zn(His)(H_2O)_3^{2+}$	4.635	3.930	3.647	3.373	2.561
	$Zn(Cys)(H_2O)_3^{2+}$	3.912	3.313	3.072	2.840	2.152
	$Zn(Met)(H_2O)_3^{2+}$	4.397	3.733	3.466	3.207	2.438
	$Zn(GS)^-$	4.311	3.655	3.392	3.137	2.381
sixfold	$Zn(H_2O)_6^{2+}$	3.854	3.263	3.026	2.797	2.119
	$Zn(Glu)(H_2O)_4^{2+}$	3.888	3.292	3.053	2.822	2.139
	$Zn(Thr)(H_2O)_5^{2+}$	3.916	3.315	3.075	2.842	2.154
	$Zn(His)(H_2O)_4^{2+}$	3.541	2.996	2.777	2.566	1.943
	$Zn(His)(H_2O)_5^{2+}$	3.724	3.150	2.921	2.699	2.043
	$Zn(Cys)(H_2O)_5^{2+}$	3.196	2.702	2.504	2.313	1.750
	$Zn(Met)(H_2O)_5^{2+}$	3.478	2.947	2.734	2.528	1.918

Table 9 Logarithm of the reduced partition function, ln β (‰), for the pair ^{65}Cu-^{63}Cu of Cu(II)-amino acid complexes, lactate, and hydrated Cu^{2+} ion.

	Temperature (K)				
	273	298	310	323	373
$Cu(H_2O)_5^{2+}$	5.355[a]	4.546[a]	4.220	3.905[a]	2.968[a]
$Cu(Glu)(H_2O)_3^{2+}$	5.230	4.436	4.117	3.808	2.891
$Cu(Thr)(H_2O)_4^{2+}$	5.220	4.429	4.110	3.803	2.889
$Cu(His)(H_2O)_3^{2+}$	5.274	4.470	4.148	3.836	2.911
$Cu(His)(H_2O)_4^{2+}$	5.299	4.492	4.168	3.855	2.926
$Cu(Cys)(H_2O)_4^{2+}$	3.981	3.369	3.124	2.888	2.187
$Cu(Met)(H_2O)_4^{2+}$	4.632	3.932	3.650	3.378	2.568
$Cu(GS)H^0$	4.945	4.194	3.892	3.600	2.734
$CuC_3H_5O_3(H_2O)_3^+$	5.530	4.695	4.359	4.034	3.068

[a] Fujii et al. (2013).

Table B1 Vibrational frequencies and ln β values.

Fe(II)

	ν_1 (cm^{-1})	ln β at 298 K (‰)	Reference
$Fe(H_2O)_6^{2+}$	325	5.095	This study
$Fe(H_2O)_6^{2+}$ + CPCM	338	4.912	This study
Raman	390	-	Kanno and Hiraishi (1982)

Fe(III)

	ν_1 (cm^{-1})	ln β at 298 K (‰)	Reference
$Fe(H_2O)_6^{3+}$	407	8.070	This study
$Fe(H_2O)_6^{3+}$ + CPCM	467	7.758	This study
Raman	509	-	Sharma (1973)
Raman	506	-	Kanno and Hiraishi (1982)

Ni(II)

	ν_1 (cm^{-1})	ln β at 298 K (‰)	Reference
$Ni(H_2O)_6^{2+}$	347	5.432	Fujii et al. (2011)
$Ni(H_2O)_6^{2+}$	347	5.412	This study
$Ni(H_2O)_6^{2+}$ + CPCM	353	5.524	This study
$Ni(H_2O)_{18}^{2+}$	394	6.046	Fujii et al. (2011)
Raman	390	-	Kanno (1977,1978)
Raman	390	-	Edwards and Knowles (1992)
Raman	395	-	Bickley et al. (1993)

Cu(I)

	ν_1 (cm^{-1})	ln β at 298 K (‰)	Reference
$Cu(H_2O)_2^{+}$	370	2.867	Fujii et al. (2013)
$Cu(H_2O)_2^{+}$ + CPCM	361	2.862	This study
Raman	410	-	Applegarth (2014)

Table B1 (continued).

Cu(II)

	ν_1 (cm^{-1})	ln β at 298 K (‰)	Reference
$Cu(H_2O)_5^{2+}$	383[a]	4.546	Fujii et al. (2013)
$Cu(H_2O)_5^{2+}$ + CPCM	383[a]	4.547	This study
$Cu(H_2O)_6^{2+}$	361	4.288	Fujii et al. (2013)
$Cu(H_2O)_6^{2+}$ + CPCM	371	4.297	This study
Raman	440	-	Hester and Plane (1964)
Raman	436	-	Davis and Chong (1972)
Raman	434	-	Kanno (1977,1978)
Raman	445	-	Castro and Jagodzinski (1991)

[a] ν_2 (A_1) mode of fivefold coordination (Raman active).

Zn(II)

	ν_1 (cm^{-1})	ln β at 298 K (‰)	Reference
$Zn(H_2O)_6^{2+}$	333	3.263	Fujii et al. (2011)
$Zn(H_2O)_6^{2+}$ + CPCM	353	3.280	Fujii et al. (2011)
$Zn(H_2O)_{18}^{2+}$	380	3.576	Fujii et al. (2011)
Raman	390	-	Irish et al. (1963)
Raman	379	-	Yamaguchi et al. (1989)
Raman	385	-	Maeda et al. (1995)
Raman	390	-	Rudolph and Pye (1999)
Raman	389	-	Mink et al. (2003)

1131

1132 Table B2 $\Delta^{56}Fe$ for Fe^{3+}_{aq}-Fe^{2+}_{aq} (295 K)

	ln β (Fe^{3+}) (‰)	ln β (Fe^{2+}) (‰)	$\Delta^{56}Fe$	Reference
6 H_2O	8.223	5.194	3.03	This study
6 H_2O (CPCM)	7.905	5.007	2.90	This study
6 H_2O	8.35[a]	5.08[a]	3.27	Ottonello and Zuccolini (2009)
18 H_2O (COSMO)	7.87	4.76	3.11	Rustad et al. (2010)
Experimental	-	-	2.75 ± 0.15	Johnson et al. (2002)
Experimental	-	-	2.95 ± 0.53	Welch et al. (2003)

1133 [a] Estimated from ln β at 298K by using $1/T^2$ dependence.

1134

1135 Figure Captions

1136

1137 Figure 1. Mole fractions of Cu(II) species and Cu isotopic variations ($^{65}Cu/^{63}Cu$) in
1138 seawater as a function of pH at 298 K. (a) Mole fractions of Cu(II) species reproduced
1139 from Zirino and Yamamoto (1972). (b) $\delta^{65}Cu$ of Cu(II) species relative to the bulk
1140 solution. (c) $\delta^{65}Cu$ of Cu(II) carbonates, chlorides, hydroxides, sulfates, and hydrated
1141 Cu^{2+} ions relative to the bulk solution. Though the metal concentration is not strictly
1142 required, total concentration of Cu was set to 1.1×10^{-8} mol kg^{-1} (Macleod et al., 1994).

1143

1144 Figure 2. Mole fractions of Zn(II) species and Zn isotopic variations ($^{66}Zn/^{64}Zn$) in
1145 seawater as a function of pH at 298 K. (a) Mole fractions of Zn(II) species reproduced
1146 from Zirino and Yamamoto (1972). (b) $\delta^{66}Zn$ of Zn(II) species relative to the bulk
1147 solution. (c) $\delta^{66}Zn$ of Zn(II) carbonates, chlorides, hydroxides, sulfates, and hydrated
1148 Zn^{2+} ions relative to the bulk solution. Total concentration of Zn was set to 7.5×10^{-8}
1149 mol kg^{-1} (Macleod et al., 1994).

1150

1151 Figure 3. Mole fractions of Ni(II) species and Ni isotopic variations ($^{60}Ni/^{58}Ni$) in
1152 seawater as a function of pH at 298 K. (a) Mole fractions of Ni(II) species were
1153 estimated from Zirino and Yamamoto (1972). Stability constants of Ni(II) species were
1154 taken from the literature (Turner et al., 1981; Foulliac and Criaud, 1984; Byrne et al.,
1155 1988). (b) $\delta^{60}Ni$ of Ni(II) species relative to the bulk solution. (c) $\delta^{60}Ni$ of Ni(II)
1156 carbonates, chlorides, hydroxides, sulfates, and hydrated Ni^{2+} ions relative to the bulk
1157 solution. Total concentration of Ni was set to 2.9×10^{-8} mol kg^{-1}(Macleod et al., 1994).

Figure 4. Mole fractions of Fe(II) species and Fe isotopic variations ($^{56}Fe/^{54}Fe$) in seawater as a function of pH at 298 K. (a) Mole fractions of Fe(II) species were estimated from Zirino and Yamamoto (1972). Stability constants of Fe(II) species were taken from the literature (Foulliac and Criaud, 1984; Byrne et al., 1988). (b) $\delta^{56}Fe$ of Fe(II) species relative to the bulk solution. (c) $\delta^{56}Fe$ of Fe(II) carbonates, chlorides, hydroxides, sulfates, and hydrated Fe^{2+} ions relative to the bulk solution. Total concentration of Fe was set to 3.6×10^{-8} mol kg^{-1} (Macleod et al., 1994).

Figure 5. Temperature dependence of ln β for aqueous Fe species. The ln β values of Fe(II) (Table 3) and Fe(III) (Table 4) species are shown as a function of T^{-2}. (a) Fe(II) and (b) Fe(III). Vertical scale factor of (b) is 3/2 of (a). The temperature dependence of ln β for aqueous species of Ni, Cu, and Zn can be found in Fujii et al. (2011a,b, 2013).

Figure 6. Mole fractions of Fe(II) species and Fe isotopic variations ($^{56}Fe/^{54}Fe$) in seawater-like matrix under sulfide-rich conditions. (a) Mole fractions of Fe(II) species were reproduced from Fig. 22a of Rickard and Luther (2007), in which total concentrations of Fe and S are reported to be 10^{-6} mol kg^{-1} and 10^{-3} mol kg^{-1}, respectively. The HS^-/SO_4^{2-} redox couple was set to be disabled in their calculation. (b) $\delta^{56}Fe$ of Fe(II) species relative to the bulk solution. The ln β values at 298 K in Table 3 were used. (c) $\delta^{56}Fe$ of Fe(II) carbonates, chlorides, hydroxides, sulfides, and hydrated Fe^{2+} ions relative to the bulk solution.

1181 Figure 7. Temperature dependence of ln β for Cu(I) species. The ln β values of hydrated
1182 Cu^{+}, Cu(I) chlorides, and hydrogensulfides (Table 5) are shown as a function of T^{-2}. The
1183 temperature dependence of ln β for aqueous species of Cu(II) can be found in Fujii et al.
1184 (2013).
1185
1186 Figure 8. ln β for Fe(II), Ni(II), Cu(II), and Zn(II) species. The metal cations are
1187 denoted as M^{2+}. The ln β values at 298 K for hydrated cation, hydroxide, chloride,
1188 sulfate, sulfide, carbonate, and simple phosphate complexes are taken from Tables 1, 2,
1189 3, 6, S8, Fujii and Albarède (2012), and Fujii et al., (2013).
1190
1191 Figure 9. ln β vs bond length. The ln β values (298 K) of hydrated complexes with the
1192 ratio M:ligand = 1:1 were taken from Tables 1, 2, 3, 4, 6, S8, Fujii and Albarède (2012),
1193 and Fujii et al., (2013), where ligands are OH^{-}, Cl^{-}, SO_4^{2-}, HS^{-}, HCO_3^{-}, CO_3^{2-}, and
1194 $H_2PO_4^{-}$. For Fe(III), the ln β value for $FeH_3PO_4^{3+}$ is also shown. For Zn(II) hydroxide
1195 and sulfide, the ln β values for $Zn(OH)_2$ and $Zn(HS)_2$ are shown. For reference, the ln β
1196 values for hydated M^{2+} (or M^{3+}) are shown. The atomic distances between M and O of
1197 the oxygen donor ligands, M and Cl, and M and S of HS were used as bond lengths. The
1198 atomic distances can be calculated from the Cartesian coordinates given in the
1199 electronic supplement. The correlation lines were drawn for complexes, except for
1200 sulfides, by least squares methods.
1201
1202 Figure 10. ln β vs group electronegativity. The ln β values (298 K) of hydrated
1203 complexes with the ratio M:ligand = 1:1 were taken from Tables 1, 2, 3, 4, 6, S8, S9,

Fujii and Albarède (2012), and Fujii et al., (2013), where ligands are OH^-, Cl^-, SO_4^{2-}, HS^-, HCO_3^-, CO_3^{2-}, $H_2PO_4^-$, and HPO_3^{2-}. For Fe(III), the ln β value for $FeH_3PO_4^{3+}$ is also shown. For Zn(II) hydroxide and sulfide, the ln β values for $Zn(OH)_2$ and $Zn(HS)_2$ are shown. The correlation lines were drawn for all complexes by least squares methods.

Figure 11. Molecular structures of hydrated Fe^{3+}, aqueous Fe(III) hydroxides, phosphates, and citrates. The structures were drawn using GaussView5 (Gaussian Inc.) (Dennington et al., 2009).

Figure 12. Temperature dependence of ln β for Fe, Ni, Cu, and Zn phosphates and citrates. The ln β values of hydrated cations, phosphates, and citrates are shown as a function of T^{-2}. Vertical scale range was fixed at 7‰. (a) Fe(II) (Table 3), (b) Fe(III) (Table 4), (c) Ni(II) (Table 2), (d) Cu(II) (Table 6 and ln β of Cu^{2+} was reproduced from Fujii et al., 2013), and (e) Zn(II) (the ln β values were taken from Fujii and Albarède, 2012).

Figure 13. Molecular structures of hydrated cations and amino acid complexes of Zn(II) and Cu(II). (a) Zn(II), fourfold complexation, (b) Zn(II), sixfold complexation, and (c) Cu(II), fivefold complexation. Abbreviations are Glu (glutamine), Thr (threonine), His (histidine), Cys (cysteine), and Met (methionine). Deprotonated glutathione (GSH) is shown as GS^-. The structures were drawn using GaussView5 (Gaussian Inc.) (Dennington et al., 2009).

1227

1228 Figure 14. Zn ($^{66}Zn/^{64}Zn$) and Cu ($^{65}Cu/^{63}Cu$) isotopic variations in model molecules of

1229 Zn^{2+}- and Cu^{2+}- amino acid complexes at 310 K. (a) Zn(II), (b) Cu(II). ln β of aqueous

1230 Cu(I) species, $Cu(H_2O)_2^+$, which is estimated to be 2.664‰ at 310 K from Fujii et al.

1231 (2013). Here shown together for comparison.

1232

Fig.1

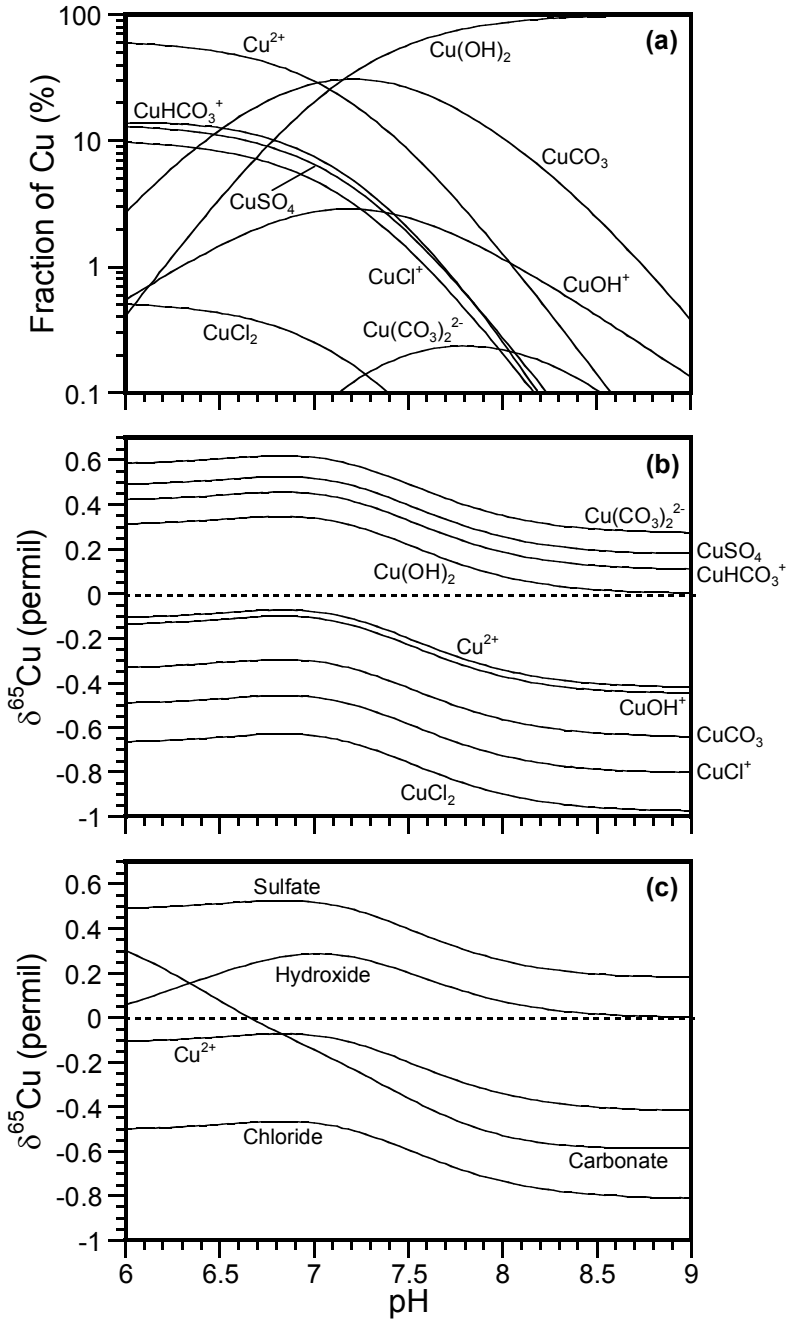
(a)
Fraction of Cu (%)
100
10
1
0.1
Cu2+
Cu(OH)2
CuHCO3+
CuCO3
CuSO4
CuCl+
CuOH+
CuCl2
Cu(CO3)22-
(b)
δ65Cu (permil)
0.6
0.4
0.2
0
-0.2
-0.4
-0.6
-0.8
-1
Cu(CO3)22-
CuSO4
CuHCO3+
Cu(OH)2
Cu2+
CuOH+
CuCO3
CuCl+
CuCl2
(c)
Sulfate
Hydroxide
Cu2+
Chloride
Carbonate
6
6.5
7
7.5
8
8.5
9
pH

Fig.2

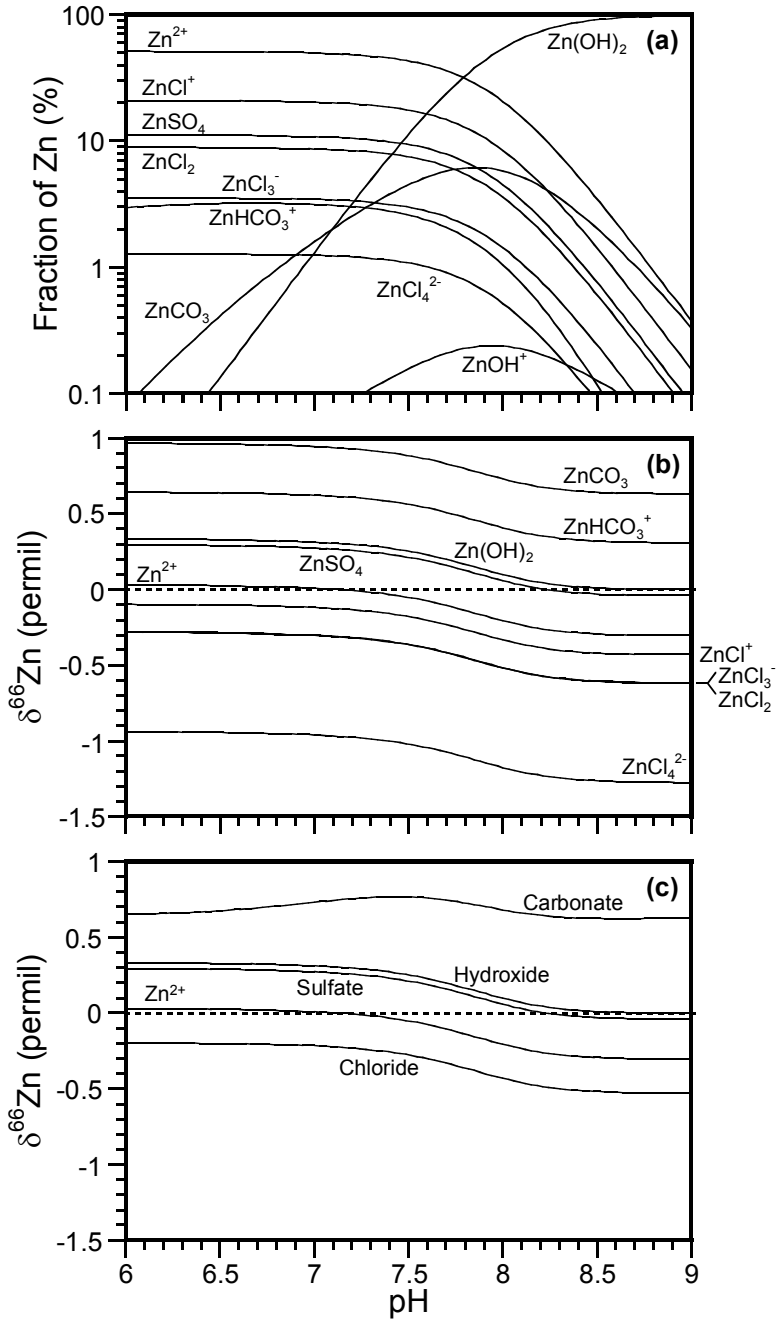
100
10
1
0.1
Fraction of Zn (%)
Zn2+
ZnCl+
ZnSO4
ZnCl2
ZnCl3-
ZnHCO3+
ZnCO3
ZnCl42-
ZnOH+
Zn(OH)2
(a)
1
0.5
0
-0.5
-1
-1.5
δ66Zn (permil)
ZnCO3
ZnHCO3+
Zn(OH)2
Zn2+
ZnSO4
ZnCl+
ZnCl3-
ZnCl2
ZnCl42-
(b)
Carbonate
Hydroxide
Zn2+
Sulfate
Chloride
(c)
6
6.5
7
7.5
8
8.5
9
pH

Fig.3

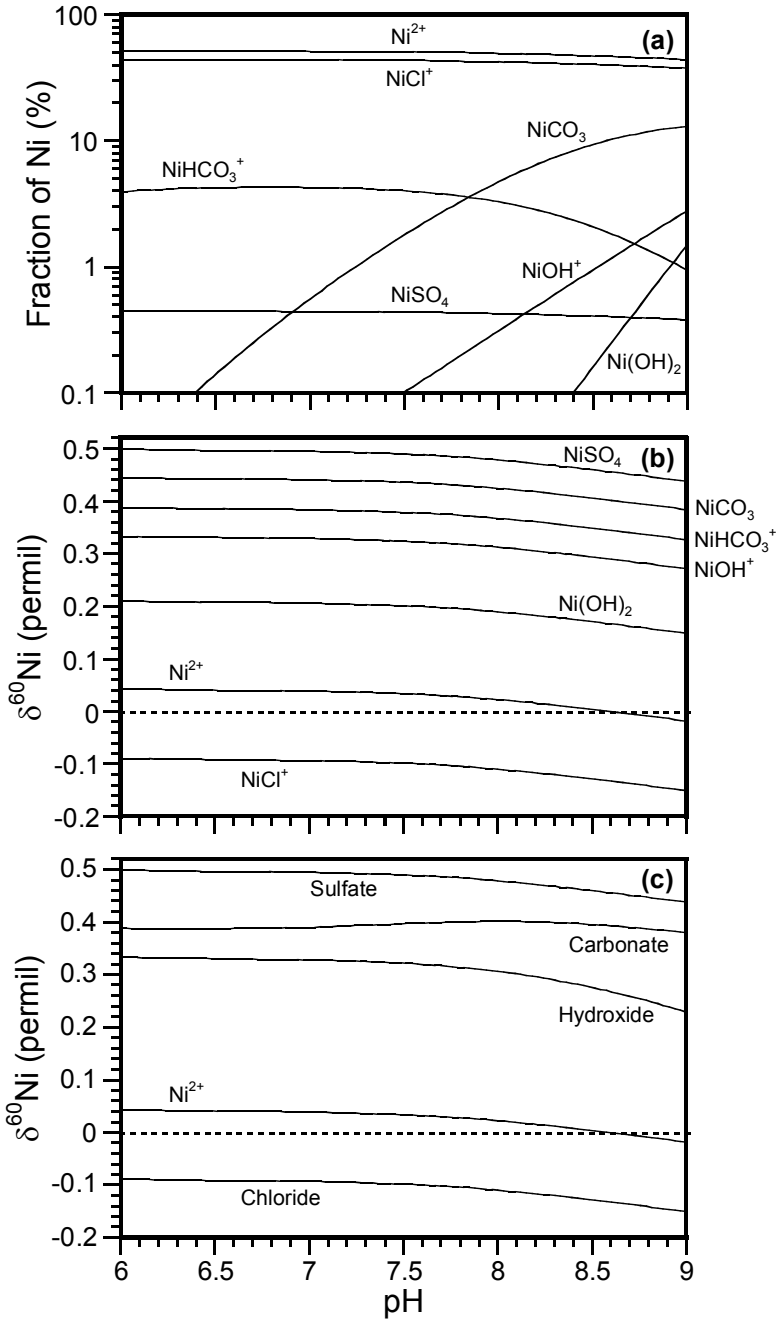
(a)
Fraction of Ni (%)
100
10
1
0.1
Ni2+
NiCl+
NiCO3
NiHCO3+
NiOH+
NiSO4
Ni(OH)2
(b)
δ60Ni (permil)
0.5
0.4
0.3
0.2
0.1
0
-0.1
-0.2
NiSO4
NiCO3
NiHCO3+
NiOH+
Ni(OH)2
Ni2+
NiCl+
(c)
δ60Ni (permil)
Sulfate
Carbonate
Hydroxide
Ni2+
Chloride
6
6.5
7
7.5
8
8.5
9
pH

Fig.4

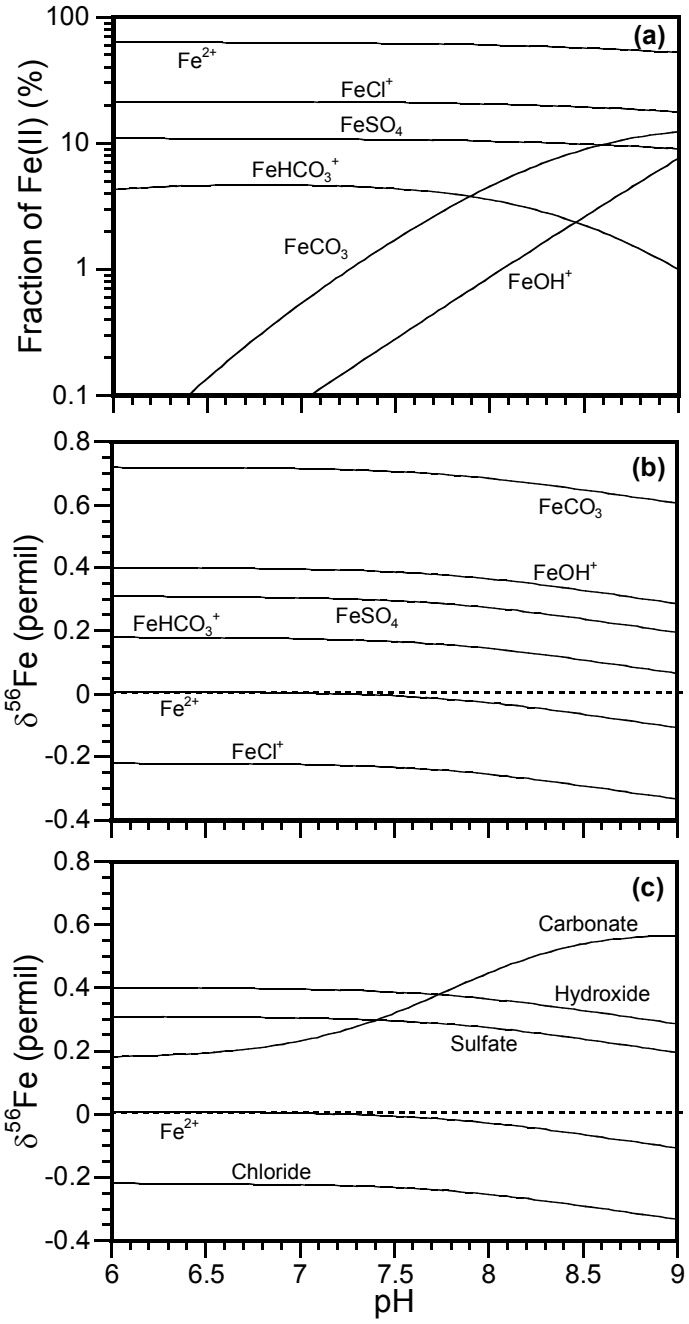
(a)
Fraction of Fe(II) (%)
100
10
1
0.1
Fe2+
FeCl+
FeSO4
FeHCO3+
FeCO3
FeOH+
(b)
δ56Fe (permil)
0.8
0.6
0.4
0.2
0
-0.2
-0.4
FeCO3
FeOH+
FeHCO3+
FeSO4
Fe2+
FeCl+
(c)
δ56Fe (permil)
Carbonate
Hydroxide
Sulfate
Fe2+
Chloride
6
6.5
7
7.5
8
8.5
9
pH

Fig.5

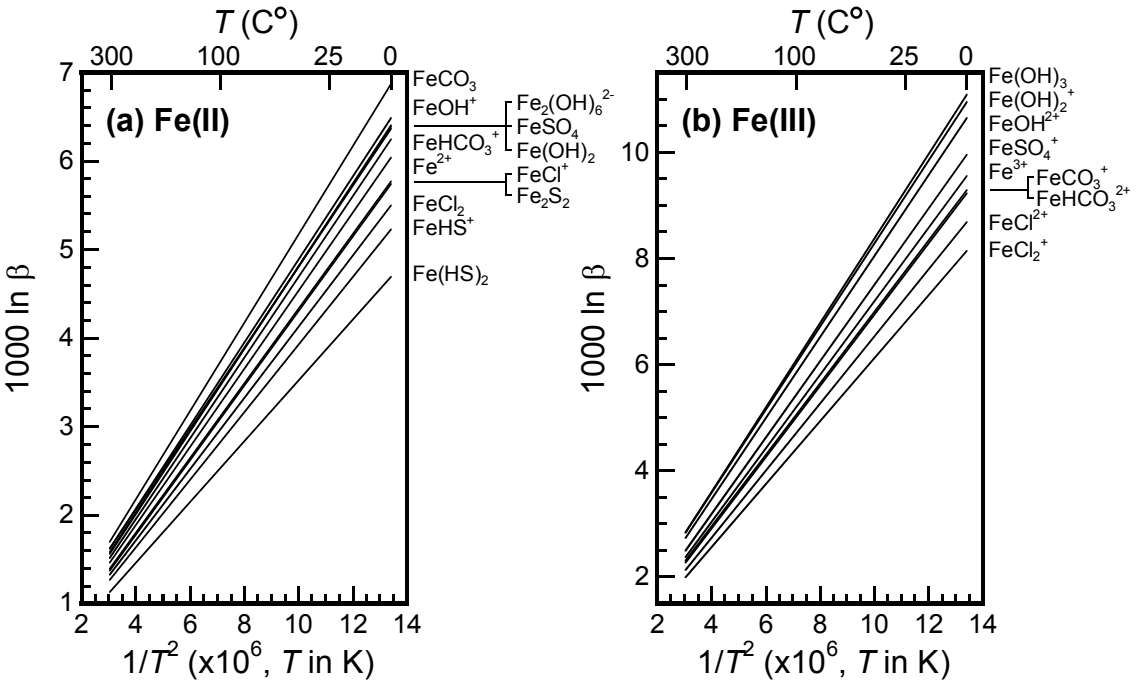
T (C°)
300
100
25
0
(a) Fe(II)
FeCO3
FeOH+
Fe2(OH)6 2-
FeSO4
FeHCO3 +
Fe(OH)2
Fe2+
FeCl+
Fe2S2
FeCl2
FeHS+
Fe(HS)2
1000 ln β
1/T2 (x10^6, T in K)
(b) Fe(III)
Fe(OH)3
Fe(OH)2 +
FeOH2+
FeSO4 +
Fe3+
FeCO3 +
FeHCO3 2+
FeCl2+
FeCl2 +

Fig.6

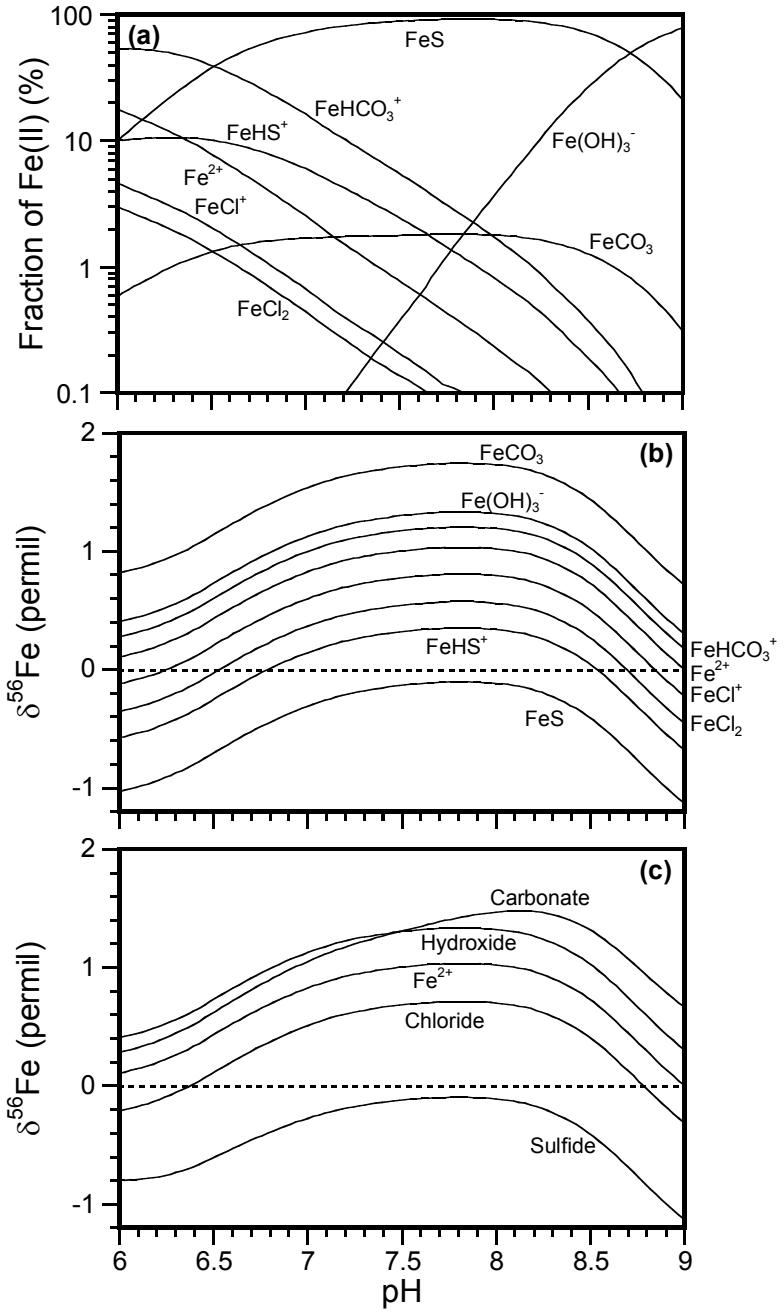
(a)
Fraction of Fe(II) (%)
100
10
1
0.1
FeS
FeHCO3+
FeHS+
Fe2+
FeCl+
FeCl2
Fe(OH)3-
FeCO3
(b)
δ56Fe (permil)
2
1
0
-1
FeCO3
Fe(OH)3-
FeHS+
FeS
FeHCO3+
Fe2+
FeCl+
FeCl2
(c)
δ56Fe (permil)
Carbonate
Hydroxide
Fe2+
Chloride
Sulfide
6
6.5
7
7.5
8
8.5
9
pH

Fig.7

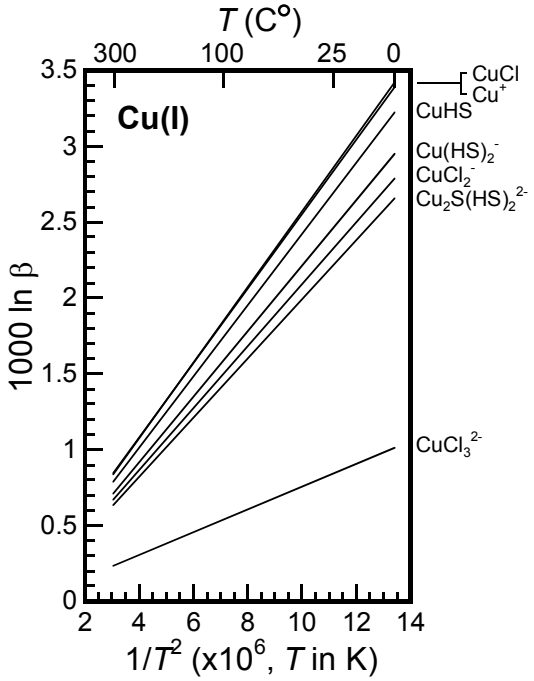
T (C°)
300
100
25
0
Cu(I)
CuCl
Cu+
CuHS
Cu(HS)2-
CuCl2-
Cu2S(HS)22-
CuCl32-
1000 ln β
3.5
3
2.5
2
1.5
1
0.5
0
2
4
6
8
10
12
14
1/T2 (x106, T in K)

Fig.8

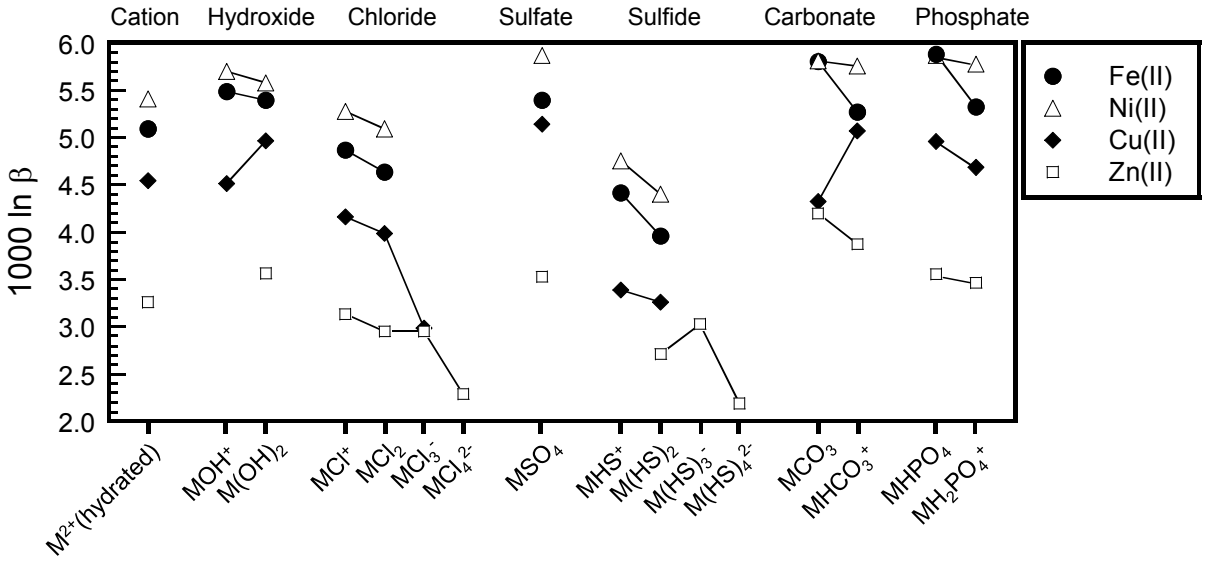
Cation
Hydroxide
Chloride
Sulfate
Sulfide
Carbonate
Phosphate
1000 ln β
6.0
5.5
5.0
4.5
4.0
3.5
3.0
2.5
2.0
Fe(II)
Ni(II)
Cu(II)
Zn(II)
M2+(hydrated)
MOH+
M(OH)2
MCl+
MCl2
MCl3-
MCl42-
MSO4
MHS+
M(HS)2
M(HS)3-
M(HS)42-
MCO3
MHCO3+
MHPO4
MH2PO4+

Fig.9

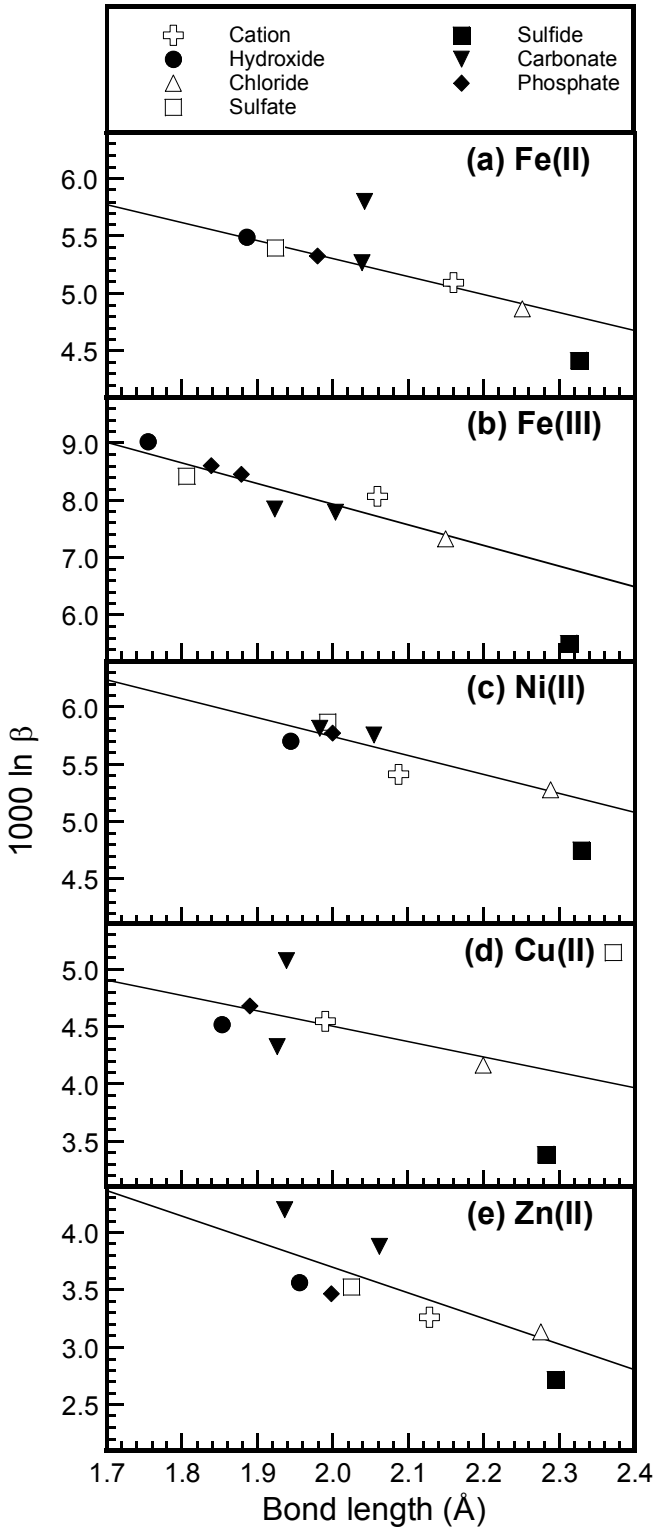
Cation
Hydroxide
Chloride
Sulfate
Sulfide
Carbonate
Phosphate
(a) Fe(II)
(b) Fe(III)
(c) Ni(II)
(d) Cu(II) □
(e) Zn(II)
1000 ln β
Bond length (Å)

Fig.10

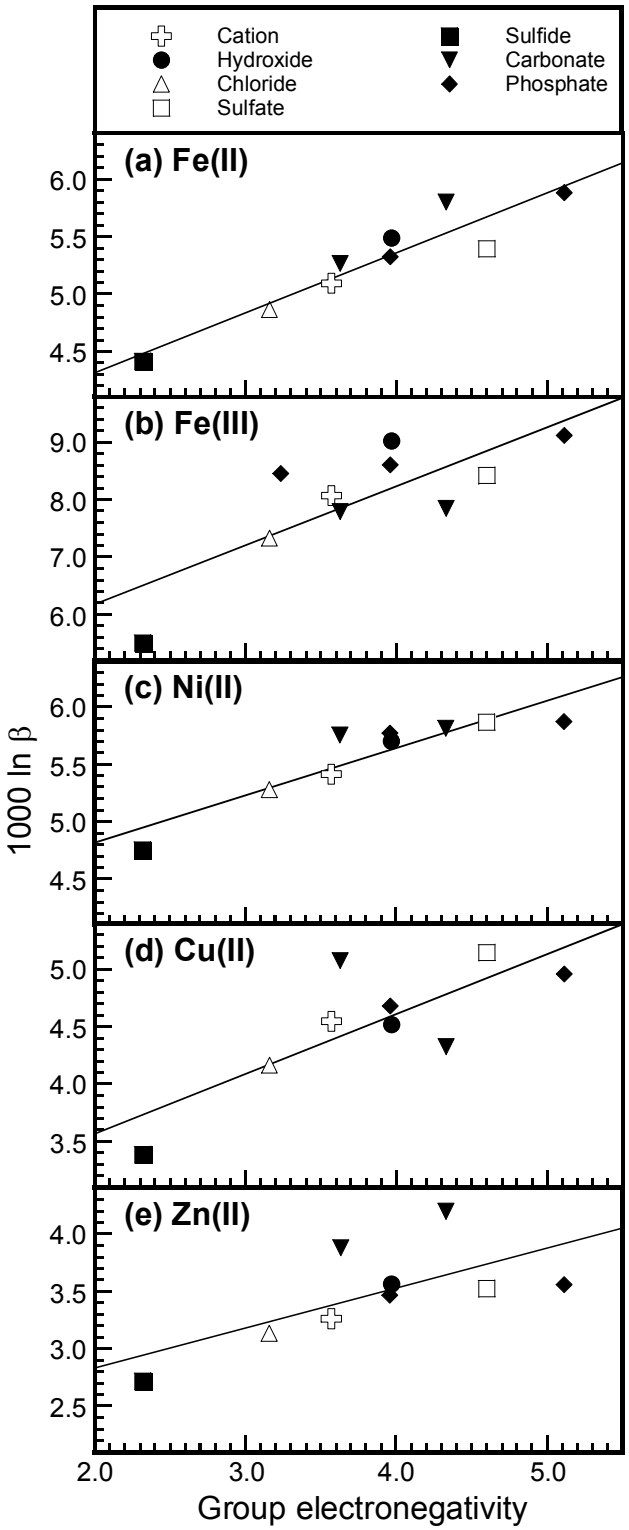
Cation
Hydroxide
Chloride
Sulfate
Sulfide
Carbonate
Phosphate
(a) Fe(II)
(b) Fe(III)
(c) Ni(II)
(d) Cu(II)
(e) Zn(II)
1000 ln β
Group electronegativity
2.0
3.0
4.0
5.0

Fig.11

(a) Fe^{3+} and Fe(III) hydroxides

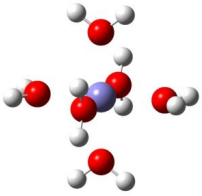

(a-1) $Fe(H_2O)_6^{3+}$

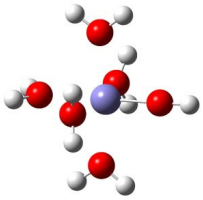

(a-2) $FeOH(H_2O)_5^{2+}$

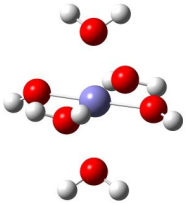

(a-3) $Fe(OH)_2(H_2O)_4^{+}$

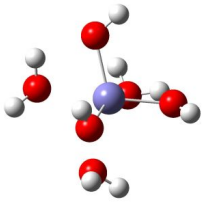

(a-4) $Fe(OH)_3(H_2O)_3^{-}$

(b) Fe(III) phosphates

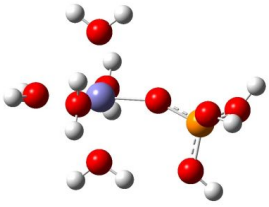

(b-1) $FeH_3PO_4(H_2O)_5^{3+}$

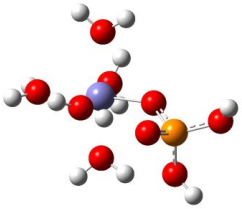

(b-2) $FeH_2PO_4(H_2O)_5^{2+}$

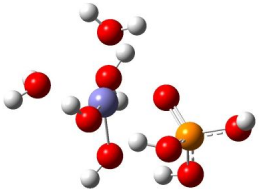

(b-3) $FeHPO_4(H_2O)_5^{+}$

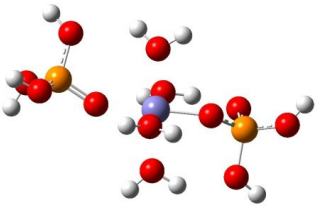

(b-4) $FeH_5(PO_4)_2(H_2O)_4^{2+}$

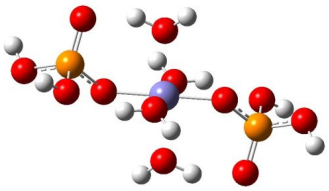

(b-5) $FeH_4(PO_4)_2(H_2O)_4^{+}$

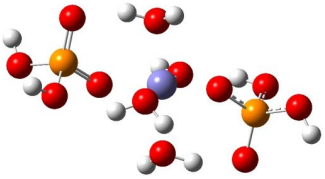

(b-6) $FeH_3(PO_4)_2(H_2O)_4$

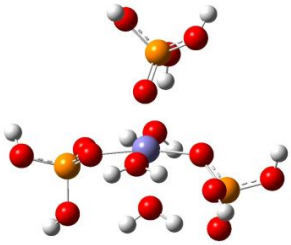

(b-7) $FeH_7(PO_4)_3(H_2O)_3^{+}$

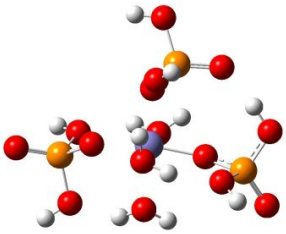

(b-8) $FeH_6(PO_4)_3(H_2O)_3$

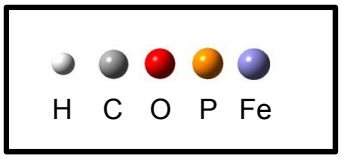

(c) Fe(III) citrates

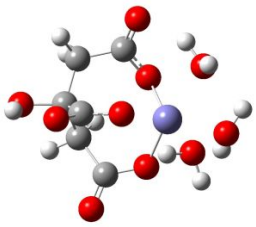

(c-1) $Fe(cit)(H_2O)_3$

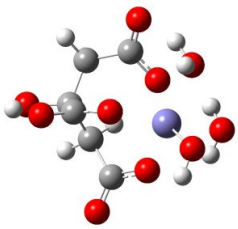

(c-2) $Fe(cit)OH(H_2O)_2^{-}$

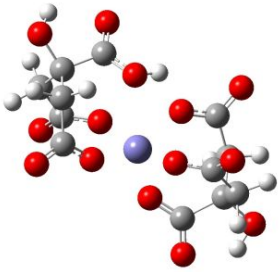

(c-3) $FeH(cit)_2^{2-}$

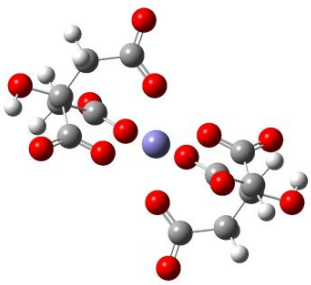

(c-4) $Fe(cit)_2^{3-}$

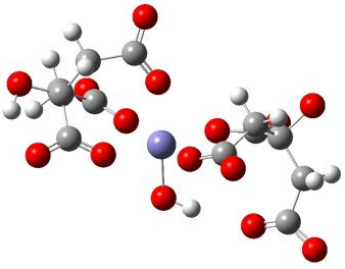

(c-5) $Fe(cit)_2OH^{4-}$

Fig.12

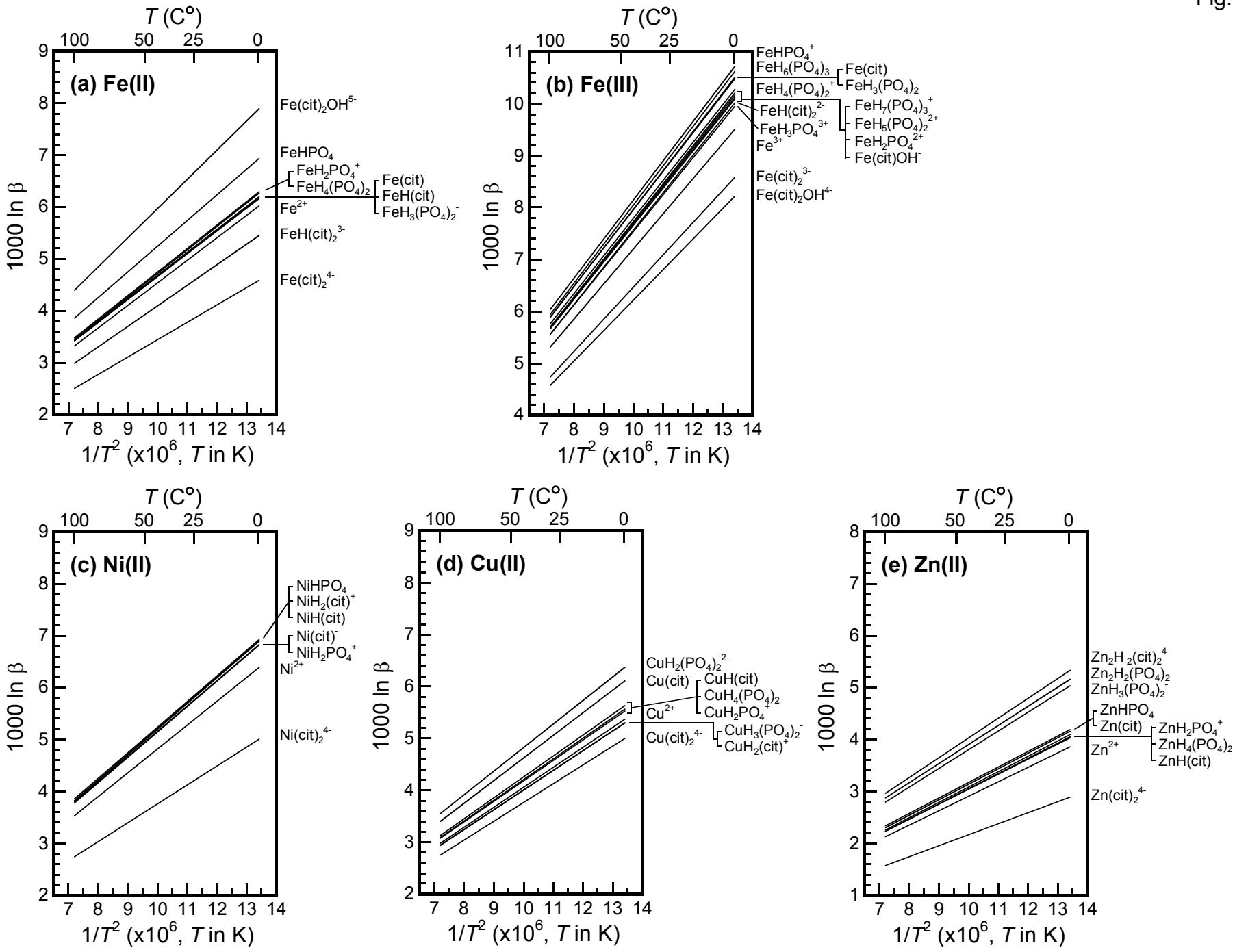
(a) Fe(II)
(b) Fe(III)
(c) Ni(II)
(d) Cu(II)
(e) Zn(II)
T (C°)
1000 ln β
1/T² (x10⁶, T in K)
Fe(cit)₂OH⁵⁻
FeHPO₄
FeH₂PO₄⁺
FeH₄(PO₄)₂
Fe(cit)⁻
FeH(cit)
FeH₃(PO₄)₂⁻
Fe²⁺
FeH(cit)₂³⁻
Fe(cit)₂⁴⁻
FeHPO₄⁺
FeH₆(PO₄)₃
Fe(cit)
FeH₃(PO₄)₂
FeH₄(PO₄)₂⁺
FeH(cit)₂²⁻
FeH₇(PO₄)₃⁺
FeH₅(PO₄)₂²⁺
FeH₃PO₄³⁺
FeH₂PO₄²⁺
Fe³⁺
Fe(cit)OH⁻
Fe(cit)₂³⁻
Fe(cit)₂OH⁴⁻
NiHPO₄
NiH₂(cit)⁺
NiH(cit)
Ni(cit)⁻
NiH₂PO₄⁺
Ni²⁺
Ni(cit)₂⁴⁻
CuH₂(PO₄)₂²⁻
Cu(cit)⁻
CuH(cit)
CuH₄(PO₄)₂
CuH₂PO₄⁺
Cu²⁺
Cu(cit)₂⁴⁻
CuH₃(PO₄)₂⁻
CuH₂(cit)⁺
Zn₂H₋₂(cit)₂⁴⁻
Zn₂H₂(PO₄)₂
ZnH₃(PO₄)₂⁻
ZnHPO₄
Zn(cit)⁻
ZnH₂PO₄⁺
ZnH₄(PO₄)₂
ZnH(cit)
Zn²⁺
Zn(cit)₂⁴⁻

(a) Zn(II), fourfold-coordination

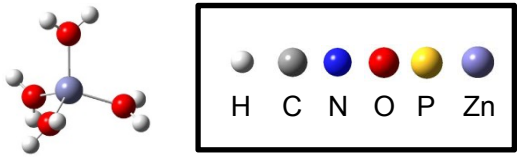

(a-1) $Zn(H_2O)_4^{2+}$

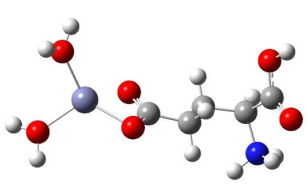

(a-2) $Zn(Glu)(H_2O)_2^{2+}$

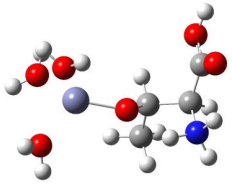

(a-3) $Zn(Thr)(H_2O)_3^{2+}$

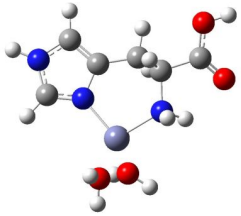

(a-4) $Zn(His)(H_2O)_2^{2+}$

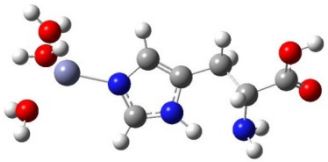

(a-5) $Zn(His)(H_2O)_3^{2+}$

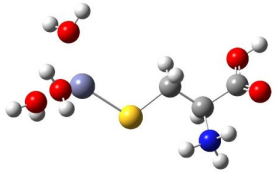

(a-6) $Zn(Cys)(H_2O)_3^{2+}$

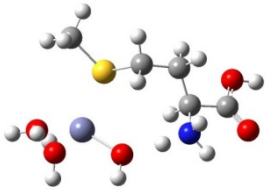

(a-7) $Zn(Met)(H_2O)_3^{2+}$

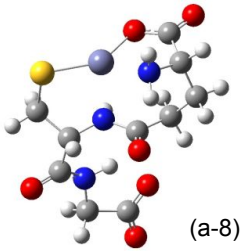

(a-8) Zn(II)-GSH complex
$[Zn(GS)]^-$

(b) Zn(II), sixfold-coordination

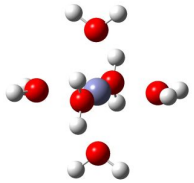

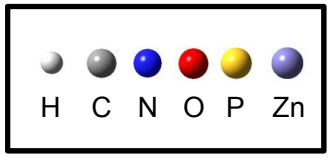

(b-1) $Zn(H_2O)_6^{2+}$

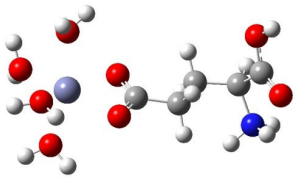

(b-2) $Zn(Glu)(H_2O)_4^{2+}$

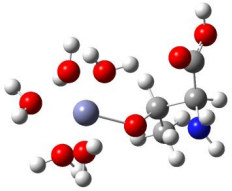

(b-3) $Zn(Thr)(H_2O)_5^{2+}$

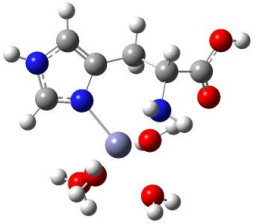

(b-4) $Zn(His)(H_2O)_4^{2+}$

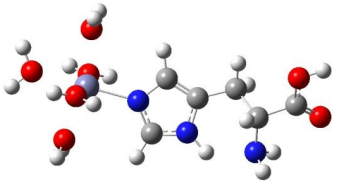

(b-5) $Zn(His)(H_2O)_5^{2+}$

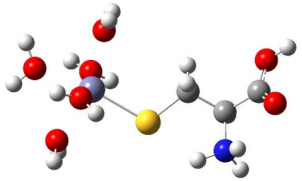

(b-6) $Zn(Cys)(H_2O)_5^{2+}$

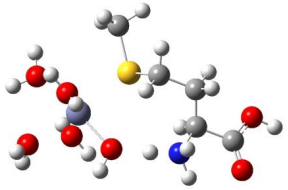

(b-7) $Zn(Met)(H_2O)_5^{2+}$

(c) Cu(II)

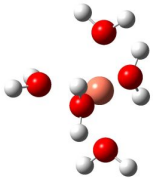

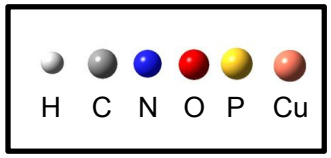

(c-1) $Cu(H_2O)_5^{2+}$

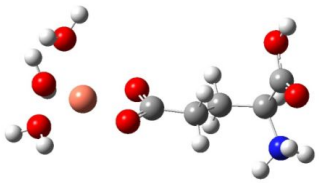

(c-2) $Cu(Glu)(H_2O)_3^{2+}$

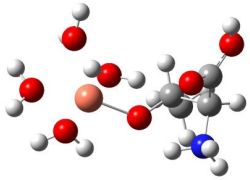

(c-3) $Cu(Thr)(H_2O)_4^{2+}$

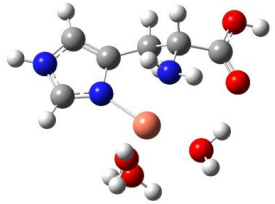

(c-4) $Cu(His)(H_2O)_3^{2+}$

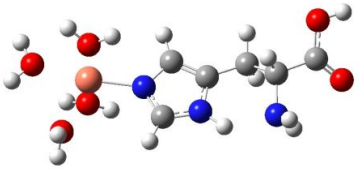

(c-5) $Cu(His)(H_2O)_4^{2+}$

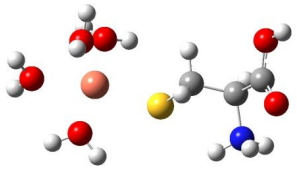

(c-6) $Cu(Cys)(H_2O)_4^{2+}$

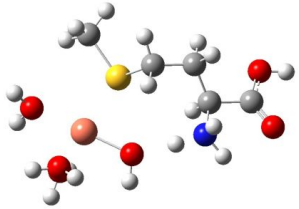

(c-7) $Cu(Met)(H_2O)_4^{2+}$

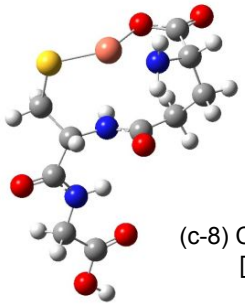

(c-8) Cu(II)-GSH complex
$[Cu(GS)H]^0$

Fig.14

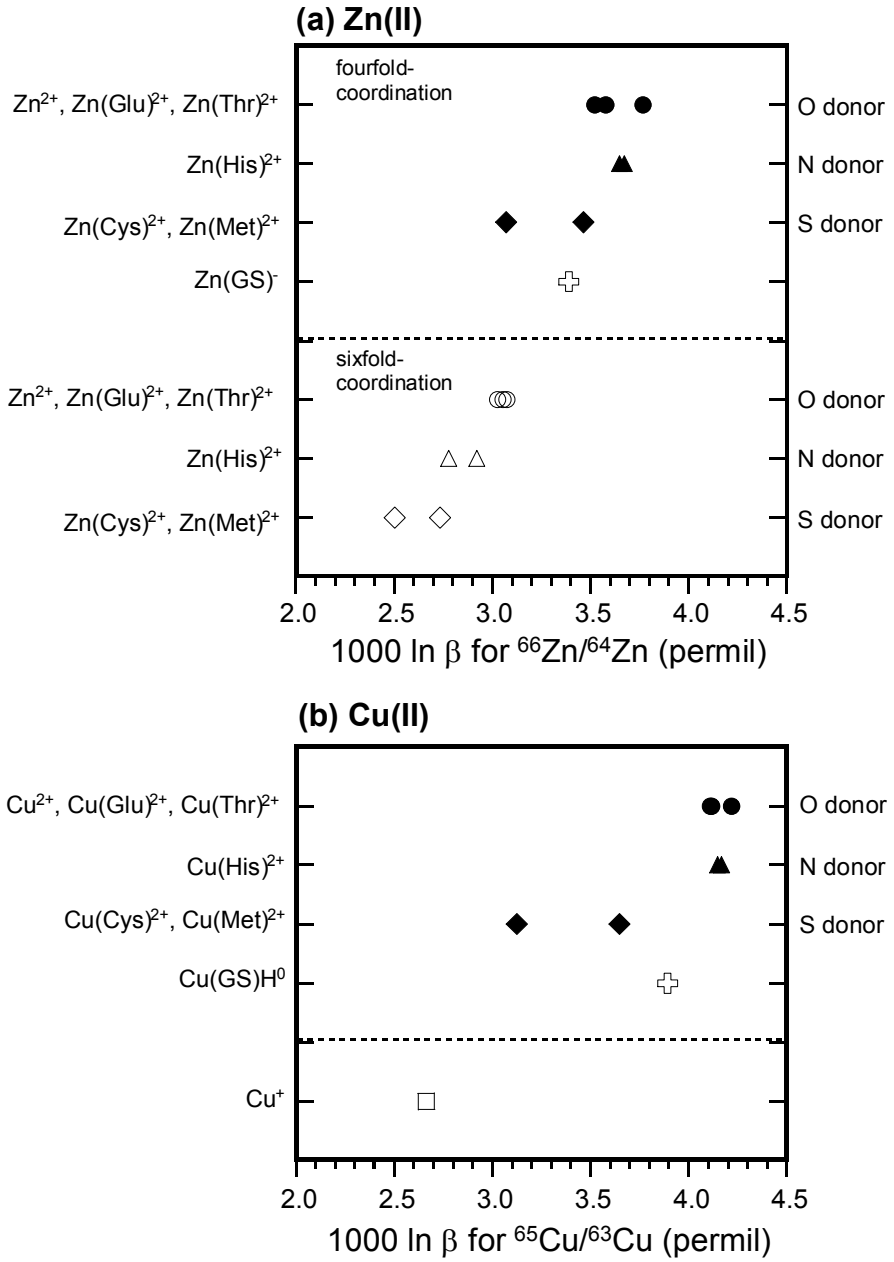
(a) Zn(II)
fourfold-coordination
sixfold-coordination
Zn2+, Zn(Glu)2+, Zn(Thr)2+
Zn(His)2+
Zn(Cys)2+, Zn(Met)2+
Zn(GS)-
O donor
N donor
S donor
2.0
2.5
3.0
3.5
4.0
4.5
1000 ln β for 66Zn/64Zn (permil)
(b) Cu(II)
Cu2+, Cu(Glu)2+, Cu(Thr)2+
Cu(His)2+
Cu(Cys)2+, Cu(Met)2+
Cu(GS)H0
Cu+
1000 ln β for 65Cu/63Cu (permil)

Supporting Information

Density Functional Theory Estimation of Isotope Fractionation of Fe, Ni, Cu, and Zn Among Species Relevant to Geochemical and Biological Environments

Toshiyuki Fujii[1]*, Frédéric Moynier[2], Janne Blichert-Toft[3], and Francis Albarède[3]

[1] Research Reactor Institute, Kyoto University, 2-1010 Asashiro Nishi, Kumatori, Sennan, Osaka 590-0494, Japan

[2] Institut de Physique du Globe de Paris, Sorbonne Paris Cité, Université Paris Diderot, CNRS, 1 rue Jussieu, 75005, Paris, France

[3] Ecole Normale Supérieure de Lyon, Université de Lyon 1, CNRS, 46, Allee d'Italie, 69364 Lyon Cedex 7, France

Table S1. Optimized structure Cartesian coordinates of Zn(II) complexes.

$Zn(H_2O)_6^{2+}$

Zn	0.000026	0.000014	-0.000010
O	0.612463	-1.838912	-0.878282
O	-1.384498	-1.050191	1.228861
O	1.503404	-0.217831	1.489653
O	1.384546	1.050202	-1.228858
O	-1.503503	0.217749	-1.489545
O	-0.612487	1.838946	0.878196
H	2.303939	1.251699	-1.006328
H	1.212923	1.409191	-2.110385
H	0.270221	-2.717425	-0.662548
H	1.280310	-1.948331	-1.569258
H	-1.212869	-1.409192	2.110381
H	-2.303892	-1.251681	1.006332
H	-1.682200	-0.393479	-2.217494
H	-2.125345	0.954279	-1.568664
H	-1.280341	1.948337	1.569170
H	-0.270256	2.717469	0.662488
H	2.125240	-0.954366	1.568780
H	1.682084	0.393386	2.217617

$ZnCl(H_2O)_5^{+}$

Zn	-0.180338	-0.029988	-0.086367
Cl	-2.359692	-0.364869	-0.464125
O	0.017984	-0.069148	2.116516
O	1.913451	0.310455	0.148381
O	-0.469724	2.134093	0.200672
O	0.289817	-0.058811	-2.249425
O	0.072240	-2.246607	0.183937
H	0.680290	0.642784	-2.785399
H	-0.547619	-0.297163	-2.674361
H	2.214903	0.256898	1.064866
H	2.622024	-0.007593	-0.423181
H	0.107589	2.896764	0.076394

H	-1.372087	2.397323	-0.027047
H	0.731065	-2.867416	-0.150595
H	-0.799596	-2.609107	-0.033948
H	-0.507402	0.595266	2.581325
H	-0.218643	-0.926438	2.494922

$ZnCl_2(H_2O)_4$

Zn	0.000057	0.001479	0.000449
Cl	2.298580	-0.009645	0.007299
Cl	-2.298479	0.012577	-0.006437
O	0.005415	1.832372	1.338329
O	-0.004213	-1.829651	-1.337181
O	-0.012441	-1.336301	1.831427
O	0.011375	1.339144	-1.830575
H	0.778046	-1.778869	-1.900637
H	-0.780481	-1.770724	-1.908088
H	0.763213	-1.908616	1.778482
H	-0.795300	-1.898317	1.774447
H	0.792398	1.903756	-1.773208
H	-0.766224	1.908934	-1.778206
H	-0.774994	1.780949	1.904335
H	0.783594	1.773879	1.906700

$ZnCl_3(H_2O)^-$

Zn	-0.014019	-0.024136	0.084944
Cl	2.270336	0.023341	0.262670
Cl	-1.077383	-1.770294	-0.812798
Cl	-1.027117	2.025090	0.264056
O	-0.021341	-0.025761	2.475465
H	0.941440	0.078216	2.427447
H	-0.377791	0.874395	2.419510

$ZnCl_4^{2-}$

Zn	0.000238	-0.000337	-0.000044
Cl	-0.515644	-0.728532	2.195323
Cl	-1.732854	-0.658214	-1.477573
Cl	0.202003	2.361543	-0.021691

Cl	2.046075	-0.974202	-0.695982

$ZnSO_4(H_2O)_5$

Zn	0.083898	-0.105521	-0.003450
S	0.282612	2.898252	0.474807
O	0.055116	0.097291	2.083435
O	2.166439	0.142821	-0.124202
O	0.008340	-0.072862	-2.241333
O	0.260230	-2.259594	0.014772
O	-0.398684	1.804597	-0.465980
O	-0.068284	4.230640	0.017707
O	-0.247189	2.564428	1.860762
O	1.762175	2.579955	0.413382
O	-2.154948	-0.097850	0.096459
H	2.515003	0.091137	-1.021640
H	2.158605	1.150490	0.115266
H	-0.083026	1.141057	2.138988
H	0.880213	-0.081483	2.547761
H	1.173226	-2.547075	0.139509
H	-0.277815	-2.740912	0.654357
H	-2.079154	0.863711	-0.078597
H	-2.495338	-0.166184	0.996914
H	-0.705841	-0.475505	-2.747270
H	-0.169005	0.887882	-2.195682

$Zn(OH)_2(H_2O)_4$

Zn	-0.063224	0.000870	-0.035787
O	-0.083285	-0.521389	1.848932
O	-0.838479	0.106545	-2.162500
O	-0.323524	-2.373685	0.085427
O	1.500768	0.531654	-1.083524
O	-2.269127	-0.121771	0.477831
O	-0.122743	2.372221	-0.324229
H	-1.295122	0.953497	-2.232241
H	0.098715	0.288563	-2.378711
H	-0.079977	-2.130015	1.008437
H	0.330925	-2.995810	-0.245339

H	-1.934474	-0.295256	1.381266
H	-2.567831	-0.974233	0.138951
H	-0.047405	2.993992	0.405488
H	0.785451	2.135836	-0.624283
H	0.533448	-0.142511	2.478088
H	2.367847	0.161213	-0.908252

$ZnHCO_3(H_2O)_3^+$

Zn	0.019328	0.198704	-0.033726
O	2.034268	-0.028613	0.344280
O	1.169426	1.905321	-0.271140
O	3.388661	1.727865	0.131851
O	-0.349392	-1.024681	-1.654930
O	-1.695870	1.374920	-0.214476
O	-0.360675	-0.931459	1.662662
C	2.181023	1.200632	0.066375
H	0.354322	-1.605697	-1.974836
H	-0.893856	-0.771390	-2.411535
H	-2.574418	1.309351	0.180177
H	-1.465476	2.312999	-0.282336
H	0.457420	-1.200743	2.104778
H	-1.081202	-1.493174	1.972429
H	3.342102	2.665258	-0.105299

$ZnCO_3(H_2O)_3$

Zn	-0.354832	-0.136112	-0.013998
O	1.710998	-0.254434	0.064240
O	2.742997	1.777514	0.017787
O	0.479534	1.610019	-0.051983
O	-0.089696	-1.346745	1.698573
O	0.081797	-1.430761	-1.642625
O	-2.234571	0.857382	0.008699
C	1.736543	1.106243	0.011089
H	-0.335515	-1.064674	2.587063
H	0.875818	-1.181957	1.581755
H	-0.036564	-1.192638	-2.569129

H	1.023181	-1.236920	-1.400225
H	-3.009807	0.794572	-0.560422
H	-1.871200	1.756124	-0.063340

Table S2. Optimized structure Cartesian coordinates of Ni(II) complexes.

$Ni(H_2O)_6^{2+}$

Ni	0.000056	0.000036	-0.000025
O	0.635333	-1.815809	-0.808912
O	-1.325485	-1.022179	1.246374
O	1.498116	-0.134704	1.445983
O	1.325691	1.022184	-1.246427
O	-1.498496	0.134410	-1.445539
O	-0.635475	1.815900	0.808641
H	2.243391	1.240743	-1.034035
H	1.137818	1.356966	-2.133909
H	0.299529	-2.691230	-0.572423
H	1.297263	-1.929057	-1.504630
H	-1.137561	-1.356958	2.133845
H	-2.243242	-1.240563	1.034047
H	-1.660503	-0.494908	-2.161596
H	-2.124628	0.864679	-1.544054
H	-1.297307	1.928970	1.504485
H	-0.299448	2.691354	0.572592
H	2.125096	-0.864347	1.543752
H	1.660551	0.494916	2.161677

$NiCl(H_2O)_5^{+}$

Ni	-0.188832	0.000008	-0.000167
Cl	2.099674	0.001078	0.000320
O	-0.281079	-1.307078	1.658158
O	-0.141090	1.741304	1.212221
O	-0.281909	1.307052	-1.658346
O	-0.138826	-1.741463	-1.212295
O	-2.320528	-0.001197	-0.000006
H	-0.433838	2.227389	-1.402632
H	0.591749	1.296049	-2.077871
H	0.592419	-1.294888	2.077990
H	-0.431569	-2.227606	1.402271
H	0.791144	-1.908928	-1.430018

H	-0.661221	-1.892194	-2.010071
H	-2.886052	-0.377906	0.684148
H	-2.886990	0.374437	-0.683973
H	0.788572	1.909849	1.430400
H	-0.664060	1.891352	2.009745

$NiCl_2(H_2O)_4$

Ni	-0.000157	0.001903	0.000672
Cl	2.339396	-0.010945	0.009962
Cl	-2.339561	0.013070	-0.010490
O	0.015470	1.731777	1.247265
O	0.005631	-1.729384	-1.244906
O	-0.022685	-1.244406	1.731386
O	0.001531	1.247600	-1.730483
H	0.799522	-1.679874	-1.794065
H	-0.765946	-1.677141	-1.824361
H	0.749276	-1.823844	1.684798
H	-0.816075	-1.793458	1.673711
H	0.775193	1.824285	-1.679310
H	-0.790338	1.799700	-1.680303
H	-0.758070	1.687023	1.824654
H	0.807359	1.674658	1.798607

$NiSO_4(H_2O)_5$

Ni	1.030205	-0.017393	-0.010801
S	-2.038870	0.021551	0.080203
O	1.511958	1.520299	1.415772
O	1.243632	-1.633589	1.405999
O	3.105673	-0.033782	-0.541456
O	0.475420	-1.492837	-1.339329
O	0.527004	1.637461	-1.160623
O	-3.204264	0.037689	0.944878
O	-1.919486	-1.242106	-0.759467
O	-1.908814	1.240736	-0.812237
O	-0.713573	0.032259	0.956047
H	1.326133	2.294752	0.863065
H	0.704577	1.411211	1.946856

H	0.612114	-1.365111	-2.283533
H	-0.576535	-1.478991	-1.180336
H	1.164854	-2.462472	0.915768
H	0.335928	-1.445342	1.721699
H	0.788304	1.731444	-2.081665
H	-0.520545	1.578390	-1.112863
H	3.612012	0.348376	0.187079
H	3.493994	-0.898158	-0.720676

$NiOH(H_2O)_5^+$

Ni	-0.011743	-0.033958	-0.019375
O	-1.369819	1.425809	-0.750138
O	-1.173161	-1.524313	-0.966001
O	1.480111	0.001303	-1.264944
O	1.083010	1.714018	0.557346
O	-1.381182	-0.154773	1.600134
O	1.442472	-1.291971	0.898868
H	1.708687	1.471289	-0.167302
H	1.590263	1.829766	1.369643
H	-1.812515	1.304794	-1.599407
H	-0.953704	2.299031	-0.760473
H	-0.750790	-2.079633	-1.632936
H	-1.812083	-2.067577	-0.488270
H	-2.047389	0.544609	1.619974
H	-1.099410	-0.310218	2.509944
H	1.408994	-2.221772	1.149977
H	1.993666	-1.204737	0.088608
H	1.432435	0.024780	-2.223559

$Ni(OH)_2(H_2O)_4$

Ni	0.000055	-0.000065	-0.000005
O	-1.140086	-1.680443	0.775350
O	-1.481103	1.456205	0.706970
O	1.589880	0.173538	1.198347
O	1.481122	-1.456282	-0.707011
O	-1.589716	-0.173738	-1.198358

O	1.140039	1.680536	-0.775165
H	1.973761	-1.075498	0.069988
H	1.967987	-1.220885	-1.503978
H	-1.642771	-1.546490	-0.067214
H	-0.626228	-2.488863	0.667806
H	-1.967934	1.220850	1.503969
H	-1.973706	1.075390	-0.070034
H	-1.525365	-0.131507	-2.154479
H	0.625768	2.488728	-0.667875
H	1.642364	1.546857	0.067662
H	1.525606	0.131373	2.154476

$NiHCO_3(H_2O)_4^+$

Ni	-0.110353	-0.099469	-0.028369
O	1.798355	0.177802	0.682150
O	2.988246	1.918155	-0.144407
O	0.908065	1.495907	-0.833658
O	-1.024864	1.239110	1.339183
O	0.487402	-1.230438	-1.725608
O	-0.613287	-1.768540	1.141127
O	-2.022640	-0.193743	-0.896406
C	1.887938	1.182948	-0.092496
H	-1.420562	-2.291387	1.070209
H	0.003099	-2.224961	1.726206
H	-0.713069	2.148383	1.231699
H	-1.034724	1.052884	2.286538
H	-2.646653	0.515230	-0.695152
H	-2.092038	-0.388108	-1.839672
H	0.926981	-2.086353	-1.646272
H	1.021527	-0.694506	-2.328648
H	3.640247	1.557173	0.473854

$NiCO_3(H_2O)_4$

Ni	-0.265136	-0.189575	-0.042189
O	1.608155	-0.126476	0.604163
O	2.818925	1.741848	0.141828

O	0.663119	1.502040	-0.541112
O	-1.215795	1.358052	1.254975
O	0.739949	-1.537356	-1.435772
O	-0.770329	-1.951614	1.082100
O	-2.211985	-0.018517	-0.934010
C	1.793679	1.100790	0.074914
H	-0.875923	-2.726314	0.516465
H	0.034077	-2.102161	1.597337
H	-0.547901	1.921046	0.791899
H	-1.016706	1.394577	2.197094
H	-2.638778	0.574557	-0.298150
H	-2.201752	0.455944	-1.773846
H	1.533055	-1.293194	-0.905345
H	0.902104	-1.200641	-2.324708

$NiHS(H_2O)_5^+$

Ni	-0.159936	0.003308	0.017467
S	2.160958	-0.157296	-0.084517
O	-0.216575	1.599864	-1.422409
O	-0.331481	-1.601626	-1.375277
O	-0.635103	-1.500886	1.459436
O	0.131673	1.620888	1.402405
O	-2.299151	0.234255	-0.057488
H	-0.638819	-2.369825	1.034805
H	-0.104622	-1.589152	2.261314
H	0.353749	1.528705	-2.199114
H	0.024514	2.429355	-0.987208
H	1.089986	1.552249	1.562211
H	-0.306800	1.866775	2.226622
H	-2.733286	0.952479	-0.532350
H	-2.907821	-0.100228	0.611248
H	0.563574	-1.753242	-1.718118
H	-0.961135	-1.688406	-2.102417
H	2.376599	-1.212273	0.728241

$Ni(HS)_2(H_2O)_4$

Ni	-0.002734	0.018011	0.004964

S	2.410727	-0.061575	0.007929
S	-2.416191	-0.042234	-0.050189
O	0.258801	1.193986	1.818633
O	-0.243885	1.814357	-1.203721
O	0.169682	-1.228121	-1.773016
O	-0.196442	-1.779824	1.217637
H	-0.199079	-0.857113	-2.583564
H	1.139500	-1.125367	-1.816684
H	1.223495	1.030151	1.811833
H	-0.091995	0.746661	2.598587
H	0.235685	-2.560803	0.850892
H	-1.151355	-1.860790	1.030869
H	-2.670671	0.708932	1.041597
H	0.034672	2.616858	-0.746065
H	-1.217894	1.767481	-1.123533
H	2.648527	1.029832	-0.748863

$NiH_2PO_4(H_2O)_5^+$

Ni	-0.103023	-0.037123	-0.043001
P	-0.191908	3.025478	0.397924
O	-0.265913	0.261352	2.003092
O	1.923107	0.481298	-0.290343
O	-0.003812	-0.578044	-2.096143
O	0.419862	-2.067284	0.243047
O	-0.619676	1.843872	-0.485433
O	-0.815778	4.391404	-0.156350
O	1.398595	3.176502	0.013423
O	-2.194292	-0.321476	-0.215109
O	-0.405059	2.845875	1.875927
H	0.382688	-0.062516	2.637884
H	-0.364819	1.256858	2.159592
H	-2.475185	0.601812	-0.320228
H	-2.716249	-0.693185	0.507089
H	0.078701	-2.652718	0.929457
H	0.463169	-2.574038	-0.578544
H	0.658401	-0.055607	-2.568601

H	-0.832510	-0.482831	-2.584009
H	2.662676	0.039345	0.141639
H	2.052853	1.450597	-0.219392
H	1.831869	3.965018	0.366116
H	-1.417802	4.819897	0.465679

$NiHPO_4(H_2O)_5$

Ni	-0.270102	-0.179779	0.036626
P	-0.145193	2.816898	0.153754
O	-0.459548	0.247129	2.091354
O	1.688075	0.111157	-0.253432
O	-0.104934	-0.420638	-2.110583
O	0.404166	-2.201530	0.293606
O	-0.966637	1.669755	-0.486934
O	-0.763123	4.218934	-0.349000
O	1.303541	2.804357	-0.535736
O	-2.390656	-0.501068	0.119124
O	-0.099144	2.761008	1.667760
H	0.163725	-0.158819	2.702051
H	-0.316496	1.254857	2.120478
H	-2.563775	0.428577	-0.115507
H	-2.599616	-0.566323	1.060041
H	0.053034	-2.824417	-0.353808
H	1.281041	-1.915594	-0.027472
H	0.849316	-0.230021	-2.095594
H	-0.521379	0.415414	-2.369142
H	2.287425	0.157566	0.497837
H	1.640885	1.868361	-0.537195
H	-0.828592	4.845707	0.380116

$NiH_2(cit)(H_2O)_3^+$

Ni	1.172985	-0.151442	0.183709
O	-0.369626	0.068338	1.372212
O	-2.437965	-0.546448	1.941342
O	0.526813	1.383695	-1.059016
O	-0.320677	3.314064	-1.590350

O	-1.339481	-3.130598	-1.214519
O	0.295163	-1.775346	-0.727440
O	-3.587127	0.166385	-0.207265
O	2.903835	-0.547916	-0.933330
O	1.842913	-1.382320	1.780260
O	2.416252	1.278921	1.150331
C	-2.185350	0.239454	-0.288800
C	-1.868157	1.710644	-0.656283
C	-1.748847	-0.732053	-1.461150
C	-1.618565	-0.130721	1.137418
C	-0.869516	-1.900786	-1.098186
C	-0.474092	2.087882	-1.099561
H	-2.127655	2.345423	0.199143
H	-2.563843	1.993447	-1.455639
H	-1.194464	-0.189090	-2.229944
H	-2.681805	-1.070237	-1.911985
H	3.544866	0.166438	-1.034715
H	2.870936	-1.039059	-1.762806
H	1.049167	-1.463582	2.332606
H	2.192441	-2.269868	1.632507
H	2.694083	0.960780	2.020013
H	2.123719	2.191630	1.261554
H	-3.774925	-0.164811	0.694963
H	-2.265246	-3.142829	-1.495396
H	-1.154829	3.803849	-1.627377

$NiH(cit)(H_2O)_3$

Ni	1.214400	-0.237596	0.053464
O	-0.354280	-0.071713	1.285019
O	-2.486007	-0.179788	1.935564
O	0.521868	0.974943	-1.404894
O	0.249992	2.884328	-0.276195
O	-1.560627	-3.200321	-0.773491
O	0.275456	-2.015752	-0.644284
O	-3.551679	0.168901	-0.345946
O	2.922993	-0.378102	-1.199232

O	1.868966	-1.456023	1.680717
O	2.194135	1.476070	0.845917
C	-2.139725	0.226168	-0.390916
C	-1.720308	1.647331	-0.866509
C	-1.683702	-0.856750	-1.450575
C	-1.622626	-0.037336	1.075036
C	-0.915854	-2.039430	-0.926992
C	-0.214555	1.893406	-0.853207
H	-2.205988	2.383080	-0.226028
H	-2.105047	1.782610	-1.882914
H	-1.027780	-0.383343	-2.178993
H	-2.599849	-1.182269	-1.945172
H	3.603907	0.152710	-0.764746
H	2.573175	0.189346	-1.904894
H	1.040100	-1.335239	2.178353
H	1.894898	-2.387351	1.428165
H	2.114623	1.563717	1.802775
H	1.635131	2.206591	0.452179
H	-3.758140	0.080233	0.606230
H	-2.495829	-3.097153	-0.994469

$Ni(cit)(H_2O)_3^-$

Ni	1.247018	-0.120799	0.156658
O	-0.313941	0.077934	1.405240
O	-2.461413	-0.067362	1.987684
O	0.660257	1.190028	-1.305813
O	0.236185	3.069514	-0.178227
O	-1.242938	-3.148416	-0.782270
O	0.550850	-1.828511	-0.640517
O	-3.457290	0.238292	-0.337971
O	2.819944	-0.467343	-1.329422
O	1.785345	-1.615930	1.691021
O	2.112636	1.589440	1.136068
C	-2.031269	0.266770	-0.345354
C	-1.634115	1.702556	-0.815525
C	-1.543283	-0.834013	-1.360957

C	-1.573343	0.060360	1.142313
C	-0.724239	-2.043191	-0.873832
C	-0.147298	2.043690	-0.766081
H	-2.178774	2.423787	-0.205669
H	-1.986818	1.803155	-1.848121
H	-0.950481	-0.346444	-2.135605
H	-2.455993	-1.229915	-1.803067
H	2.488049	0.285353	-1.845171
H	2.314665	-1.230927	-1.655196
H	1.007745	-1.373431	2.220540
H	1.431794	-2.282529	1.069418
H	1.688178	1.582573	2.002712
H	1.644152	2.315272	0.649025
H	-3.677976	0.091351	0.602077

$Ni(cit)_2^{4-}$

Ni	-0.000202	-0.002402	-0.000524
O	1.767611	-0.052490	-1.156130
O	3.891461	-0.194414	-1.849616
O	0.646092	-1.685758	1.104346
O	1.707338	-3.235136	2.326307
O	2.260714	2.226565	2.947971
O	0.940601	1.229555	1.436990
O	4.985111	-0.547281	0.352533
O	-1.768037	0.044813	1.155035
O	-3.893118	0.172971	1.847365
O	-0.643747	1.680601	-1.106676
O	-1.704402	3.234571	-2.323258
O	-2.264341	-2.225371	-2.951545
O	-0.944100	-1.234405	-1.436691
O	-4.984670	0.550622	-0.351729
C	3.530380	-0.417957	0.507946
C	3.110065	-1.768515	1.136941
C	3.371358	0.819047	1.424865
C	2.985542	-0.200456	-0.953132
C	2.052498	1.446670	1.975008
C	1.680085	-2.231945	1.557469

C	-3.530208	0.419016	-0.507668
C	-3.107035	1.773318	-1.126552
C	-3.373274	-0.811538	-1.433624
C	-2.986300	0.189825	0.951952
C	-2.055266	-1.446230	-1.978200
C	-1.677723	2.231139	-1.554721
H	3.454288	-2.544581	0.440988
H	3.733255	-1.887331	2.030223
H	3.991782	0.617881	2.305130
H	3.870625	1.646420	0.903907
H	5.044531	-0.445758	-0.628262
H	-3.440872	2.544922	-0.420573
H	-3.736541	1.903915	-2.013635
H	-3.985388	-0.599009	-2.317134
H	-3.883052	-1.638900	-0.923044
H	-5.045061	0.437622	0.627737

Table S3. Optimized structure Cartesian coordinates of Fe(II) complexes.

$Fe(H_2O)_6^{2+}$

Fe	0.000854	0.001698	0.002572
O	2.180247	-0.000258	-0.000286
O	-0.000085	2.169469	0.048148
O	-0.000079	0.019597	2.143082
O	-2.179755	-0.000258	-0.000306
O	-0.000083	-2.168247	-0.048653
O	-0.000067	-0.019935	-2.141410
H	2.757238	0.758701	-0.163289
H	2.756999	-0.759457	0.162445
H	-2.756749	0.758877	-0.162394
H	-2.756510	-0.759631	0.161516
H	-0.000132	2.727559	0.838279
H	-0.000099	2.761464	-0.716868
H	-0.000096	-2.760761	0.715924
H	-0.000131	-2.725777	-0.839134
H	0.778586	0.035119	2.717459
H	-0.778875	0.035167	2.717278
H	0.778537	-0.035638	-2.715771
H	-0.778801	-0.035689	-2.715591

$FeCl(H_2O)_5^{+}$

Fe	-0.047300	-0.000408	0.000859
Cl	2.203867	0.003597	-0.003518
O	-0.457746	-1.508774	1.578056
O	-0.020171	1.916027	1.244654
O	-0.462908	1.507311	-1.578014
O	-0.016908	-1.917274	-1.242924
O	-2.209371	0.000166	0.000466
H	-0.276160	2.392027	-1.235421
H	-0.006131	1.443737	-2.426347
H	-0.001871	-1.446736	2.426955
H	-0.272815	-2.393633	1.234867
H	0.902338	-2.083057	-1.496692

H	-0.573264	-2.220548	-1.970658
H	-2.769369	-0.516006	0.592185
H	-2.764733	0.517121	-0.594965
H	0.898299	2.085132	1.498940
H	-0.578192	2.218574	1.971433

$FeCl_2(H_2O)_4$

Fe	-0.000024	0.001477	0.000504
Cl	2.334141	-0.009280	0.007543
Cl	-2.334144	0.012223	-0.006716
O	0.078543	1.840318	1.349602
O	0.069227	-1.838303	-1.347894
O	-0.085932	-1.346992	1.839492
O	-0.061731	1.350505	-1.839056
H	0.911186	-1.784062	-1.818346
H	-0.631022	-1.791656	-2.010036
H	0.613001	-2.010870	1.798032
H	-0.928624	-1.815339	1.778651
H	0.643723	2.007186	-1.793583
H	-0.899928	1.827488	-1.783544
H	-0.625452	1.800068	2.008185
H	0.917582	1.778202	1.824302

$FeSO_4(H_2O)_5$

Fe	0.963581	-0.036794	-0.006732
S	-2.103307	0.091907	0.053528
O	1.649029	1.782860	1.255139
O	1.477238	-2.007631	1.096753
O	3.131664	-0.118186	-0.265691
O	0.328662	-1.668384	-1.340920
O	0.473868	1.753323	-1.191188
O	-3.230431	0.100233	0.967668
O	-2.062834	-1.114766	-0.863859
O	-1.957490	1.365442	-0.756542
O	-0.742512	-0.001777	0.881951
H	1.256671	2.404394	0.618548
H	1.084063	1.821831	2.037428

H	0.509710	-1.731155	-2.284017
H	-0.706114	-1.528039	-1.232110
H	1.039658	-2.539019	0.410149
H	0.899802	-2.057485	1.869350
H	0.663152	1.882966	-2.125814
H	-0.569766	1.692259	-1.091180
H	3.503611	0.619263	0.237352
H	3.441460	-0.926858	0.164570

$FeOH(H_2O)_5^+$

Fe	0.000222	-0.082203	-0.234095
O	-1.385300	1.499494	-0.807072
O	-1.362396	-1.640465	-1.038600
O	1.626413	-0.015355	-1.187092
O	1.015261	1.962395	0.444104
O	-1.216390	-0.232987	1.565299
O	1.340695	-1.470531	1.051196
H	1.733272	1.684574	-0.157804
H	1.421939	2.305812	1.247746
H	-1.982650	1.568073	-1.560725
H	-0.932503	2.347947	-0.695090
H	-1.276481	-2.048690	-1.908185
H	-1.834126	-2.265937	-0.475686
H	-1.923493	0.392835	1.765067
H	-0.752909	-0.432276	2.388484
H	1.345997	-2.420502	1.215583
H	2.062374	-1.290899	0.421844
H	1.847915	-0.134837	-2.112884

$Fe(OH)_2(H_2O)_4$

Fe	-0.000260	0.000061	-0.000029
O	-1.058841	-1.938205	0.755668
O	-1.582364	1.723203	0.679660
O	1.579209	0.145930	1.133767
O	1.581590	-1.721695	-0.682316
O	-1.579980	-0.147432	-1.133066

O	1.061003	1.937944	-0.753685
H	2.030643	-1.233419	0.047770
H	2.137739	-1.643064	-1.463873
H	-1.641739	-1.754874	-0.007114
H	-0.462848	-2.639917	0.465932
H	-2.138700	1.647132	1.461216
H	-2.031509	1.233371	-0.049300
H	-1.587178	-0.072456	-2.089430
H	0.464940	2.640072	-0.465133
H	1.641982	1.753578	0.010360
H	1.585987	0.069477	2.090023

$Fe_2(OH)_6^{2-}$

Fe	-0.038997	0.017342	0.054048
Fe	2.456853	0.099663	-1.979911
O	-0.033815	0.176443	2.041927
O	1.859052	-0.792624	-0.199426
O	0.558526	0.908855	-1.726623
O	2.451545	-0.062361	-3.967606
O	4.394981	0.327263	-1.569708
O	-1.977758	-0.204885	-0.356247
H	2.457183	-0.667884	0.542061
H	-0.041131	0.783283	-2.466730
H	3.206491	-0.589848	-4.243923
H	4.794989	0.889356	-2.239515
H	-2.378752	-0.768444	0.311756
H	-0.787289	0.706048	2.318358

$FeHCO_3(H_2O)_4^{+}$

Fe	-0.162404	-0.065415	-0.013894
O	1.922838	0.208264	0.788573
O	3.030830	1.980540	-0.080097
O	0.950870	1.498195	-0.702496
O	-1.579472	0.507537	1.460397
O	-0.151883	-1.655909	-1.417747
O	0.080700	-1.620341	1.631585
O	-1.500684	0.759945	-1.673705

C	1.962653	1.206530	0.018041
H	-0.131287	-2.557387	1.716685
H	1.006939	-1.498062	1.888816
H	-2.052502	1.343501	1.547868
H	-1.477784	0.117200	2.338406
H	-2.444842	0.931213	-1.771508
H	-1.028722	1.541848	-1.996280
H	0.474766	-2.384036	-1.504625
H	-0.507536	-1.454083	-2.293197
H	3.716299	1.648794	0.517592

$FeCO_3(H_2O)_4$

Fe	-0.422145	-0.278536	0.004348
O	1.613924	-0.237547	0.160285
O	2.680734	1.765842	-0.004654
O	0.418263	1.577865	-0.161918
O	-1.684261	0.995589	1.365073
O	0.242421	-1.943393	-1.359961
O	-0.078193	-1.831778	1.590645
O	-1.708692	0.646220	-1.589203
C	1.671744	1.101790	-0.002484
H	-0.063810	-2.747624	1.287163
H	0.853811	-1.538319	1.587301
H	-1.007703	1.685249	1.197250
H	-1.699613	0.835286	2.315188
H	-2.546142	1.023755	-1.293974
H	-1.069054	1.385236	-1.583246
H	1.143671	-1.593028	-1.197602
H	0.082435	-1.891365	-2.308839

$FeHS(H_2O)_5^+$

Fe	-0.048342	-0.011667	0.026668
S	2.256730	-0.248663	-0.175267
O	-0.277421	1.731376	-1.371323
O	-0.351898	-1.793478	-1.417257
O	-0.719907	-1.646013	1.378368
O	0.228017	1.787126	1.438293

O	-2.197966	0.334713	0.061537
H	-0.664687	-2.494870	0.918691
H	-0.445888	-1.794775	2.291278
H	0.096778	1.747232	-2.260844
H	0.024774	2.535731	-0.928118
H	1.175475	1.797060	1.638744
H	-0.239491	2.093368	2.225168
H	-2.646113	0.999552	-0.474209
H	-2.854296	-0.185647	0.538556
H	0.556783	-1.952978	-1.715328
H	-0.934422	-1.945198	-2.171950
H	2.448199	-1.137923	0.821848

$Fe(HS)_2(H_2O)_4$

Fe	0.000245	-0.000211	-0.000454
S	1.760517	0.157825	1.643969
S	-1.759883	-0.157490	-1.644850
O	-1.022401	-1.849206	0.908895
O	-1.416849	1.644483	0.883469
O	1.416550	-1.645240	-0.883810
O	1.022224	1.850069	-0.908245
H	2.124316	-1.478983	-0.238019
H	1.795934	-1.557778	-1.765622
H	-1.493686	-2.146263	0.115657
H	-0.360082	-2.525631	1.094704
H	-1.796964	1.555959	1.764851
H	-2.123870	1.477756	0.236940
H	-1.108031	0.214862	-2.764208
H	0.359572	2.526724	-1.092050
H	1.493790	2.145437	-0.114503
H	1.108292	-0.212606	2.763726

$Fe_2S_2(H_2O)_4$

Fe	0.257577	-0.256141	0.070816
Fe	2.106584	0.270263	1.574775
S	2.405917	0.011903	-0.681692
S	-0.041641	0.001504	2.327142

O	2.422189	2.080682	2.795251
O	3.886707	-0.936719	2.067388
O	-0.584911	0.941502	-1.579213
O	-0.984481	-2.079540	0.002154
H	1.512396	2.156280	3.124635
H	2.647380	2.916885	2.371088
H	3.796261	-1.730477	2.606928
H	4.090593	-1.220622	1.162090
H	-1.101490	1.733422	-1.391538
H	0.261755	1.227430	-1.957768
H	-1.120977	-2.158333	0.959746
H	-0.599937	-2.908721	-0.304516

$FeH_2PO_4(H_2O)_5^+$

Fe	-0.169024	0.000675	-0.054911
P	-0.078159	3.064937	0.479448
O	-0.027447	0.206389	2.106745
O	1.991386	0.549931	-0.349914
O	0.019383	-0.676676	-2.138068
O	0.263956	-2.081088	0.306873
O	-0.673480	1.894527	-0.326046
O	-0.871327	4.416306	0.144781
O	1.359830	3.288377	-0.273824
O	-2.379637	-0.281081	-0.366905
O	0.077681	2.828678	1.953640
H	-0.681469	-0.109927	2.739820
H	0.069553	1.192405	2.267295
H	-2.757963	0.608661	-0.398467
H	-3.038326	-0.866154	0.024531
H	0.600778	-2.461582	1.126701
H	0.456563	-2.688962	-0.417590
H	0.760117	-0.313964	-2.640755
H	-0.758435	-0.645856	-2.709146
H	2.693253	0.275497	0.252001
H	2.067300	1.521268	-0.437713
H	1.828140	4.095993	-0.024308
H	-1.286776	4.816134	0.919529

$FeHPO_4(H_2O)_5$, $[FeH_2PO_4OH(H_2O)_3]\cdot H_2O$

Fe	-0.337893	0.106012	0.255407
P	-0.288527	3.103394	0.749932
O	0.382426	0.318253	2.269365
O	1.194712	0.496035	-0.874913
O	0.990382	-1.887125	-2.075182
O	-0.279674	-2.077685	0.245497
O	-1.270686	1.969472	0.388930
O	-1.093669	4.500524	0.791672
O	0.683020	3.318504	-0.516594
O	-2.243436	-0.034789	-0.826690
O	0.458566	2.878967	2.048964
H	0.023453	-0.041693	3.085257
H	0.473864	1.325858	2.374244
H	-2.508251	0.885766	-0.643756
H	-2.992621	-0.620147	-0.679629
H	0.285337	-2.531779	0.879601
H	0.106236	-2.253837	-0.652546
H	1.164158	-0.933061	-1.856347
H	0.710840	-1.930400	-2.993824
H	2.065360	0.489554	-0.462480
H	0.964558	2.447403	-0.871942
H	-0.850398	5.009270	1.573061

$FeH_4(PO_4)_2(H_2O)_4$

Fe	0.003758	0.001170	0.002735
P	0.148926	-3.183234	0.365685
P	-0.152621	3.185187	-0.354165
O	-0.262402	-0.507203	2.111910
O	2.174293	-0.478191	-0.087391
O	-0.335720	-2.007413	-0.462456
O	1.754535	-3.266766	-0.015094
O	-0.400645	-4.582644	-0.241782
O	-0.051502	-3.144668	1.858907
O	0.281579	0.513455	-2.109511

O	-2.168676	0.476961	0.058120
O	0.329886	2.009043	0.474752
O	-1.759544	3.267339	0.020244
O	0.392186	4.585070	0.256255
O	0.054360	3.147321	-1.846629
H	2.292714	-1.442190	-0.183607
H	2.529310	-0.072712	-0.887196
H	-0.171876	-1.484697	2.273239
H	0.256227	-0.022135	2.761271
H	2.222598	-3.954127	0.474266
H	-1.006577	-5.008477	0.375506
H	-2.294019	1.437532	0.176396
H	-2.562259	0.044966	0.824981
H	0.186176	1.492138	-2.263418
H	-0.242653	0.032950	-2.757850
H	-2.226132	3.953880	-0.471691
H	1.008077	5.007443	-0.353478

$FeH_3(PO_4)_2(H_2O)_4^-$

Fe	0.087042	-0.000140	-0.054055
P	0.406349	-2.991807	0.382882
P	-0.363186	3.163468	-0.556261
O	-0.562529	-0.474527	2.078171
O	2.277269	-0.387927	-0.036967
O	-0.246937	-1.866404	-0.513873
O	1.924739	-2.940016	0.296215
O	-0.065638	-4.432752	-0.262146
O	-0.226721	-2.912980	1.792762
O	0.366034	0.422777	-2.299946
O	-2.323633	0.451562	0.176184
O	0.264322	2.032157	0.255851
O	-1.844289	3.515559	0.069827
O	0.443988	4.528513	-0.131271
O	-0.519591	2.992612	-2.031869
H	2.296637	-1.396358	0.105014
H	2.527718	-0.255113	-0.957701

H	-0.457048	-1.544748	2.064726
H	0.010722	-0.142578	2.774943
H	-0.975158	-4.602197	0.005111
H	-2.490420	1.402936	0.211830
H	-2.138937	0.174290	1.090234
H	-0.029543	1.309552	-2.462070
H	-0.206600	-0.246254	-2.690914
H	1.347936	4.301436	0.114366
H	-1.768026	3.826070	0.979712

$FeH(cit)(H_2O)_3$

Fe	1.269537	-0.258146	0.089848
O	-0.386824	-0.182106	1.240771
O	-2.518824	-0.111273	1.909262
O	0.534416	1.014547	-1.400870
O	0.209259	2.872675	-0.201385
O	-1.689373	-3.159765	-0.627599
O	0.250903	-2.132176	-0.690410
O	-3.559045	0.114980	-0.414104
O	2.953450	-0.241390	-1.317467
O	1.881110	-1.607955	1.742501
O	2.228948	1.551273	0.891109
C	-2.145677	0.195572	-0.429450
C	-1.728640	1.627423	-0.886517
C	-1.648450	-0.872339	-1.480307
C	-1.653989	-0.057317	1.043146
C	-0.950433	-2.080386	-0.912428
C	-0.224575	1.897134	-0.830655
H	-2.241829	2.351693	-0.254308
H	-2.086407	1.761926	-1.912576
H	-0.938048	-0.404490	-2.157620
H	-2.538272	-1.171183	-2.037002
H	3.741068	0.195783	-0.971294
H	2.527084	0.405113	-1.906219
H	1.074042	-1.462191	2.264017
H	1.856477	-2.535802	1.477551

H	2.245627	1.683813	1.845070
H	1.620035	2.251459	0.513184
H	-3.790751	0.108509	0.535203
H	-2.623171	-2.984115	-0.807488

$Fe(cit)(H_2O)_3^-$

Fe	1.292308	-0.117141	0.133833
O	-0.366594	-0.011088	1.409565
O	-2.533632	-0.041979	1.959919
O	0.681633	1.276247	-1.311981
O	0.187697	3.030769	-0.026408
O	-1.213299	-3.126627	-0.643346
O	0.598517	-1.818134	-0.673719
O	-3.464261	0.215427	-0.399934
O	2.843891	-0.450795	-1.594710
O	1.741090	-1.610188	1.890151
O	2.146624	1.629865	1.141391
C	-2.039555	0.250325	-0.365065
C	-1.638276	1.691371	-0.827430
C	-1.515905	-0.850185	-1.365016
C	-1.620556	0.039279	1.135404
C	-0.690492	-2.039067	-0.837722
C	-0.160449	2.055025	-0.720119
H	-2.214575	2.403057	-0.236279
H	-1.954598	1.782753	-1.872200
H	-0.918353	-0.360249	-2.134882
H	-2.414671	-1.264337	-1.819373
H	2.425289	0.297225	-2.048537
H	2.299673	-1.217992	-1.835073
H	0.878897	-1.321616	2.243176
H	1.505078	-2.345154	1.301762
H	1.876046	1.607376	2.066473
H	1.586072	2.345757	0.725077
H	-3.709948	0.101338	0.538999

$FeH(cit)_2^{3-}$

Fe	-0.251682	-0.259662	0.489097
O	1.796340	-0.094579	-1.251012
O	3.366514	1.523342	-1.230135
O	0.916022	-1.671448	1.373704
O	2.413983	-2.978514	2.398633
O	2.262284	2.049444	3.080993
O	1.144062	1.185469	1.326899
O	4.987350	-0.260132	-0.024364
O	-2.010599	0.404679	1.309215
O	-4.206721	0.590357	1.669126
O	-0.384499	0.993084	-1.292642
O	-1.203343	1.743370	-3.234605
O	-2.687825	-2.809497	-2.040803
O	-1.388514	-1.665698	-0.618336
O	-4.878041	1.144768	-0.687851
C	3.576140	-0.247243	0.371826
C	3.194624	-1.735513	0.522173
C	3.470331	0.574791	1.683091
C	2.867146	0.500080	-0.780333
C	2.157427	1.325735	2.071097
C	2.084187	-2.150193	1.528633
C	-3.513588	0.641325	-0.620059
C	-2.682042	1.730088	-1.356820
C	-3.553549	-0.739196	-1.327658
C	-3.202488	0.525371	0.917844
C	-2.424016	-1.816067	-1.327068
C	-1.329347	1.443249	-2.038039
H	2.917359	-2.132326	-0.458587
H	4.104069	-2.242284	0.848363
H	3.740928	-0.077332	2.519224
H	4.239162	1.351726	1.635525
H	5.104321	0.597938	-0.458232
H	-2.509087	2.552637	-0.652530
H	-3.338220	2.106469	-2.142788
H	-3.797821	-0.551010	-2.378649
H	-4.426910	-1.256057	-0.915512

H	-5.158858	1.033341	0.245686
H	1.046708	0.522849	-1.594775

$Fe(cit)_2^{4-}$

Fe	-0.000039	-0.000247	-0.000155
O	1.885867	-0.050911	-1.118802
O	3.990389	-0.353559	-1.830187
O	0.790434	-1.745435	1.097688
O	1.847505	-3.334686	2.282121
O	2.318697	2.082475	3.057594
O	1.037826	1.177295	1.455078
O	5.102813	-0.539206	0.387058
O	-1.885822	0.049366	1.118675
O	-3.990362	0.351354	1.830245
O	-0.790116	1.745372	-1.097413
O	-1.847134	3.333712	-2.283101
O	-2.319215	-2.082474	-3.057992
O	-1.038184	-1.1771	-1.455713
O	-5.102719	0.539612	-0.386765
C	3.645747	-0.436959	0.540271
C	3.248895	-1.781132	1.203685
C	3.46567	0.81847	1.428891
C	3.096209	-0.265166	-0.927156
C	2.138441	1.374733	2.029283
C	1.815859	-2.29926	1.556174
C	-3.645691	0.437042	-0.540121
C	-3.248544	1.781689	-1.202391
C	-3.466004	-0.817638	-1.429878
C	-3.096155	0.263812	0.927159
C	-2.138831	-1.374533	-2.029847
C	-1.815549	2.298958	-1.5562
H	3.669505	-2.564131	0.56033
H	3.824522	-1.838557	2.13506
H	4.139544	0.675932	2.279885
H	3.886434	1.658806	0.860139
H	5.156305	-0.522278	-0.598597

H	-3.667572	2.564297	-0.557498
H	-3.825395	1.840693	-2.132888
H	-4.139158	-0.673733	-2.281232
H	-3.887923	-1.658168	-0.862275
H	-5.156247	0.521548	0.598873

$Fe(cit)_2OH^{5-}$

Fe	-0.757539	-1.111181	0.176199
O	1.175641	-1.535013	-0.513485
O	3.180802	-1.695194	-1.488592
O	3.427629	-3.243721	2.170168
O	5.487182	-2.553376	2.790323
O	1.432463	-0.035502	3.635196
O	0.10703	-0.703887	1.971413
O	3.83392	0.564958	-0.281846
O	-2.626277	-0.312838	0.925144
O	-4.36954	1.028559	1.360913
O	-0.522447	0.996243	-0.426297
O	-0.505576	3.044333	-1.335137
O	-2.543259	-1.136838	-3.736912
O	-1.538156	-1.282147	-1.740861
O	-4.945206	1.581245	-1.015482
O	-1.225097	-2.861719	0.663112
C	3.13496	-0.4544	0.540327
C	4.32734	-1.141404	1.285645
C	2.188456	0.406575	1.40077
C	2.419982	-1.331347	-0.556966
C	1.19631	-0.188016	2.423358
C	4.369645	-2.435033	2.173926
C	-3.644644	0.914415	-0.915722
C	-2.598202	1.976777	-1.342963
C	-3.752264	-0.306292	-1.862465
C	-3.510792	0.503188	0.59135
C	-2.493582	-0.942926	-2.499517
C	-1.071158	1.973953	-1.000143
H	5.04816	-1.366199	0.490519

H	4.788238	-0.344953	1.880266
H	2.831589	1.092945	1.961745
H	1.591249	0.991714	0.696413
H	4.008071	0.058973	-1.092948
H	-2.961169	2.925938	-0.937775
H	-2.658481	2.079549	-2.433956
H	-4.392525	0.00964	-2.689158
H	-4.276082	-1.109579	-1.329568
H	-5.159721	1.653081	-0.056333
H	-0.675581	-3.108034	1.417057

Table S4. Optimized structure Cartesian coordinates of Fe(III) complexes.

$Fe(H_2O)_6^{3+}$

Fe	0.000665	0.001616	0.002405
O	2.059449	0.000436	0.001405
O	0.002334	2.059899	0.000385
O	0.001336	0.002406	2.060211
O	-2.058763	0.000551	0.001372
O	0.002385	-2.058314	0.000325
O	0.001293	0.002383	-2.058008
H	2.640669	0.785328	0.000424
H	2.639610	-0.785380	0.001320
H	-2.639949	0.785451	0.002084
H	-2.639061	-0.785136	0.000320
H	0.001459	2.641222	0.785229
H	0.002234	2.639994	-0.785507
H	0.000746	-2.639681	0.785057
H	0.001514	-2.638393	-0.785502
H	0.786184	0.002297	2.641483
H	-0.784561	0.000632	2.640411
H	0.785999	0.001344	-2.639294
H	-0.784543	0.002346	-2.638121

$FeCl(H_2O)_5^{2+}$

Fe	0.08745	0.00003	-0.00019
Cl	2.23693	0.00121	0.00136
O	-0.25426	-1.39619	1.58008
O	-0.08868	1.56805	1.38586
O	-0.25618	1.39628	-1.57975
O	-0.08593	-1.56810	-1.38639
O	-2.07999	-0.00116	-0.00012
H	-0.06264	2.34120	-1.47626
H	-0.06762	1.17643	-2.50568
H	-0.06214	-1.17601	2.50507
H	-0.06075	-2.34125	1.47640
H	0.67175	-2.02243	-1.78849

H	-0.89916	-1.96425	-1.73549
H	-2.64810	-0.52184	0.58720
H	-2.64866	0.51930	-0.58711
H	0.66817	2.02336	1.78841
H	-0.90264	1.96265	1.73499

$FeCl_2(H_2O)_4^+$

Fe	-0.000194	0.000959	0.000898
Cl	2.238809	-0.009528	0.010218
Cl	-2.239100	0.011578	-0.008603
O	0.002701	1.624522	1.396117
O	-0.000750	-1.621850	-1.395337
O	-0.014419	-1.395095	1.623324
O	0.012496	1.397188	-1.621920
H	0.788502	-1.870555	-1.894401
H	-0.787365	-1.863683	-1.901837
H	0.769824	-1.901307	1.873362
H	-0.806109	-1.893138	1.866156
H	0.803865	1.895396	-1.865556
H	-0.772016	1.903274	-1.871170
H	-0.785828	1.875021	1.895374
H	0.790130	1.868184	1.900512

$FeSO_4(H_2O)_5^+$

Fe	0.809247	-0.058921	0.075939
S	-2.332699	0.056166	-0.287204
O	1.687785	1.408490	1.411783
O	1.232885	-1.434528	1.675553
O	2.910070	-0.199370	-0.520830
O	0.341153	-1.459374	-1.341406
O	0.437738	1.606630	-1.094606
O	-3.437375	0.026549	0.629788
O	-2.146595	-1.143741	-1.159063
O	-2.077758	1.337130	-1.007457
O	-0.905692	-0.048861	0.642478
H	1.345133	2.301869	1.260913

H	1.660125	1.248163	2.365443
H	0.704780	-1.666031	-2.210158
H	-0.693759	-1.474112	-1.393475
H	1.913263	-2.118453	1.723163
H	0.419712	-1.793949	2.061029
H	0.842384	1.874342	-1.928460
H	-0.586428	1.662322	-1.177875
H	3.544248	0.428462	-0.149223
H	3.381500	-0.768396	-1.141952

$FeOH(H_2O)_5^{2+}$

Fe	0.150273	-0.018595	-0.267140
O	-1.364489	1.411791	-0.815210
O	-1.136793	-1.576563	-0.867882
O	1.088840	-0.039500	-1.750483
O	1.268477	1.537826	0.611615
O	-1.003796	0.007618	1.552843
O	1.275204	-1.439309	0.897696
H	2.017672	1.967959	0.171437
H	1.149996	1.949788	1.480385
H	-2.046227	1.203829	-1.472169
H	-1.159289	2.353061	-0.922408
H	-1.063384	-2.024192	-1.724791
H	-1.878616	-1.968460	-0.383494
H	-1.794377	0.543096	1.714272
H	-0.818575	-0.511766	2.348925
H	1.273046	-2.385358	0.686468
H	2.162804	-1.234606	1.229140
H	1.607076	-0.050170	-2.567113

$Fe(OH)_2(H_2O)_4^{+}$

Fe	0.005429	0.018578	-0.006113
O	-1.111523	-1.731989	0.699426
O	-1.496417	1.357976	0.805143
O	1.051701	0.017089	1.498451
O	1.531302	-1.257942	-0.903065

O	-1.065723	0.054330	-1.493574
O	1.153855	1.737572	-0.644173
H	2.345329	-1.254441	-0.381827
H	1.773459	-1.242147	-1.837174
H	-1.718717	-2.154288	0.079131
H	-0.748146	-2.414094	1.276975
H	-1.723797	1.479871	1.734428
H	-2.302994	1.389699	0.273643
H	-1.220666	-0.329424	-2.359097
H	0.768124	2.407644	-1.222107
H	1.636553	2.180834	0.066090
H	1.121904	-0.259562	2.414296

$Fe(OH)_3(H_2O)_3$

Fe	-0.098495	0.172435	0.099263
O	0.220292	0.380546	1.953476
O	2.158162	-0.224161	0.406825
O	-0.101343	-2.139330	0.094166
O	0.534807	-0.217417	-2.089375
O	0.092354	1.877492	-0.700115
O	-1.907240	-0.347253	-0.104780
H	-0.518415	0.417089	2.567145
H	-1.068674	-2.142091	0.191948
H	0.277853	-2.504865	0.900591
H	2.706605	0.373776	-0.112148
H	2.102034	0.131035	1.310076
H	0.121608	2.665004	-0.150530
H	-0.106890	-0.756280	-2.564225
H	0.363849	0.713725	-2.310305
H	-2.566883	0.297989	-0.372221

$FeHCO_3(H_2O)_4^{2+}$

Fe	-0.131045	-0.099925	-0.000627
O	1.762920	0.155316	0.713852
O	2.930076	1.956064	-0.060055
O	0.853814	1.491978	-0.714309

O	-1.275980	0.762911	1.478961
O	0.168719	-1.504302	-1.477679
O	-0.030440	-1.754095	1.329780
O	-1.600841	0.676194	-1.327560
C	1.888916	1.209849	-0.008019
H	-0.661027	-2.462000	1.535529
H	0.777979	-1.907644	1.845518
H	-1.786491	1.582178	1.377945
H	-1.228994	0.548760	2.424077
H	-2.507989	0.402973	-1.535653
H	-1.397701	1.477228	-1.838683
H	0.673094	-2.327429	-1.380020
H	0.018499	-1.350769	-2.424162
H	3.655271	1.651049	0.515518

$FeCO_3(H_2O)_4^+$

Fe	-0.130866	-0.087524	0.000878
O	1.683426	0.043237	0.625923
O	2.877204	1.885231	-0.001922
O	0.711528	1.523472	-0.627294
O	-1.377693	0.791295	1.464008
O	0.174244	-1.581193	-1.462793
O	-0.158576	-1.698073	1.520388
O	-1.621365	0.528626	-1.518248
C	1.882801	1.232933	-0.001253
H	-0.519426	-2.594057	1.502573
H	0.727018	-1.739854	1.913874
H	-1.385033	1.754809	1.554786
H	-1.404721	0.405495	2.350546
H	-2.586890	0.555579	-1.499434
H	-1.306547	1.357296	-1.912041
H	1.054840	-1.971643	-1.556436
H	-0.192555	-1.450386	-2.348180

$FeHS(H_2O)_5^{2+}$

Fe	0.082822	-0.024258	0.013251

S	2.382431	-0.225020	-0.138489
O	0.023681	1.579188	-1.407883
O	-0.401761	-1.391133	-1.556433
O	-0.370906	-1.549542	1.431171
O	0.044788	1.409920	1.595590
O	-2.133847	0.309399	0.023542
H	-0.458146	-2.493394	1.231399
H	-0.296104	-1.462274	2.393017
H	0.104001	1.462210	-2.366381
H	0.271644	2.495184	-1.212073
H	0.800914	1.790046	2.066411
H	-0.757546	1.822318	1.947848
H	-2.599780	0.976838	-0.499789
H	-2.801014	-0.164737	0.539476
H	0.209970	-1.911132	-2.097984
H	-1.299304	-1.571366	-1.872341
H	2.604480	-1.237301	0.734519

$FeH_3PO_4(H_2O)_5^{3+}$

Fe	-0.152437	0.027702	0.088825
P	-0.115691	3.358669	0.478663
O	-0.045277	-0.393104	2.145923
O	1.877005	0.416061	0.028404
O	-0.199052	-0.065573	-2.007714
O	0.273274	-2.020443	-0.078643
O	-0.484837	1.869401	0.255877
O	-0.641367	4.310383	-0.629634
O	1.456826	3.363838	0.336700
O	-2.170861	-0.438507	0.117250
O	-0.630763	3.690050	1.908681
H	-0.813420	-0.489773	2.734254
H	0.736865	-0.283787	2.712691
H	-2.895017	0.205738	0.201200
H	-2.568743	-1.325316	0.066606
H	0.411227	-2.638724	0.659343
H	0.376293	-2.519875	-0.906879

H	0.528641	0.179460	-2.603993
H	-1.004353	-0.128459	-2.548974
H	2.623967	-0.202007	-0.051192
H	2.226001	1.325831	0.091391
H	1.945354	4.199462	0.214821
H	-1.516231	4.737807	-0.636816
H	-0.574371	4.566699	2.330600

$FeH_2PO_4(H_2O)_5^{2+}$

Fe	-0.179799	0.101945	-0.050992
P	-0.010111	3.181871	0.563853
O	-0.200945	0.348816	1.961763
O	1.876551	0.497350	-0.309357
O	-0.081798	-0.520299	-2.088900
O	0.272426	-1.963784	0.272275
O	-0.488642	1.901565	-0.268270
O	-0.726911	4.466792	0.018265
O	1.492027	3.291805	0.004355
O	-2.224049	-0.394106	-0.259998
O	-0.149543	2.881802	2.020746
H	-0.360563	-0.203083	2.739225
H	-0.197019	1.344632	2.221165
H	-2.897302	0.303622	-0.268906
H	-2.663593	-1.227680	-0.035432
H	0.494224	-2.445586	1.082558
H	0.391609	-2.572361	-0.472671
H	0.671372	-0.260247	-2.641264
H	-0.864479	-0.550291	-2.659726
H	2.632560	-0.021426	0.001370
H	2.127086	1.444576	-0.312772
H	1.954286	4.140546	0.092675
H	-1.401495	4.888031	0.573758

$FeHPO_4(H_2O)_5^{+}$

Fe	-0.032490	-0.034990	0.119867
P	0.003018	3.019679	0.328898
O	-0.098746	0.166963	1.974439

O	1.753019	0.460423	-0.251411
O	0.005466	-0.661324	-2.013718
O	0.088314	-2.209653	0.252187
O	-0.719650	1.812242	-0.285370
O	-0.654738	4.406802	-0.008077
O	1.451328	3.154026	-0.260601
O	-2.187515	-0.450490	-0.295551
O	-0.002913	2.905413	1.906191
H	-0.611462	-0.314477	2.632005
H	-0.006845	1.961545	2.212846
H	-2.709511	0.361854	-0.247822
H	-2.723187	-1.176094	0.047126
H	0.525183	-2.665894	0.982481
H	0.311134	-2.669830	-0.568364
H	0.796497	-0.291339	-2.430626
H	-0.748064	-0.485241	-2.591626
H	2.469116	0.166544	0.324400
H	1.841674	2.252517	-0.398859
H	-1.238020	4.785265	0.662626

$FeH_5(PO_4)_2(H_2O)_4^{2+}$

Fe	-0.014976	-0.109037	-0.273615
P	0.189740	-3.108630	0.665674
P	-0.255092	3.275053	-0.354083
O	-0.037619	-0.156523	1.780976
O	2.060128	-0.460257	-0.315265
O	-0.288049	-1.948263	-0.309026
O	1.728933	-3.221624	0.193807
O	-0.453006	-4.472783	0.203849
O	-0.025980	-2.714501	2.088841
O	-0.044440	-0.110115	-2.398181
O	-2.097872	0.284457	-0.300783
O	0.284623	1.868214	-0.313942
O	-1.759849	3.242157	0.145520
O	0.424805	4.311549	0.613699
O	-0.156450	3.751728	-1.854529

H	2.358088	-1.388825	-0.251629
H	2.788564	0.100229	-0.610923
H	-0.061093	-1.103163	2.147945
H	0.446631	0.416878	2.389007
H	2.215591	-4.018310	0.454932
H	-1.115280	-4.868071	0.790433
H	-2.497485	1.092919	0.054327
H	-2.751718	-0.427527	-0.265703
H	-0.064897	0.630861	-3.018004
H	-0.141293	-0.934234	-2.895869
H	-2.153420	4.040338	0.532845
H	1.339918	4.603004	0.480430
H	-0.434412	4.644566	-2.112419

$FeH_4(PO_4)_2(H_2O)_4^+$

Fe	-0.000024	0.000116	-0.000016
P	0.171448	-3.126351	0.430507
P	-0.171106	3.126422	-0.430636
O	-0.107395	-0.424297	2.037871
O	2.091766	-0.418252	0.020062
O	-0.31494	-1.8558	-0.33115
O	1.716206	-3.202239	-0.072325
O	-0.479218	-4.425653	-0.223055
O	0.007676	-3.033087	1.914368
O	0.106401	0.424251	-2.037929
O	-2.091883	0.41816	-0.019881
O	0.315725	1.855872	0.330759
O	-1.715672	3.202189	0.072944
O	0.480058	4.425558	0.222752
O	-0.00814	3.033306	-1.914576
H	2.342934	-1.343065	-0.16573
H	2.736029	0.178286	-0.379839
H	-0.055393	-1.398938	2.271256
H	0.306359	0.119655	2.718571
H	2.198981	-4.000153	0.183802
H	-1.136739	-4.865229	0.332553

H	-2.342745	1.34302	0.166159
H	-2.735548	-0.178246	0.381226
H	0.054663	1.398773	-2.271624
H	-0.306985	-0.119942	-2.718651
H	-2.198767	3.999765	-0.183646
H	1.13631	4.865879	-0.333768

$FeH_3(PO_4)_2(H_2O)_4$

Fe	-0.249926	-0.020554	0.072560
P	0.208167	-3.172794	0.435980
P	-0.212896	3.026506	-0.371405
O	-0.136553	-0.472443	2.151315
O	2.023286	-0.432943	0.154760
O	-0.395501	-1.963269	-0.291515
O	1.699608	-3.278093	-0.221384
O	-0.479602	-4.532289	-0.097808
O	0.226865	-3.108142	1.934932
O	0.251491	0.328977	-2.009186
O	-2.046755	0.473124	-0.082747
O	0.355875	1.793867	0.406321
O	-1.740205	3.193103	0.063807
O	0.457130	4.350856	0.244860
O	0.025270	2.921028	-1.857639
H	2.264699	-1.283293	-0.246387
H	2.438756	0.265319	-0.364506
H	0.039619	-1.436039	2.323163
H	0.521402	0.056306	2.616777
H	2.225499	-4.003205	0.138370
H	-1.096876	-4.896632	0.547959
H	-2.175719	2.310139	0.060494
H	-2.739543	-0.189017	-0.171089
H	0.168270	1.322355	-2.168761
H	-0.314544	-0.127644	-2.641016
H	0.880948	4.875011	-0.444204

$FeH_7(PO_4)_3(H_2O)_3^+$

Fe	-0.478399	-0.254569	-0.546881

P	1.964221	-2.298021	-0.545740
P	-3.343060	-1.911226	-0.547349
P	-1.265793	2.675749	0.352334
O	-1.294137	-0.331327	1.519390
O	0.252230	-0.154817	-2.510849
O	1.236383	0.574655	0.389261
O	0.457082	-1.926657	-0.398210
O	2.169858	-3.822441	-0.134158
O	2.127753	-2.234616	-2.179530
O	-2.198006	-1.093590	-1.090255
O	-4.769289	-1.400899	-1.015071
O	-3.163465	-3.408558	-1.042728
O	-1.079514	1.565762	-0.715686
O	-1.803004	2.152096	1.656770
O	0.218286	3.307068	0.445984
O	-2.125754	3.879565	-0.243001
O	-3.462752	-1.895142	1.016041
O	2.923453	-1.407337	0.162571
H	0.936281	-0.796649	-2.781207
H	0.320376	0.661241	-3.020360
H	1.426732	1.524534	0.400155
H	2.063291	0.014874	0.424176
H	-0.616489	-0.599085	2.156309
H	-1.546572	0.645461	1.738425
H	1.554692	-4.453770	-0.529996
H	3.036110	-2.366385	-2.486075
H	-4.923689	-1.357478	-1.968757
H	-3.804980	-4.056191	-0.717915
H	0.298492	4.110297	0.978163
H	-3.041564	3.906581	0.063990
H	-2.749926	-1.364910	1.447187

$FeH_6(PO_4)_3(H_2O)_3$

Fe	-0.465389	0.020141	-0.137766
P	1.498694	-2.680298	-0.186206
P	-2.672477	-2.293855	-0.567857

P	-1.233906	3.213215	0.222161
O	-0.430778	0.428122	1.986870
O	-0.329376	-0.404101	-2.211580
O	1.429858	1.084738	-0.329333
O	0.646977	-1.453040	0.280919
O	0.665894	-3.982244	0.168955
O	1.352418	-2.504007	-1.844278
O	-2.166830	-0.922941	-0.069912
O	-4.227283	-2.396339	-0.167933
O	-2.658776	-2.066662	-2.202593
O	-1.245426	1.785066	-0.334412
O	-1.490411	2.946528	1.831105
O	0.372508	3.602339	0.179704
O	-2.075952	4.302854	-0.306657
O	-1.970181	-3.549599	-0.194790
O	2.918897	-2.744730	0.209853
H	0.357595	-1.099945	-2.321335
H	-1.161998	-0.803080	-2.523328
H	1.382745	2.045408	-0.165733
H	2.142523	0.700492	0.195725
H	-0.560229	-0.323313	2.576149
H	-0.961413	1.191055	2.284465
H	-0.315906	-3.889576	0.058242
H	2.098217	-2.908879	-2.303481
H	-4.694751	-1.555165	-0.245251
H	-2.766313	-2.896105	-2.685830
H	0.511403	4.535721	-0.021280
H	-1.881380	3.707562	2.276388

$Fe(cit)(H_2O)_3$

Fe	1.069944	-0.211234	-0.014539
O	-0.403464	-0.034044	1.233597
O	-2.503289	-0.195237	1.961374
O	0.454523	1.141178	-1.230282
O	0.112230	3.014865	-0.077092
O	-1.377440	-3.085918	-0.844896

O	0.394372	-1.732680	-0.887835
O	-3.641073	0.266126	-0.326712
O	2.961756	-0.662048	-1.002685
O	1.874141	-1.282278	1.762557
O	2.225964	1.495852	0.793658
C	-2.228295	0.278751	-0.375663
C	-1.817913	1.738108	-0.772403
C	-1.781932	-0.788116	-1.455354
C	-1.706524	-0.021151	1.061616
C	-0.923325	-1.981075	-1.019535
C	-0.336268	2.044149	-0.677190
H	-2.359025	2.433919	-0.131701
H	-2.154075	1.899360	-1.801525
H	-1.252375	-0.279480	-2.261399
H	-2.711304	-1.199910	-1.843397
H	3.491918	0.112459	-1.229202
H	2.810196	-1.172094	-1.809397
H	1.057739	-1.328693	2.286100
H	2.160637	-2.190799	1.606801
H	2.397245	1.539327	1.741432
H	1.668258	2.277748	0.549677
H	-3.874977	0.074175	0.597953

$Fe(cit)OH(H_2O)_2^-$

Fe	1.170506	-0.293435	0.423406
O	-0.519085	0.100923	1.378565
O	-2.691790	-0.001837	1.864051
O	0.618392	1.083837	-1.083351
O	0.174703	3.046201	-0.114284
O	-1.359221	-3.145603	-0.948094
O	0.370551	-1.816293	-0.497519
O	-3.573193	0.313614	-0.513718
O	2.682234	-0.530438	-1.318104
O	2.232037	-1.088435	1.731081
O	2.117545	1.593716	1.123433
C	-2.149820	0.306800	-0.445443

C	-1.679202	1.726486	-0.885843
C	-1.638942	-0.810099	-1.426737
C	-1.769017	0.097639	1.058717
C	-0.867157	-2.030479	-0.901095
C	-0.195848	2.009723	-0.683103
H	-2.255436	2.468669	-0.332936
H	-1.925145	1.835855	-1.948079
H	-0.997260	-0.343314	-2.176109
H	-2.533660	-1.192522	-1.914617
H	2.253815	0.207831	-1.782023
H	2.243885	-1.327652	-1.648389
H	1.950800	-1.974337	1.981833
H	2.084544	1.590144	2.085995
H	1.553040	2.332193	0.786363
H	-3.850267	0.182876	0.413156

$FeH(cit)_2^{2-}$

Fe	-0.218898	-0.110580	0.359954
O	1.765294	-0.219397	-1.317881
O	3.447214	1.274253	-1.425941
O	0.749466	-1.448266	1.390620
O	2.070164	-2.834026	2.526101
O	1.987615	1.998290	2.937107
O	1.059861	1.250036	1.040021
O	4.916741	-0.439415	0.070600
O	-1.826659	0.411239	1.316816
O	-3.997531	0.424852	1.793905
O	-0.400664	1.042806	-1.308121
O	-1.264829	2.017151	-3.110172
O	-2.158796	-2.441476	-2.404158
O	-1.139277	-1.512506	-0.655569
O	-4.837047	0.969823	-0.535494
C	3.500071	-0.327546	0.360882
C	3.036965	-1.778129	0.622795
C	3.350259	0.618516	1.580876
C	2.890386	0.340642	-0.885088

C	2.015473	1.332714	1.908357
C	1.877683	-2.040900	1.607749
C	-3.444747	0.595628	-0.526274
C	-2.720322	1.772875	-1.237166
C	-3.385599	-0.754601	-1.289865
C	-3.064621	0.453246	0.984543
C	-2.120987	-1.619011	-1.492386
C	-1.381167	1.587722	-1.965810
H	2.779244	-2.253664	-0.327387
H	3.903357	-2.297714	1.031346
H	3.665649	0.074780	2.474845
H	4.072008	1.429663	1.442601
H	5.135596	0.364220	-0.422206
H	-2.578001	2.578301	-0.507709
H	-3.422181	2.138538	-1.986234
H	-3.800634	-0.571836	-2.283857
H	-4.099578	-1.417433	-0.787340
H	-5.105362	0.825075	0.392247
H	1.185662	0.419494	-1.812378

$Fe(cit)_2^{3-}$

Fe	-0.075745	-0.333239	-0.031024
O	0.130439	-0.579650	2.004182
O	0.890147	-0.937747	4.068913
O	1.623894	0.745941	-0.072907
O	3.713199	1.522550	-0.100047
O	2.564426	-3.578061	-0.596984
O	1.010615	-1.999128	-0.349121
O	3.275573	-1.436167	3.502015
O	-0.281731	-0.086576	-2.066190
O	-1.037043	0.291166	-4.129037
O	-1.775371	-1.412679	0.014701
O	-3.858393	-2.206235	0.029889
O	-2.728795	2.898000	0.539535
O	-1.162285	1.332985	0.283350
O	-3.429190	0.759651	-3.565104

C	2.495300	-1.143471	2.311104
C	3.188147	0.101179	1.706183
C	2.606918	-2.433980	1.464329
C	1.042469	-0.859945	2.826253
C	2.024079	-2.664260	0.048242
C	2.810382	0.823556	0.389335
C	-2.648704	0.468014	-2.374071
C	-3.331905	-0.785554	-1.776795
C	-2.773290	1.753320	-1.521084
C	-1.192611	0.198915	-2.887771
C	-2.184255	1.988534	-0.108199
C	-2.957791	-1.501675	-0.455706
H	3.140956	0.882033	2.475327
H	4.247486	-0.154922	1.615063
H	3.675153	-2.655522	1.388729
H	2.182885	-3.240323	2.075582
H	2.587650	-1.340721	4.197296
H	-3.267892	-1.565863	-2.545299
H	-4.394977	-0.542090	-1.695621
H	-3.843998	1.960043	-1.438145
H	-2.364427	2.567485	-2.132267
H	-2.738069	0.678408	-4.259013

$Fe(cit)_2OH^{4-}$

Fe	-0.510640	-0.870021	0.111101
O	1.357832	-1.168550	-0.743071
O	3.388151	-1.689664	-1.522295
O	2.364879	-3.125576	1.805892
O	4.287977	-3.225984	2.983388
O	1.658834	0.882178	3.322883
O	0.327813	-0.030346	1.780861
O	4.456797	0.249770	-0.185741
O	-2.455853	-0.424627	0.934820
O	-4.607290	0.052754	1.317548
O	-0.547886	1.114498	-0.758798
O	-0.876746	3.053824	-1.832626

O	-2.749472	-1.660948	-3.532956
O	-1.566256	-1.369032	-1.656293
O	-5.068820	1.342295	-0.766305
O	-0.508387	-2.601897	0.803804
C	3.345466	-0.438069	0.503366
C	4.045690	-1.365498	1.543446
C	2.524836	0.725971	1.096566
C	2.614206	-1.190976	-0.665003
C	1.433979	0.482921	2.160991
C	3.476268	-2.688105	2.164449
C	-3.710574	0.795232	-0.773428
C	-2.807398	2.041844	-0.926236
C	-3.698028	-0.175561	-1.978129
C	-3.554842	0.069087	0.609630
C	-2.547384	-1.132747	-2.411484
C	-1.276945	2.038570	-1.210177
H	4.975279	-1.684992	1.061188
H	4.352411	-0.732479	2.383831
H	3.254351	1.399801	1.554794
H	2.047256	1.246284	0.260941
H	4.584593	-0.349775	-0.945007
H	-2.927916	2.633736	-0.009127
H	-3.258703	2.636085	-1.726200
H	-3.933955	0.426535	-2.862866
H	-4.563748	-0.834885	-1.840675
H	-5.382448	0.985693	0.097391
H	0.378036	-2.814858	1.147242

Table S5. Optimized structure Cartesian coordinates of Cu(I) complexes.

$CuCl(H_2O)$

Cu	0.036942	0.074314	0.043155
Cl	-2.057940	-0.063980	0.074830
O	2.004689	0.205762	0.009429
H	2.502159	-0.106062	0.774133
H	2.473097	-0.085036	-0.781548

$CuCl_2^-$

Cu	-0.000055	0.043433	0.043431
Cl	2.169412	-0.018947	0.082887
Cl	-2.169357	0.105513	0.003682

$CuCl_3^{2-}$

Cu	-0.005126	0.506655	0.034208
Cl	2.106385	-0.653066	0.075348
Cl	-2.066920	-0.735974	0.128658
Cl	-0.054341	2.912384	-0.098214

$CuHS(H_2O)$

Cu	-0.011636	-0.248242	-0.030432
S	2.118534	-0.441174	-0.041410
O	-1.999404	-0.132648	-0.070277
H	2.342706	0.584117	0.810873
H	-2.504543	-0.362548	0.717514
H	-2.425131	0.628496	-0.481195

$Cu(HS)_2^-$

Cu	0.000067	-0.279988	-0.000206
S	2.204089	-0.30569	-0.150469
S	-2.205099	-0.295192	0.127476
H	2.446249	0.510525	0.900414
H	-2.420237	0.760894	-0.689656

$Cu_2S(HS)_2^{2-}$

Cu	0.133977	-0.122383	2.110868
Cu	-1.786975	-0.104253	-0.745506
S	0.277476	-0.331589	-0.061234

S	0.192536	0.089698	4.364498
S	-3.855727	0.102047	-1.642872
H	-4.058614	1.398392	-1.311408
H	-0.652741	-0.926301	4.657057

Table S6. Optimized structure Cartesian coordinates of Cu(II) complexes.

$CuH_2PO_4(H_2O)_4^+$

Cu	-0.410131	0.052746	0.548220
P	-0.084032	3.057843	0.729853
O	0.221424	0.346939	2.444874
O	1.468939	0.388902	-0.646826
O	-0.137745	-1.930471	0.822551
O	-0.903862	1.852526	0.192761
O	-0.924592	4.401601	0.547857
O	1.066116	3.223744	-0.403029
O	-1.653150	-0.413237	-1.054587
O	0.456009	2.863712	2.118343
H	-0.370659	0.132506	3.177067
H	0.413673	1.349287	2.502253
H	-1.819901	0.438400	-1.487374
H	-2.513067	-0.836960	-0.934075
H	0.490533	-2.210974	1.501282
H	-0.045072	-2.517917	0.060867
H	2.343796	-0.013082	-0.614255
H	1.595401	1.332399	-0.848165
H	1.598948	4.028082	-0.340006
H	-1.347796	4.724939	1.354077

$CuHPO_4(H_2O)_4$

Cu	-0.609161	-0.021907	0.630228
P	-0.052556	2.883407	0.526304
O	0.256383	0.048185	2.332598
O	1.470221	0.161312	-0.581758
O	-0.079656	-2.023616	0.692530
O	-1.201017	1.811462	0.470717
O	-0.736930	4.340408	0.546184
O	0.931164	2.792667	-0.596546
O	-1.753077	-0.191718	-1.102412
O	0.588091	2.766441	2.001119
H	-0.375042	0.071311	3.061054

H	0.637112	1.816222	2.277505
H	-2.012773	0.746492	-1.125878
H	-2.549743	-0.730557	-1.157156
H	0.407836	-1.877492	1.526101
H	0.584376	-2.123106	-0.004263
H	2.235072	0.161952	0.005023
H	1.373492	1.119191	-0.826213
H	-1.267907	4.492248	1.336555

$CuH_4(PO_4)_2(H_2O)_3$

Cu	-0.273859	0.104002	-0.253640
P	0.504466	2.982905	0.800121
P	0.602414	-2.783471	0.143895
O	-0.489817	-0.272879	1.918198
O	1.622372	0.259201	-1.018969
O	-0.390882	2.006601	0.033434
O	0.571624	-2.780402	1.642152
O	0.256045	4.440303	0.816929
O	0.558979	2.339280	2.315992
O	2.035209	2.653603	0.241518
O	-0.283416	-1.787349	-0.612701
O	2.105183	-2.452297	-0.441444
O	0.339396	-4.262572	-0.454818
O	-2.349055	0.272643	-0.623185
H	2.134887	-0.559696	-0.904740
H	2.099680	1.029065	-0.656543
H	-0.081403	-1.137389	2.142085
H	-0.075032	0.435887	2.432373
H	-2.565838	1.137232	-0.247424
H	-2.866330	-0.391897	-0.153521
H	-0.115915	-4.821051	0.186098
H	2.794965	-2.989856	-0.033604
H	0.802631	2.996805	2.978233
H	2.535042	3.467607	0.107901

$CuH_3(PO_4)_2(H_2O)_3^-$

Cu	-0.263817	0.254663	-0.314626
P	0.665632	3.071986	0.803683
P	0.411803	-2.709366	0.043567
O	-0.740807	-0.141032	1.822244
O	1.664120	0.298258	-1.068340
O	-0.233759	2.189651	-0.040147
O	0.428349	-2.376808	1.540720
O	0.592952	4.557419	0.792640
O	0.508505	2.466645	2.330285
O	2.232208	2.612001	0.439490
O	-0.402024	-1.593129	-0.749634
O	1.984456	-2.282940	-0.515023
O	0.114106	-4.102374	-0.405346
O	-2.500440	-0.034709	-0.394230
H	2.015361	-0.610207	-0.893520
H	2.179547	0.961021	-0.580690
H	-0.258720	-1.044283	1.884484
H	-0.287788	0.519110	2.362533
H	-2.526850	-0.026440	0.574812
H	-2.244619	-0.951625	-0.613081
H	2.642799	-2.827901	-0.072637
H	0.856825	3.078140	2.988005
H	2.749422	3.399247	0.237052

$CuH_2(PO_4)_2(H_2O)_2^{2-}$

Cu	0.030985	-0.000223	-0.115202
P	1.226935	-2.907117	-0.048313
P	-1.168548	2.903396	-0.192081
O	1.945516	-0.045406	0.198185
O	-0.020981	-2.001970	-0.208990
O	1.059252	-4.386253	-0.143258
O	1.926588	-2.494434	1.381324
O	2.336136	-2.379254	-1.140754
O	0.080268	2.001257	-0.021194
O	-1.003888	4.383267	-0.104559
O	-2.280837	2.379124	0.899172

O	-1.862640	2.481951	-1.621386
O	-1.883823	0.040292	-0.428433
H	2.177584	0.884644	0.280713
H	2.067797	-1.521522	1.328070
H	2.441804	-1.417365	-0.957342
H	-2.112172	-0.891180	-0.503837
H	-2.383528	1.416071	0.720975
H	-2.006595	1.509824	-1.562774

$CuH_2(cit)(H_2O)_2^+$

Cu	1.232197	-0.207584	0.128561
O	-0.156048	0.035530	1.372068
O	-2.238743	-0.081455	2.117049
O	0.537981	1.454367	-1.095552
O	-0.358696	3.414719	-1.434891
O	-1.366748	-3.173514	-0.855924
O	0.405005	-1.928217	-0.589383
O	-3.434574	-0.031866	-0.125843
O	2.886464	-0.472149	-1.013311
O	2.415844	0.597985	1.629346
C	-2.050617	0.188680	-0.238995
C	-1.858875	1.667408	-0.685035
C	-1.552044	-0.784124	-1.369254
C	-1.441885	0.004859	1.203612
C	-0.784330	-1.995481	-0.906966
C	-0.470892	2.143945	-1.067250
H	-2.244244	2.315636	0.109850
H	-2.516446	1.830139	-1.547927
H	-0.885494	-0.269246	-2.060599
H	-2.448363	-1.072008	-1.919618
H	3.143831	0.252708	-1.599276
H	2.969117	-1.298456	-1.507855
H	1.902336	0.662579	2.447348
H	3.315941	0.330744	1.851024
H	-3.626808	-0.061127	0.832255
H	-2.300783	-3.132486	-1.108849

H	-1.200705	3.890818	-1.396330

$CuH(cit)(H_2O)_2$

Cu	1.173822	-0.227277	0.090587
O	-0.218395	0.021607	1.356417
O	-2.318049	0.127551	2.064606
O	0.510312	1.038894	-1.606061
O	0.298816	2.845992	-0.306419
O	-1.448925	-3.252238	-0.626384
O	0.334728	-2.016437	-0.387865
O	-3.462808	0.131184	-0.210460
O	2.744783	-0.350840	-1.217404
O	2.129201	1.429783	0.896408
C	-2.056028	0.229213	-0.304370
C	-1.693327	1.633381	-0.887773
C	-1.607349	-0.908257	-1.300858
C	-1.496097	0.102729	1.160476
C	-0.843980	-2.072638	-0.731273
C	-0.188218	1.901721	-0.956220
H	-2.167730	2.390452	-0.264131
H	-2.129865	1.688998	-1.889395
H	-0.944325	-0.470835	-2.049056
H	-2.523610	-1.247324	-1.785394
H	3.527061	0.084752	-0.854484
H	2.326231	0.302145	-1.816922
H	1.882810	1.501328	1.828145
H	1.593914	2.155437	0.433743
H	-3.654950	0.199661	0.744947
H	-2.375011	-3.182515	-0.894108

$Cu(cit)(H_2O)_2^-$

Cu	1.192643	-0.241528	0.243424
O	-0.278277	0.021000	1.452377
O	-2.418747	0.164468	2.017834
O	0.600705	1.337709	-1.767604
O	0.383383	2.866966	-0.143598

O	-1.170138	-3.201642	-0.877502
O	0.564916	-1.877338	-0.470847
O	-3.401186	0.232489	-0.329081
O	2.639305	-0.213249	-1.259252
O	2.036128	1.386053	1.170240
C	-1.974834	0.267998	-0.331568
C	-1.586200	1.695002	-0.860384
C	-1.489003	-0.859806	-1.310249
C	-1.532304	0.122163	1.165540
C	-0.690096	-2.079946	-0.821766
C	-0.088711	2.013362	-0.940778
H	-2.072545	2.428512	-0.216723
H	-2.023255	1.765633	-1.860787
H	-0.878662	-0.393687	-2.086661
H	-2.398595	-1.248433	-1.764205
H	2.119297	0.516929	-1.691247
H	2.366938	-1.021594	-1.716181
H	1.530708	1.387029	1.995352
H	1.583718	2.121764	0.637576
H	-3.632426	0.233297	0.619067

$Cu(cit)_2^{4-}$

Cu	0.002093	-0.283947	-0.309252
O	1.778911	-1.029903	-0.883764
O	3.939473	-1.325145	-1.338886
O	2.850677	-3.771515	1.298160
O	4.667681	-3.938347	2.633581
O	1.189856	-0.992232	3.545949
O	0.204227	-0.777376	1.558809
O	4.493279	0.339280	0.633697
O	-1.006580	1.402687	0.065572
O	-2.527140	2.878884	0.759781
O	-2.384071	3.049091	-2.910327
O	-4.535655	3.350302	-3.537692
O	-2.615438	-0.905673	-3.368456
O	-0.848266	-0.597192	-2.044888

O	-4.315758	0.904849	0.500451
C	3.485874	-0.714263	0.903788
C	4.298201	-1.834127	1.616867
C	2.470478	0.030060	1.791421
C	2.999120	-1.087072	-0.544982
C	1.213798	-0.666605	2.350689
C	3.856287	-3.317599	1.873242
C	-3.370764	1.139184	-0.616885
C	-4.176064	2.022943	-1.612781
C	-3.068913	-0.292768	-1.096570
C	-2.183611	1.877182	0.094349
C	-2.114920	-0.584776	-2.279826
C	-3.610398	2.866923	-2.808390
H	5.214128	-1.939394	1.024785
H	4.611974	-1.421877	2.581912
H	3.035801	0.393773	2.654466
H	2.136718	0.904010	1.223281
H	4.867737	0.023835	-0.205742
H	-4.674599	2.771633	-0.987244
H	-4.974443	1.390157	-2.015018
H	-4.034819	-0.729355	-1.366927
H	-2.697523	-0.836521	-0.221219
H	-4.177345	1.700882	1.038049

Table S7 Logarithm of the reduced partition function, ln β (‰), for the pair ^{65}Cu-^{63}Cu of Cu_2^0.

Species	Temperature (K)					
	273	298	323	373	473	573
$Cu_2^{0\,a}$	1.026	0.864	0.738	0.556	0.348	0.238

[a] Atomic distance of Cu^0-Cu^0 was calculated to be 2.28Å.

Table S8 Logarithm of the reduced partition function, ln β (‰), for the pair ^{65}Cu-^{63}Cu of Cu(II) mono-hydrogen phosphate.

Species	Temperature (K)					
	273	298	323	373	473	573
$CuHPO_4(H_2O)_4$	5.827	4.958	4.268	3.254	2.064	1.422

Table S9 Logarithm of the reduced partition function, ln β (‰), for the pair ^{56}Fe-^{54}Fe of Fe(III) mono-hydrogensulfide.

Species	Temperature (K)					
	273	298	323	373	473	573
$FeHS(H_2O)_5^{2+}$	6.502	5.507	4.722	3.580	2.255	1.547

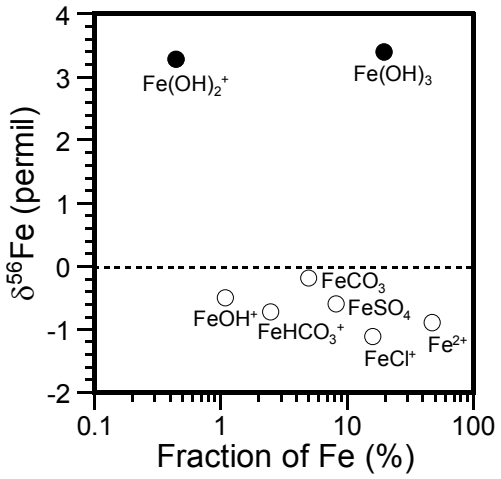

Figure S1. Mole fractions of Fe(II) and Fe(III) species and Fe isotopic variations ($^{56}Fe/^{54}Fe$) in seawater at pH = 8.2 and 298 K. Total concentration of Fe was set to 3.6×10^{-8} mol kg^{-1}. The ratio of concentrations was set to [Fe(II)]/[Fe(III)] = 4. Mole fractions of Fe(II) species were taken from Fig. 4. Mole fractions of Fe(III) hydroxides were estimated by using stability constants (Byrne and Kester, 1976).

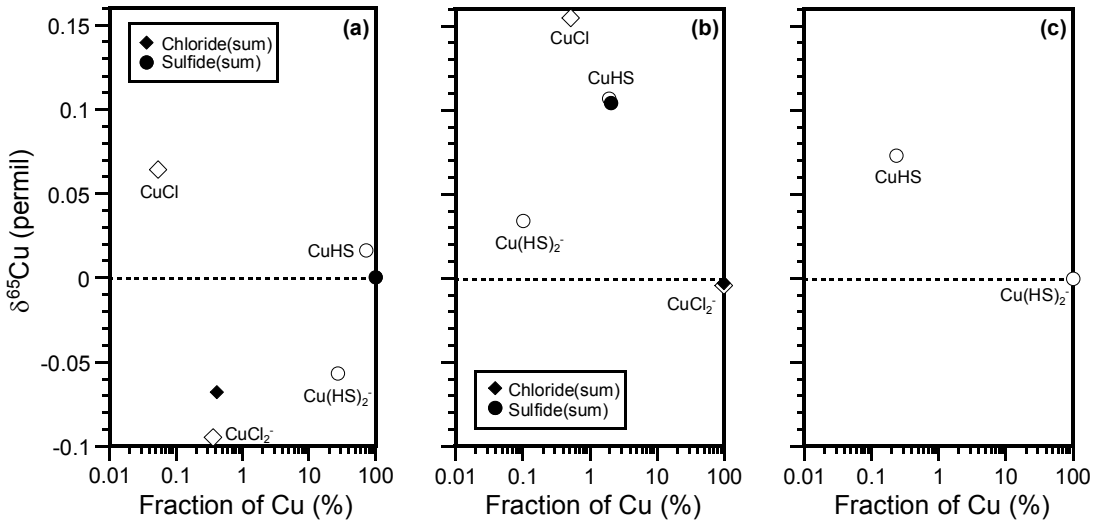

Figure S2. Copper, Cu(I), isotopic variations ($^{65}Cu/^{63}Cu$, $\delta^{65}Cu$) under hydrothermal conditions at 573 K. (a) The conditions for Broadlands fluid. (b) The conditions of high salinity at low pH. (c) The conditions of high sulfur concentration at high pH. Estimated mole fractions are from Mountain and Seward (1999), where the detailed conditions of pH, concentrations of Cl and S, and H_2 fugacity can be found.

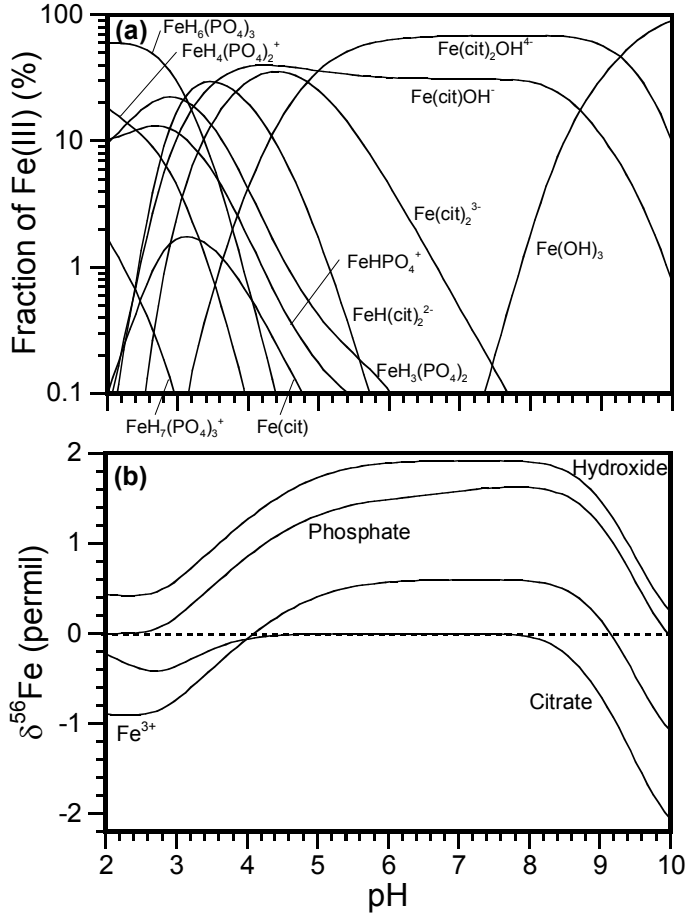

Figure S3. Mole fractions of Fe(III) species and Fe isotopic variations ($^{56}Fe/^{54}Fe$) in a soil-plant system as a function of pH at 298 K. (a) Dissociation constants of citric acid and stability constants of orthophosphates and Fe(III) species were taken from the literature (Childs, 1970; Baes and Mesmer, 1976; Ciavatta and Iuliano, 1995; Königsberger et al., 2000). (b) $\delta^{56}Fe$ of Fe(III) phosphates, citrates, hydroxides, and hydrated Fe^{3+} ions relative to the bulk solution. Total concentrations of Fe, P, and citrate were set to 0.005, 0.05, and 0.01 mol kg^{-1}, respectively. Activity coefficients of related species were set to unity.

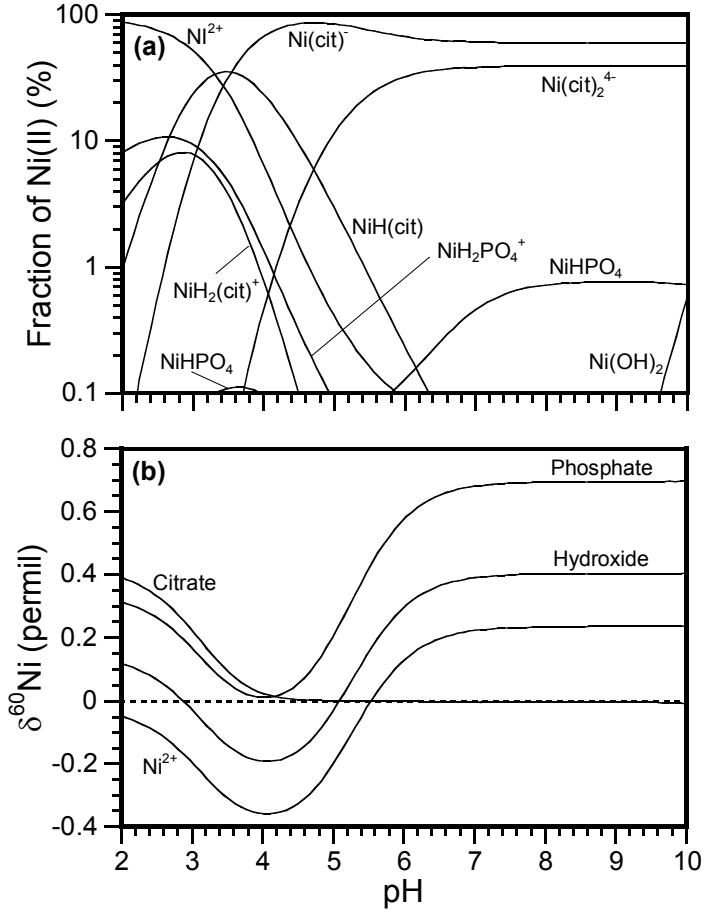

Figure S4. Mole fractions of Ni(II) species and Ni isotopic variations ($^{60}Ni/^{58}Ni$) in a soil-plant system as a function of pH at 298 K. (a) Dissociation constants of citric acid and stability constants of orthophosphates and Ni(II) species were taken from the literature (Childs, 1970; Baes and Mesmer, 1976; Taylor and Diebler, 1976; Hedwig et al., 1980). (b) $\delta^{60}Ni$ of Ni(II) phosphates, citrates, hydroxides, and hydrated Ni^{2+} ions relative to the bulk solution. Total concentrations of Ni, P, and citrate were set to 0.005, 0.1, and 0.01 mol kg^{-1}, respectively. Activity coefficients of related species were set to unity.

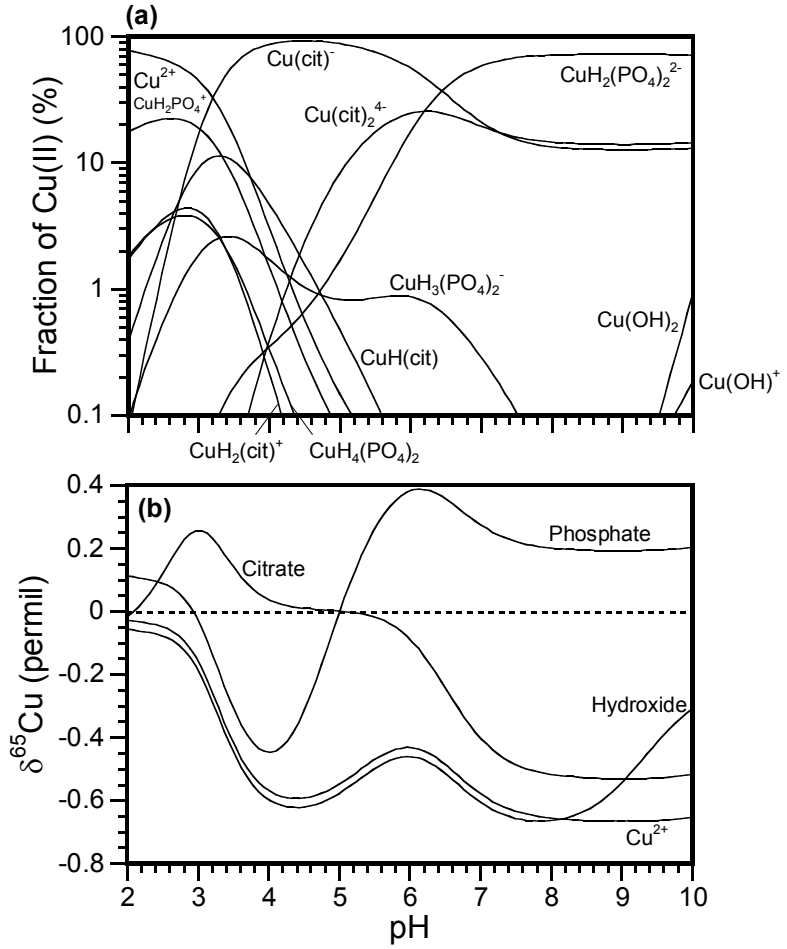

Figure S5. Mole fractions of Cu(II) species and Cu isotopic variations ($^{65}Cu/^{63}Cu$) in a soil-plant system as a function of pH at 298 K. (a) Dissociation constants of citric acid and stability constants of orthophosphates and Cu(II) species were taken from the literature (Childs, 1970; Baes and Mesmer, 1976; Petit-Ramel and Khalil, 1974; Ciavatta et al., 1993). (b) $\delta^{65}Cu$ of Cu(II) phosphates, citrates, hydroxides, and hydrated Cu^{2+} ions relative to the bulk solution. Total concentrations of Ni, P, and citrate were set to be 0.005, 0.05, and 0.01 mol kg^{-1}, respectively. Activity coefficients of related species were set to unity.

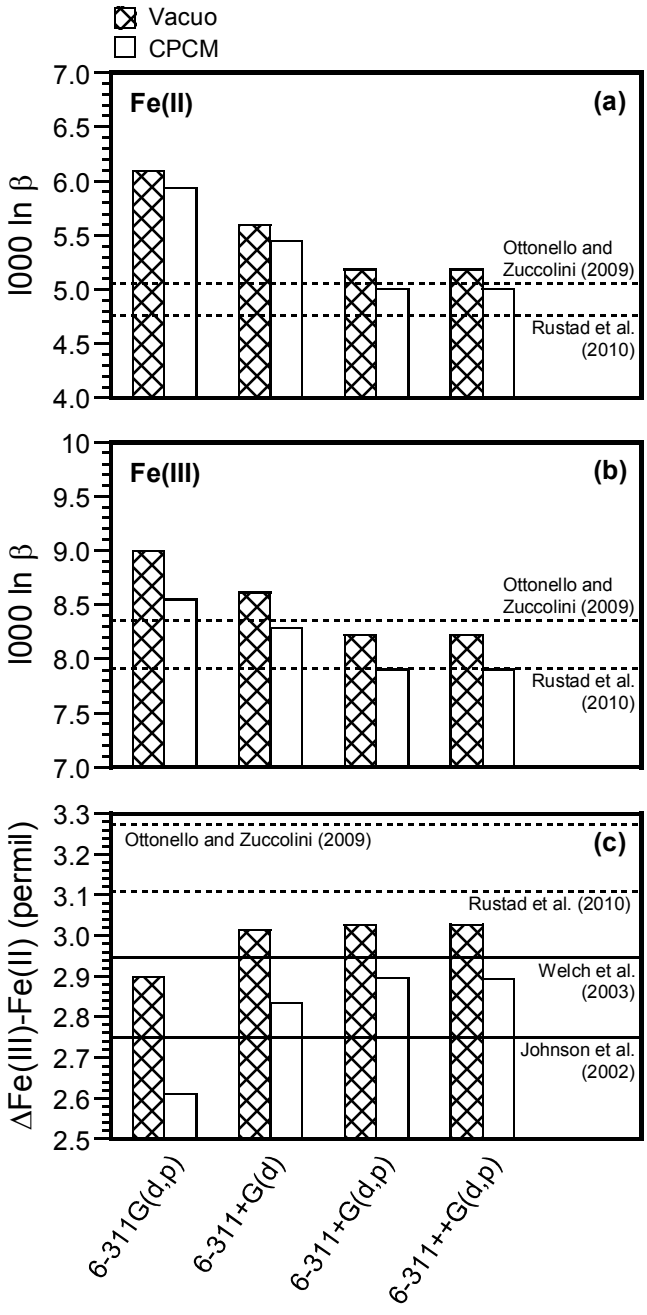

Figure S6. Fe isotopic variation ($^{56}Fe/^{54}Fe$) for hydrated Fe^{2+} and Fe^{3+} species at 295 K. DFT calculations of B3LYP/6-311G for various diffuse and polarization functions were tested with or without CPCM. (a) ln β for hydrated Fe^{2+}. (b) ln β for hydrated Fe^{3+}. (c) Isotope fractionation $\Delta^{56}Fe$ between hydrated Fe^{3+} and Fe^{2+}. Literature data (see Table B2) of theoretical values (Ottonello and Zuccolini, 2009; Rustad et al., 2010) (dotted lines) and experimental values (Johnson et al., 2002; Welch et al., 2003) (bold lines) are shown together.